HEAVY ION IRRADIATION INDUCED CHANGES IN POLYMERS AND C_{60}

ABSTRACT

BY

STEPHEN LOTHA

THESIS SUBMITTED

IN FULFILMENT OF THE DEGREE OF

DOCTOR OF PHILOSOPHY IN PHYSICS

OF

NORTH - EASTERN HILL UNIVERSITY

SHILLONG - INDIA

JUNE 1999

SYNOPSIS

HEAVY ION IRRADIATION INDUCED CHANGES IN POLYMERS AND C_{60}.

The advent of heavy ion accelerators has given rise to numerous applications in material technology, which is emerging as a new field with possibilities of engineering new materials. Heavy ion beams has become a versatile handle in studying and characterizing materials because of its possibilities of varying and controlling the ion species and their energies to a great extend. Over the years accelerator based studies on materials has played a vital role in the progress of material science. With the advances in technology the field is now wide open with immense possibilities for inter-disciplinary research and developments.

Energetic Heavy ions passing through a material lose their energy mainly by inelastic scattering with the target electrons. This energy loss can be varied by choosing appropriate ions and their energies. This provide a flexibility to engineer properties of the material, so that the desired optical, electrical and mechanical properties can be obtained.

Owing to their inherent properties like its lightness, high corrosive resistance, high electrical resistivity etc., polymers are at present fast replacing metals and alloys in many applications and detailed studies on their properties has therefore assumed great importance. The only major disadvantage is their limited mechanical strength [1].

The interaction of ion beam with polymers have been extensively studied in the past many years and it has been found that bombardment of heavy ions drastically changes the electrical, mechanical and thermal properties in them [2-4]. The breaking of bonds, formation of free radicals, excited species, and a secondary chemical processes take place, which modify their properties and structures [5, 6]. Along the ion trajectory, cylindrical zones of defects called latent tracks are formed. These tracks consists of atomic displacements, broken molecular chains, free radicals etc. If the dose is high such that track overlapping takes place then the material is changed to such an extent that it can be considered to be as a new material. The range of such radiations in polymers is extremely small and therefore microscope observations are required to measure the tracks, holes or abrasions. The density of ionization and the radius of the core region depend on the projectile and its velocity and has been observed that three parameters are needed viz., atomic number, velocity and fluence to give satisfactory physical aspects of ion irradiation in polymers [7].

The hydrogen content in materials effects its electrical, mechanical, chemical and spectroscopic properties in materials. Therefore the detection of hydrogen in a material and the determination of concentration at various depths is of great importance. It is known that the hydrogen content of hydrogenous materials decreases with incident ion fluence. It is therefore possible to tailor the properties of materials by altering hydrogen concentration using ion beams. Polymers have different strengths of hydrogen concentrations which play an important role in their properties. Therefcre in this work we have investigated the hydrogen loss behavior in different polymers using the technique known as Elastic Recoil Detection Analysis (ERDA).

Buckminsterfullerene (C_{60}) has exhibited properties that prompt possible widespread technological applications [8]. The interaction of energetic ions with C_{60} may be of particular relevance to C_{60} applications as a new material, as well

as problems related to the occurrence of C_{60} in space [9]. With the above information there has been a great interest among researchers on the question of stability of C_{60} and the products which arise on irradiation with ion beams. The possibility of metal doped K^+ fullerene for application in high temperature superconductivity prompted researchers [10-11] to attempt low energy ion implantation. However this led to the damage and destruction of C_{60}. Several workers[12-15] also investigated the process of damage of C_{60} at low energies, where the elastic collision process dominated. From their work [15] it was evident that complete destruction of C_{60} takes place when the product of the nuclear energy loss and the ion dose exceeds a critical value of 0.04 - 0.12eV/Å^3. The natural question then arises about the fate of C_{60} when they are exposed to a large electronic excitation. There are a few studies [16-18] on this aspect but the complete understanding of the process has not been achieved. We have therefore taken the interest to characterize the induced modification on C_{60} at high electronic excitation using different ions and energies.

This thesis consists of seven Chapters. **Chapter I** introduces the problem and also outlines the interpretations and limitations by earlier workers working on relevant and related systems.

Chapter II describes in general the mechanism and the effect that takes place in the material when an energetic ion interacts with matter.

In **Chapter III**, we describe the irradiation parameters and the experimental techniques used to characterize the induced modification on the irradiated Polymers and C_{60} thin films.

Chapter IV describes on the investigation of hydrogen loss under heavy ion irradiation in different Polymers using various energetic heavy ions and to determine the dependence of this loss on the electronic stopping power and the

relationship between the loss and the chemical composition such as their different bonding. The non-destructive nuclear technique Elastic Recoil Detection Analysis was used for the study.

In **Chapter V** we try to analyze the Physical and Chemical induced modification on the irradiated Polymers by swift heavy ions. The radiochemistry and melting behavior of semicrystalline polyethylene terephthalate (PET) polymer irradiated by 180 MeV Ag ion was studied. For the characterization study we have employed techniques of Differential Scanning Calorimetry (DSC), Fourier Transformed Infra-red Spectroscopy (FTIR) and X-ray diffraction spectrometer. The effect on polyvinyledyene fluoride (PVDF) by irradiation with 180 MeV Ag ions and 95 MeV Ni ions at various fluences have also been described in this chapter.

In **Chapter VI** we describe the effect of heavy ion irradiation on C_{60}. Thin films of C_{60} of thickness ~500nm deposited on float glass substrates were subjected to swift heavy ion irradiation spanning the region from 2 to 11keV/nm of electronic excitation, using 189 MeV $^{107}Ag^{13+}$ 110 MeV $^{58}Ni^{17+}$ 50 MeV $^{28}Si^{5+}$ ions. Studies on the irradiated films were investigated using the techniques of Raman and Photoluminescence spectroscopy. To get more information on the effect of energetic heavy ions on C_{60}, techniques of X-ray diffraction (XRD), Atomic force microscopy (AFM) and Fourier transformed infra-red (FTIR) spectroscopy were also utilized to study the topographic morphology, the crystalline structure and in the chemical modifications.

Finally a summary of the thesis and the important conclusions are given in **Chapter VII** along with the prospective for future scope on this field.

References:

1. R. Ochsner, A. Kluga, S. Z. Malon, L. Cong and H. Ryssel, Nucl. Instr. Meth. B 80/81 (1993) 1050.
2. L. Calgagno and G. Foti, Nucl. Instr. Meth. B 59/60 (1991) 1153.
3. E. H. Lee, M. B. Lewis, P. J. Blau and L. K. Mansur, J. Mat. Res. 6 (1991) 610.
4. L. B. Bridwell and Y. Q. Wong, Int. Conf. on Thin Films Physics and Applications SPIE Vol.1519 (1991) 879.
5. P.Mazzaldi and G. W. Arnold, Ion beam modification of Insulators Vol. 2 (Elsevier, Amsterdam, 1987).
6. L.Calgno, G. Compagaini and G. Foti, Nucl. Inst. Meth. B 65 (1992) 850.
7. S. Bouffard, B. Gervais and C. Leroy, Nucl. Inst. and Meth. B 105 (1995) 1.
8. W. Kratschmer, L. D' Lamb, K. Fostiropoulos and D. R. Huffman, Nature 347 (1990) 354.
9. J. Hare and H. Kroto, Acc. Chem. Res. 25 (1992) 106.
10. F. P. Bundy, H. T. Hall, H. M. Strong and R.H. Wentorf, Nature, 176, (1995) 51
11. H. Liander and E. Lundbad Ark. Kemi, 16 (1960) 139.
12. H. W. Kroto, J. R. Health, S. C. O'Brien, R. F. Curl and R. E. Smalley, Nature, 318 (1985) 162.
13. C. S. Sunder, A. Bharathi, Y. Hariharan, J. Janaki, V. S. Sastry, T. S. Radhakrishnan, Solid State Commun, 84 (1992) 823.
14. M. E. Kozlov, M. Harabayashi, K. Noxaki, M. Tokumoto and H. Ihara, Appl. Phys. Lett., 66 (1995) 1199.
15. B. Dischler, A. Bubenzer and P. Koidl Solid State Commun., 48 (1985) 105.
16. R. M. Papelo, A. Hallen, J. Eriksson, G. Brinkmalm, P. Demirev, P. Hakansson and B. U. R. Sundqvist, Nucl. Instr. and Meth. B 91 (1994) 124.
17. D. Fink, R. Kleet, P. Szimkoviak, J. Kastner, L. Palmetshofer, L. T. Chadderton, L. Wang and H. Kuxmany, Nucl. Instr and Meth. B 108 (1996) 114.

HEAVY ION IRRADIATION INDUCED CHANGES IN POLYMERS AND C_{60}

BY

STEPHEN LOTHA

THESIS SUBMITTED

IN FULFILMENT OF THE DEGREE OF

DOCTOR OF PHILOSOPHY IN PHYSICS

OF

NORTH - EASTERN HILL UNIVERSITY

SHILLONG - INDIA

JUNE, 1999

TO MY

PARENTS

NORTH-EASTERN HILL UNIVERSITY
SHILLONG

CERTIFICATE

I, Stephen Lotha, hereby, declare that the subject matter of the thesis entitled "Heavy ion irradiation induced changes in polymers and C_{60}" is the record of work done by me, that the contents of this thesis did not form basis of the award of any previous degree to me or to the best of my knowledge to anybody else, and that the thesis has not been submitted by me for any research degree in any other University/ Institute.

This is being submitted to the North Eastern Hill University for the degree of **DOCTOR OF PHILOSOPHY** in Physics.

Mr. Stephen Lotha

Dr. D. T. Khathing
(Supervisor)

Dr. D. K. Avasthi
(Joint Supervisor)

(Head) 19/6/98
Department of Physics
North Eastern Hill University
Shillong

Professor and Head,
Department of Physics,
North-Eastern Hill University
Shillong-793003

ACKNOWLEDGEMENTS

With great pleasure I wish to express my deepest sense of gratitude to my supervisors Dr. D. T. Khathing, department of physics NEHU and Dr. D. K. Avasthi (Joint supervisor) Nuclear Science Centre New Delhi, for their keen interest in my work, constant encouragements, advice and help, without which this work would not have been possible.

I am also deeply grateful to my collaborators, Dr. V. K. Mittal, Dr. A. Ingale and Prof. A. Gupta for their immense sacrifice and help which has contributed much towards the completion of this work.

A very special feeling of acknowledgment goes to my dear and close friends Dr. Dhrubo, Dr. V. R. Rao, Dr. R. Das, Dr. S. Khetri, Dr. Sujit, Mr. Dipankar, Mr. Prasantha Mr. A. Biswas and Mr. I. Jamir, who were always at my side during the days of hardships and disappointments with their brotherly support, encouragement, help and advice. The association and interaction with them has contributed a lot.

I am grateful to Prof. G. K. Mehta, Director NSC New Delhi, and his colleagues for allotting me the beam time to perform my experiments successfully. I am also thankful to the staff and my friends particularly Mr. J. P. Singh, Mr. R. Singh, Mr. S. Ghosh, Buddhadev and Dr. T. Som who have been very helpful during my stay at NSC.

I extend my gratefulness to Mr. P. S. Dkhar, Mr. E. J. Philip of Chemistry department, Mr. C. R. Das, Mr. A. K. Rathore of Physics department NEHU, for their cooperation and help in taking the spectras of my samples.

When I look back those long long hard four years it reminds me how much pain and sacrifice my wife and children have undergone in letting me complete this work . This column therefore remains incomplete if I forget to acknowledge their love. I certainly shall ever remain grateful to them.

I also must not forget to express my gratefulness to the Centre Director Prof. A. Gupta (IUC), Dr. V. Ganesan (scientist) and the research scholars who have been very kind and helpful to me during my stay at IUC. Indore.

.

I gratefully acknowledge the financial support and hospitality extended to me by Nuclear Science Centre, New Delhi during my work.

Finally I am very much thankful to the government of Nagaland for granting me the leave to undergo my Ph. D studies.

(STEPHEN LOTHA)

Dated: 6th. June 1999
Shillong.

CONTENTS

CHAPTER- I

I.0. Introduction:

The last three decades has witnessed intense research activities in many laboratories on the modifications of the properties of materials by ion bombardment. The driving force behind such immense interest is the possibility that ion bombardment may improve certain properties of materials that could have certain important applications. In Material Science many low energy ions have been exploited so far to give rise to cascades of collisions and displacing the atoms causing certain defects. It is observed that not much work has been reported on the modification of materials using high energetic heavy ions, where the process of energy transfer to the system is different from that of low energy ions. We have therefore made an attempt here to study the induced effects in Polymers and Fullerene (C_{60}) using swift heavy ion (SHI) where a large fraction of the energy is locked into the electronic excitation.

Swift heavy ions, (SHI), passing inside a material, predominantly interact with the target atoms through inelastic collisions producing a trail of excited and ionized atoms. This is in contrast to the familiar elastic damage in a lattice. The slowing down of swift heavy ions in the material and consequently the energy

transfer to the target is dominated by the so called electronic stopping power denoted by $(dE/dx)_e$. The specificity of swift heavy ions is that it gives high $(dE/dx)_e$ values of some tens of keV/nm. One important consequence of high $(dE/dx)_e$ is that the highly localized electronically deposited energy is transferred from the excited target electrons in the atoms by processes which could be very different from those occurring during irradiation with 'classical' low ionizing particles like γ-rays or electrons. As a result significant changes in the radiation induced damage processes occur when SHI irradiation are performed.

Using MeV ions for the modifications of materials offers a number of advantages e.g., (i) minimizing of surface damage, (ii) greater range in material and (iii) uniform electronic excitation, where collision energy damage occurs only at the end of the range.

SHI can also effect the lattice as is evident from the well known phenomenon of tracks produced in insulators. If the electronic energy loss S_e exceeds a certain threshold value structural changes can occur leading to etchable tracks in the material.

Another advantage using high energetic ions is that the electronic energy loss deposited in the material can be varied from a level of a few keV/nm to some tens of keV/nm by choosing appropriate ions and their energies. This provides remarkable flexibility and opportunities to engineer properties of the

materials, so that they can acquire the desired optical, electrical and the chemical properties.

At high ion energies ($E \geq 1$ MeV/u) where the energy loss mechanism is through electronic excitation, the structural modifications in the material is not as straightforward as for nuclear energy loss (S_n), because an efficient energy is required to convert electronic excitation to atomic motion. The energy conversion may arise from electron- phonon couplings or interactions [1], from a formation of self localized excitons [2], from a mechanical instability due to modified interatomic potentials [3, 4] or from coulomb repulsion of the ionized target [5]. All these mechanisms are more effective in insulators than metals where rapid de-excitation can occur due to the availability of free electrons. We have therefore chosen Polymers and Fullerene (C_{60}) both of which offers a large electronic excitation to energetic heavy ions. Further they exhibit attractive properties that promise exciting results in the present fast expanding field of technology.

Numerous works have been reported in literature [6-8] since a long time on irradiation induced modification of various polymers using conventional ionizing radiations such as γ, x-rays, electrons and low energy ions in the keV range where the elastic energy loss is predominant. With the advent of heavy ion accelerators in the seventies, there has been a lot of enthusiasm

among researchers specially in the field of material science to study the high energy heavy ion induced modification on polymers and other materials.

The interaction of high energetic ions with polymers is different from those of light ionizing radiations. This is due to the fact that the mechanism of energy transfer to the material is different. Bouffard et al.[9] reports that to have a nonambiguous description of irradiation on polymers three parameters are needed - the atomic number, the velocity and the fluence. Therefore the modification induced by energetic ions in materials can be understood only if the particulars of the energy transfer from the ion to the target are considered.

Energetic heavy ions in the energy range of MeV/amu passing through matter produces excited and ionized atoms along its path. The energetic secondary electrons or δ-electrons produced thereby trigger secondary ionizations, excited species, radicals etc. in its own surrounding the ion trajectory. Due to their highly charged states associated with high energy transfer, cylindrical zones of irreversible chemical and structural changes are created. These zones are known as latent tracks, which are responsible for the modifications of the material. The latent tracks consists of atomic displacements, broken molecular chains, free radicals, and chemical decomposition products [10].

In polymers hydrogen and other gases are formed within these tracks of damaged zones and diffuses out of it. This results in loss of hydrogen in polymers on irradiation. It is also observed that in polymers the dimension of the tracks and defects depend on the composition and molecular weight of the polymer, the mass and energy of the ion and on the irradiation temperature[11].

There are already few studies reported relating to modification of polymers using high electronic excitation (few keV/nm) [12-21] but the complete understanding of the mechanism of the fundamental process involved and the results that arise in the interaction using swift heavy ions at high electronic excitation is still wanting and more data and experiments are required to arrive at a satisfactory understanding.

1.1 POLYMER:

During the last few decades the importance of polymers has increased very rapidly because of their low cost, easy processibility, low weight, high corrosion resistance, high electric resistance, durability, etc. At present they are fast replacing metals and alloys in many applications. They are widely used in

the field of industries, science and technologies particularly in space and nuclear technology. It is seen that no field is left untouched by the influence of polymers. This rightly tells why this age is called the " Polymer age".

The word polymer is derived from the Greek word "poly" meaning many and "mer" meaning part. Polymers are substances composed of long chain repeating units, built up from shorter molecules and usually based on organic(carbon) materials. A polymer is made up of many small molecules which have combined to form a single long or large molecule (macromolecule).The individual small molecules from which the polymer is formed are called "monomer" (single part). The small molecules which combine to form a big molecule can be of one or more chemical compounds. e.g. Butadiene with a molecular weight of 54, combines nearly 4,000 times and gives a polymer known as polybutadine with a molecular weight of about 200,000. This process by which the monomer are linked to form a big polymer molecule is called "polymerization".

Generally polymers are held together as large molecules by covalent bonds, while separate segments or molecules are held by Vander Waals forces. Single molecules may be linear or branched.

Branching interferes with the ordering of molecules so that crystallinity decreases with branching. In the solid state polymers can be completely amorphous, partially crystalline or almost completely crystalline [22]. Depending on their chemical structures, physical properties, mechanical behavior and thermal characteristics polymers can be classified as (i) Natural and Synthetic polymer (ii) Organic and Inorganic polymers and (iii) Thermo plastic and Thermosetting polymers.

In the last few decades different scientific and technological laboratories have increasingly reported on polymers with better properties than conventional structural materials such as metals, ceramics and alloys and their overall advantage of economical viability. Improvement in the qualities of polymers like rigidity, strength, toughness, resistance and dimensional stability is making it to compete or even to surpass steel. The superior properties of polymers have also played a vital role in space and nuclear technology, in sensor applications and in medical sciences.

Interest in the applications of ion beams to polymers has arisen to the fact that the characteristic properties of polymers can be modified by irradiation under suitable conditions. Interest has also evolved in the peculiar nature of the ion-polymer interactions.

Material modification and characterization by ion beam has become a very interesting and challenging field owing to the vast technological implications [23-27]. Modifications of the physical and chemical property of material like metals, semiconductors, insulators and polymers [28-32] have been successfully achieved by ion implantation techniques. These reports showed that mechanical surface properties like friction and wear can be greatly reduced, super conducting properties of alloys can be improved and doping of impurities in semiconductors materials can be done. Chemical and electrochemical surface properties can also be suitably modified to produce desired results like prevention of corrosion and oxidation[25].

In the present work some commercial polymer films obtained from Good fellow Industries UK have been used to study the induced modifications effects on the polymers by swift heavy ions irradiation at high electronic excitation. A brief description of the polymers are given below :

(a) Polypropylene (PP)

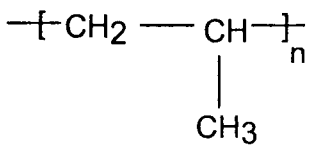

It is produced by the polymerization of propylene. The propylene is obtained from gasoline refineries. Being highly

crystalline it exhibits high stiffness, hardness and tensile strength. It has a density of (0.90 gm/ cm^3), high melting point and is more easily oxidized. Components made of polypropylene are used in appliances such as refrigerators, radios, and TV's. It is also used for making pipes, storage tanks, etc.

(b) Polymethyl methacrylate (PMMA)

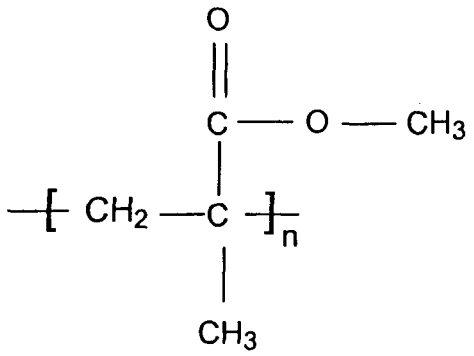

This polymer is produced from poly acrylic acid. It is a transparent glassy material, and is amorphous by nature. The main application of PMMA arise from the combination of its transparency and its good outdoor weathering properties. It is used for signboards and street lamp fittings. It is also used for decorations in buildings.

(c) Polystyrene (PS)

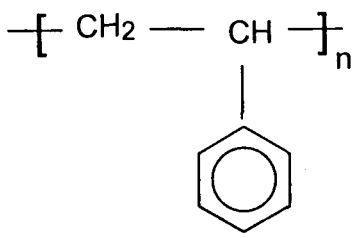

It is produced from ethylene and benzene. PS has heat distortion temperature(85 °C). It has poor weathering properties and brittleness. Besides these defects it is used widely in the manufacture of articles like lids, jars, bottles, radio and television cabinets.

(d) Polyvinylidene flouride (PVDF)

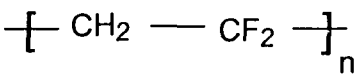

It is a crystalline polymer with a melting point at 170 °C. It does not undergo distortion over a wide range of temperature. It is resistant to many solvents and finds use in coating composition.

(e) Polyimide (PI).

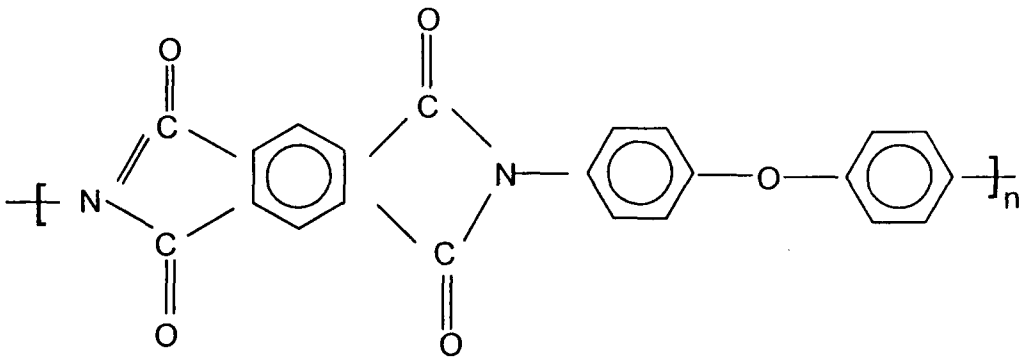

Polyimide finds applications in electrical industry for insulation coating. It can withstand temperature up to 425 °C, because of which it is used in surface coating of supersonic aircraft.

(f) Polyethylene terephthalate (PET)

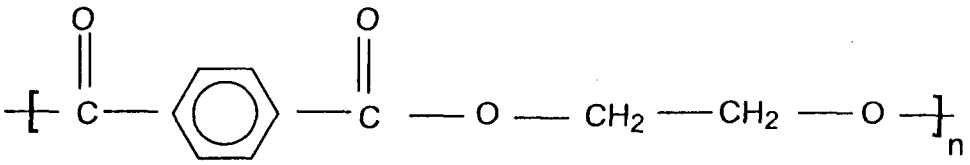

It has high melting point of 265 °C and can withstand heat and moisture. It is used extensively in making textile fibers, and Clothes made from its fibers do not wrinkle. It is also used in the manufacture of magnetic recording tapes.

In Polymers the latent tracks can be easily etched and therefore etched tracks in polymers films are generally used commercially for making calibrated pore filters [11]. However little is known on the physical chemical modifications induced in polymers by energetic swift heavy ions, and specially no detail work has been reported on the loss of Hydrogen during irradiation using high energetic ions.

The presence of hydrogen in materials greatly effects the properties of materials, like electrical, mechanical, chemical etc. In some materials hydrogen gets introduced unintentionally and causes undesirable effects, while in some materials it is introduced intentionally for advantageous results. It is known that the hydrogen content in materials decreases with increase in ion dose. It would then be possible to tailor the properties of materials by altering the hydrogen concentration using ion beams to achieve desired the properties. In order to have a detailed understanding of hydrogen loss in materials by ion beam bombardment, we have tried to investigate the hydrogen loss behavior in polymers employing various energetic heavy ions at different energies and fluences. An estimate has been made on the ion track dimensions in relation to the hydrogen loss from the studied polymers for different energetic heavy ions.

In our work a non destructive analytical nuclear technique, namely Elastic Recoil Detection Analysis(ERDA) [33,34] has been employed to monitor the changes in the hydrogen concentration under ion irradiation. Studies were done on the release of hydrogen from different polymers as a result of bombardment of 100 MeV Ag ions on Polyvinylidene(PVDF), 110 MeV Ni ions on polystyrene(PS), Polymethylmethacrylate(PMMA) and Polyvinylidene fluoride (PVDF), 85MeV Ni ion on Polypropylene(PP) and Polyimide(PI) and 50 MeV Si on Polypropylene(PP) and Polyimide(PI).

In order to get a deeper insight into the chemical modification of the irradiated polymers, Fourier transformed infrared spectroscopy measurements of some irradiated polymers were also made.

Differential Scanning Calorimetry(DSC) measurements was used to see the change in the crystallinity with respect to changes in the melting point of polyethylene terephthalate(PET) on irradiation.

In this thesis an attempt to characterize the effects of swift heavy ion on some polymers using various experimental techniques has been made. It is hoped that the findings in this work would be of important relevance to material science applications of polymers.

1.2 BUCKMINSTER-FULLERNE (C_{60}):

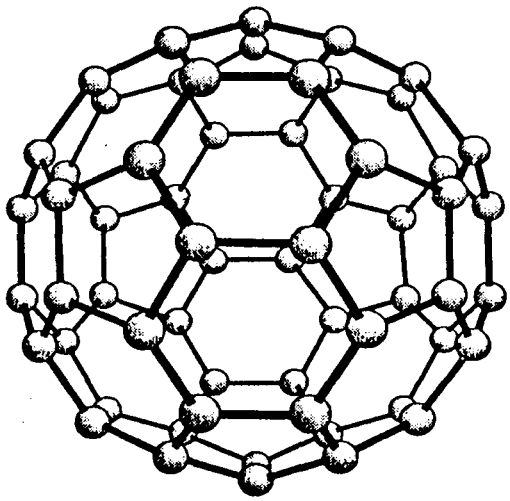

The Noble prize for chemistry 1996 was awarded jointly to H. W. Kroto, J. R. Heath, S. C. O'Brien, R. F. Curl, and R. E. Smalley for discovery of fullerenes. Since the discovery in 1985 there has been unprecedented research activities among scientists in multi disciplinary fields, including chemistry, physics, materials science and even biology.

Fullerenes constitute a new allotrope of carbon. Unlike graphite and diamond this new allotrope of carbon is the only pure and finite form of carbon consisting of hollow carbon cages. The number of carbon atoms in each fullerene cage can vary and therefore can be represented by the formula C_n, where n denotes the number of carbon atoms present in the cage. All these

clusters [35] ranging from C_{32} - C_{960} have a common property, viz. they have a network of hexagons and pentagons. It was realized that carbon clusters with only even number of atoms of carbons were rather stable than other clusters having odd number of atoms. Among the fullerene family, C_{60} is the most abundant and most stable and therefore has dominated over others in fullerene research.

C_{60} has a graphitic closed cage structure consisting of 12 five-membered rings (Pentagons) separated by 20 Hexagons distributed in a nearly spherical surface. This molecule containing 60 carbon atoms lying at the vertices of a truncated icosahedron is typified by a soccer ball looks and is known as BUCKMINSTER-FULLERENE[36], because the geodesic structures of Buckminster Fuller led to the initial proposal of the structure. Each carbon of the C_{60} molecule shares one double bond(1.40Å) and two single bonds(1.46Å) with its neighbors. At room temperature C_{60} has an f. c. c structure having inter cluster separation of 10Å. The hollow cage has a diameter of 7.1Å and a cavity of 3.8Å which is large enough to trap any atom of the periodic table. Fullerene molecule has sp^2 (curved) bonding and a specific formula and molecular weight. It has no dangling bonds but just a pi- electron cloud around.

The discovery of a method for mass production of C_{60} [37] sparked tremendous research interest among scientists in varying fields. There has been

numerous techniques reported in the last few years for obtaining purified macroscopic quantities of C_{60} molecules [38-40], and various approaches in its characterization. These studies include Time of flight, mass spectroscopy [39-41], electron and X-ray diffraction from ordered arrays of C_{60} in crystals and powder[38], Infrared absorption spectroscopy[38,40,41], Visible-ultra-violet absorption[37,38,41,42], Raman spectroscopy[39], Nuclear magnetic resonance (NMR) [40-45], electron spin resonance [45,46], Photoelectron spectroscopy [47,48] and Scanning tunneling microscopy (STM) [49,50]. All the above results show consistent result with the proposed structure of fullerene.

This super atom having truncated Icosahedral symmetry, spinning at the rate of about>100million/sec has exhibited properties that prompt tremendous Technological potential [51]. After the discovery of the method to produce gram quantities of fullerene there has been much research on their commercial importance, few of much commercial applications include being described below :-

(i) Fullerene photoconductors.

In Facsimile machines, paper copy machines and laser printers, selenium is usually used for coating the imaging drum which makes it photo conductive. Modern machines are now replacing selenium with advanced organic photo conductive polymers. Du Pont researchers has shown that doping a PVK polymer with 1%

C_{60} can create a new class of high performance photo conductors with image resolution as good or better than some of the best commercial photo conductors.

(ii) CVD Diamond films.

C_{60} has a low sublimation temperature(600 °C) at which makes vapor coating of irregularly shaped surfaces easy. Fullerenes being pure carbon molecules may have an important role to play as materials to provide uniform nucleation sites for growth of diamond thin films. Fullerenes are also soluble in polar solvents such as benzene or toluene. The preparation may be applied directly to complex surfaces in a room temperature process, leaving a film of bucky balls behind after the solvent evaporates.

Applications of diamond thin films include optical particle-beam windows, semi conductors wafers, hard surfaced gear teeth, temperature and radiation hardened electronic components and defence applications such as impact resistant armor coating.

(iii) Catalysts.

Fullerenes offer a new class of catalysts, as shown by Nagashima of Toyohasi University of Technology where C_{60} was used to

produce a palladium carrying polymer complex with high catalytic activity.

(iv) Lubricants and Abrasives.

Fluorinated bucky balls ($C_{60}F_{60}$) known as "teflon balls" have been generated by British workers in recent years. These balls may serve as one of the world's best lubricants. On a molecular level the individual C_{60} molecules are unusually hard, and due to their structure makes them resistant to compressive forces. However their weak intermolecular bonds between the molecules result in low shear strength. Fullerene as abrasives when they are converted to diamond directly, by the application of high pressure at room temperature.

(v) Super Conductivity.

It has been reported that when fullerite is doped with alkali metals such as potassium and rubidium, it becomes a superconductor. A. F. Hebard of AT and T's Bell Labs,[52] reports that K C_{60} has a transition temperature, T_c of 18K while Rb C_{60} of 28K. However recent reports show T_c of 45K (Bucky balls 1991). It is thus seen that only ceramic "high temperature" superconductors have higher transition temperature than the fullerene class.

Possible applications include mag-lev trains, high speed computer chips, long distance power transmission, super conducting motors and generators and electronic shielding for supercomputers.

C_{60} are created in the laboratory by directing an intense beam of laser onto a graphite or any other carbon surface. It is also observed that heavy ions in the GeV range, impinching onto carbonaceous materials (e.g., graphite, kapton or sugar) give rise to formation of fullerenes [53] in the ion tracks.

Although C_{60} is industrially being produced, the microscopic mechanisms underlying the formation and the fragmentation of fullerenes are yet to be understood fully. Another important issue on fullerite-based devices is the stability of C_{60} under different chemical environments and excitations [54]. Better in-depth understanding has been sought by researchers in the use of ions of various types and energies to irradiate C_{60}.

Great interest has also been recently shown on surface modifications with MeV cluster beams. Cluster may be considered as the simultaneous arrival of many closely spaced atoms at the surface. This may lead to totally different kinds of effects from those produced by single ions. In addition to being a target of energetic ions, ionized C_{60} MeV beams have also been applied in the fabrication of materials.

The advent of heavy ion accelerators gave rise to numerous applications in material technology, of the versatility in varying and controlling the ion species and their energies have made them powerful tools in the study and characterization of materials. Much work has been done on the interaction of energetic particles with the C_{60} fullerene as a new material, as well as to problems related to the occurrence of C_{60} in space [55]. Studies on the interaction of keV ions with C_{60} has been reported at large. The possibility of metal doped fullerene for applications in high temperature superconductivity prompted the researchers [56,57] to carry out low energy K^+ ion implantation in C_{60}. This process however led to radiation damage causing the destruction of fullerene. Several workers [58-60] also investigated the process of the damage of fullerene at low energies, where the elastic collision process dominates. As a result of these studies, it was shown [60] that complete destruction of fullerene takes place when the product of nuclear loss deposition and the ion dose exceeds a critical value of 0.044 - 0.12eV/Å^3. A question then arises about the fate of fullerene when they are subjected to large electronic excitation. There are few studies[61-63] on this aspect but the complete understanding of the process is still lacking. We have therefore attempted to characterize and study the induced modifications of irradiated C_{60} at high electronic excitation using various energetic ions at varying energies and fluences.

A number of techniques has been employed to characterize the thin samples of irradiated C_{60} samples with energetic ions of 189, 180 MeV Ag, 110 MeV Ni, and 50 MeV of Si, at fluences ranging from $1x10^{9}$ to $5x10^{13}$ ions/cm^2. The irradiation were all performed using the 15UD Pelletron at the Nuclear Science New Delhi.

Atomic Force Microscopy (AFM) and X ray Diffraction (XRD) was used to see the surface morphology and the structure that was modified by irradiation.

Fourier Transformed Infra-red (FTIR), Raman and Photoluminescence spectroscopy studies were undertaken to characterize the induced modification of C_{60} on irradiation using various heavy ions at different energies.

References:

1. I. M. Lifshits, M. I. Kagnov and L. V. Tanatarov, J. Nucl. Energy, Reactor Science, A12.(1960) 69: Translated from Atomnaya Energiya 6 (1959) 391.
2. N. Itoh, Radiat. Eff. Def. Solids 110 (1989) 19.
3. C. C. Watson and T. A. Tombrello, Rad. Eff. 89 (1985) 263.
4. P. Stampfli and K. H. Bennemann, Phys. Rev. B46 (1992) 10686.
5. R. L. Fiesher, P. B. Price and R. M. Walker, in Nuclear Tracks in Solids, University of California Press, 1975.
6. M. Dole, The Radiation Chemistry of Macromolecules (Academic press, New York, (1973).
7. A. Charlesby, Atomic Radiation and Polymers (Pergamon London,1960).
8. L. Calcagno and G. Foti, Nucl. Inst and Meth. B 59/60 (1991) 1159.
9. S. Bouffard, Benoit and C. Larry, Nucl. Instr. and Meth. B105 (1995)1.
10. T. Venkatesan, L. Calcagno, B. S. Elman and G. Foti in Ion Beam Modification of Insulators, eds. P. Mazzaldi, G. W. Arnol(Elsevier1987)309.
11. P. Apel. Proceedings, Nucl Instr. and Meth. B105 (1995) 91.
12. S. A. Durrani and R. K. Bull, in: Solid State Nuclear Track Detection Pergamon, Oxford, (1987).
13. R. Spohr, Ion Tracks and Microtechnology (Vieweg, Braunschweig,1990).
14. R. Spohr, P. Armbruster and K. Schaupert, Radiat. Eff. and Defects in Solids 110 (1989)27.

15. J. P. Moliton, Thesis, Universite de Limoges (1980).

16. J. C. Vareille, J. L. Decossas, J. P. Moliton and J. L. Teyssier, J. Appl. Phys.56 (1984) 211.

17. A. Chambaudet, A. Bernas and J. Roncin, Radiat. Eff. 34 (1977) 57.

18. M. I. Chipara, I. Bunget, R. Georgescu, E. Georgescu and I. Vilcov, Nucl. Inst. and Meth. 209/210 (1983) 395.

19. K. Kimura, M. Ogawa, M. Matsui, T. Karasawa, M. Imamura, Y. Tabata and K. Oshima, J. Chem. Phys. 63 (1975) 1797.

20. C. J. Sofield, S. Sugden, C. J. Bedell, P. R. Graves and L. B. Bridwell Nucl.Inst. and Meth. B 67 (1992) 432.

21. E. Ferain and R. Legras, Nucl. Instr. and Meth. B 82 (1993) 359

22. Ferdinand Rodriquez "Principles of Polymer Systems". T M H editions (1974)

23. T.Venkatesan, S. R. Forrest, M. L. Kaplan, P. H. Schmidt, W. L. Murray, B. J. Wilkans, R. F. Raberts, L. Rupp and H. Shonborn Jr, J. Appl. Phys, 56 (1984) 2778.

24. M. I. Kaplan, S. R. Forrest , P. H. Schmidt and T. Venkatesan, J. Appl. phys. 55 (1984) 732.

25. Guang-Rou Wang et al. Nucl. Instr. and Meth. B 7/8 (1985) 497

26. T. Venkatesan, Nucl. Instr. and Meth. B 7/8 (1985).

27. A. Le Moel, J. P. Duraud, C. Darnez, E. Balanzat and C. M. Demanet Nucl. Instr. and Meth. B 32 (1988) 115.

28. T. M. Hall, A. Wagner and L. F. Thompson, J. Appl. phys. 53 (1982)3997

29. G. Dearnally, J. H. Freeman, R. S. Nelson and J. Stephen, Ion Implantation (North Holland 1973).

30. G. Dearnally, Rep. prog. phys. 2 (1969) 405.

31. J. W. Mayer and O. J Marsh, Applied Solid State Science (1969) 239.

32. J. W. Mayer L. Eriksson and J. H. Davies, Ion Implantation in Semiconductors (Academic press) 1970.

33. D. K. Avasthi, D. Kabiraj, A. Bhagwat, G. K. Mehta, V. D. Vankar, and S. B. Ogale, Nucl. Instr. and Meth. B 93 (1993) 480.

34. J. L 'Ecuyer, C. Brassard, C. Cardinal and B. Terreault, Nucl. Instr. and Meth. 149 (1987) 271.

35. R. F. Curl and R. E. Smalley, Scientific American, 33 (1991)

36. H. W. Kroto, J. R, Heath, S. C. O'Brien, R. F. Curl and R. E. Smalley. Nature 318 (1985)162.

37. W. Krätschmer, L. D' Lamb, K. Fostiropoulos and D. R. Huffman, Nature 347 (1990) 354.

38. W. Krätschmer, K. Fostiropoulous, and D. R. Huffman, Chem. Phys. Lett., 170 (1990)167.

39. D. S. Bethune, G. Meijer, W. C. Tang and H. J. Rosen. Chem. Phys. Lett. 174 (1990) 219.

40. R. E. Haufer, J. C. Onceicao, L. P. F. Chibante, Y. Chai, N. E. Byrne Flanagan, M. M. Haley. S. C. O'Brien , C. Pan, Z. Xiao, W. E. Billips, M. A. Ciufaline, R. H. Hauge, J. E. Margrave. L. J. Wilson. R. F. Curl and R. E. Smalley, J. Phys. Chem. 94 (1990) 8634.

41. H. Ajie , M. M Alvarez, S. J. Anz, R. D. Beck, F. Diederich, K. Fostiropolous, D. R. Huffman, W. Kratschmer, Y. Rubin, K. E. Schriver, D. Sensharma, R. I. Whetten, J. Phys. Chem 94 (1990) 8630.

42. J. P. Hare H. W. Kroto, and R. Taylor. Chem. Phys. Lett. 177 (1994) 394.

43. R. D. Johnson, G. Meijer, and D. S. Bethune, J. Am. Chem. 95 (1991) 9.

44. C. S. Yannoni, R. D. Johnson, G. Meijer, D. S. Bethune and J. R. Salem, J. Phys. Chem. 95 (1991) 9.

45. R. Tycko, R. C. Hadden, G. Dabbagh, S. H. Glarum, D. C. Douglas and A. M. Mujsec, J. Phys. Chem. 95 (1991) 518

46. M. R. Wasielewski, M. P. O'Neil, K. R. Lykke, M. J. Pellin and D. M. Gruen, J. Am. Chem. Soc. 113 (1991) 2774.

47. D. L. Lichtenberger, K. W. Nebesny, C. D. Ray, D. R. Huffman and L. D. Lamb, Chem. Phys. Lett. 176 (1991) 203.

48. S. H. Yang, C. L. Pettiette, J. Conceicao, O. Cheshnovsky and R. E. Smalley, Chem. Phys. Lett. 139 (1987) 233.

49. R. J. Wilson, G. Meijer, D. S. Bethune, R. D. Johnson, D. D. Chambliss, M. S. de Vries, H. E. Hunziker and H. R. Wendt, Nature 348 (1990) 621.

50. J. L. Wragg, J. E. Chamberlain, H. W. White, W. Kratschmer and D. R. Huffman, Nature 348 (1990) 623.

51. For an account of the plethora of unusual fullerene properties ranging from superconductivity to non-linear optical response ,see: The fullerenes eds. H. Kroto, J. Fisher and D. Cox (Pergamon, Oxford, 1993).

52. D. Koruga, S. hameroff, J. Withers, R. Loutfy and M. Sundarshan "Fullerene C_{60} History, Physics, Nanobiology ". Elsevier Science Publishers (1993).

53. L. T. Chadderton, D. Fink, H. Moeckel and K. K. Dwivedi, Rad. Eff. Def. in Solids, 1217 (1993a) 163.

54. H. Warner, J. Blocker, U. Goebel, B. Henschke, W. Bensch and Schloegel-Angew. Chem, 31 (1992) 868.

55. J. Hare and H. Kroto, Acc. Chem. Res. 25 (1992) 106.

56. F. P. Bundy, H. T. Hall, H. M. Strong and R.H. Wentorf, Nature, 176, (1995) 51.

57. J. Kastner, H. Kuzmany, L. Palmetshofer, P. Bauer and G. Stingeder., Nucl. Instr. and Meth. B 80/81 (1993) 1456.

58. C. S. Sunder, A. Bharathi, Y. Hariharan, J. Janaki, V. S. Sastry, T. S. Radhakrishnan, Solid State Commun, 84 (1992) 823.

59. M. E. Kozlov, M. Harabayashi, K. Noxaki, M. Tokumoto and H. Ihara, Appl. Phys. Lett. 66 (1995) 1199.

60. B. Dischler, A. Bubenzer and P. Koidl, Solid State Commun, 48 (1985) 105.

61. R. M. Papelo, A. Hallen, J. Eriksson, G. Brinkmalm, P. Demirev, P. Hakansson and B. U. R. Sundqvist, Nucl. Instr. and Meth. B 91 (1994) 124.

62. D. Fink, R. Kleet, P. Szimkoviak, J. Kastner, L. Palmetshofer, L. T Chadderton, L. Wang and H. Kuzmany, Nucl. Instr. and Meth. B 108 (1996) 114.

63. A. Itoh, H. Tsuchida, K. Miyabe, M. Imai and B. Imanishi, Nucl. Instr. and Meth. B 129 (1997) 363.

CHAPTER - II

INTERACTION OF ENERGETIC IONS WITH MATTER

2.0 Introduction:

The use of Heavy energetic ions has opened up many new challenging fields of research not only in nuclear and atomic physics, but also in other disciplines such as solid state physics, bio physics, radiomedicine and material research. Energetic ions have been used to induce modifications in materials, such modifications depend on the ion parameters and the target material and can often be tailored to obtain desired properties. For better understanding of ion beam modification of materials it is therefore necessary to understand the interaction of swift heavy ion the matter.

2.1 Energy loss:

When an energetic ion penetrate a material, they interact with the target atoms along their trajectories and deposit their kinetic energy E_i mainly through the electronic loss, S_e, and nuclear energy loss, S_n. The energy loss mechanism is described below.

Electronic energy loss :

This energy loss is important at high velocities E >>10 keV/u [1], where the ion velocity is close or higher than the Bohr velocity in the atom. Fast ions transfer their energies to the target electrons and promote some of the target atoms into excited and ionized states. The energy loss due to excitation and ionization is called electronic energy loss (S_e), also refereed to as linear energy transfer (LET) or inelastic energy loss.

Nuclear energy loss :

This is significant for projectiles at E ≤ 0.1 MeV/u [2]. Projectiles transfer their energies to the target nuclei by elastic collisions and consequently the target atom recoils and produces a cascade of collisions. As a result it produces damage and vacancies in the material. Energy loss due to this mechanism is called nuclear energy loss (S_n) or elastic energy loss.

Ions of energy greater than about 1 MeV lose energy mainly by Coulomb interactions with the orbital electrons of the target atoms and the nuclear collision losses are small compared to electronic energy losses. Nuclear collisions are important near the end of the range of the ions, where they get buried.

We may therefore write the total rate of energy loss in the form

$$(dE/dx)_{total} = (dE/dx)_{electronic} + (dE/dx)_{nuclear}$$

2.2 Range:

The charge particle loses its energy continuously while traversing through the stopping medium. Therefore to a first approximation it can be regarded as having a well defined range. The range of a charge particle is the distance before coming to rest. The reciprocal of the stopping power gives the distance traveled per unit energy loss. Therefore the range R(T) of a particle of kinetic energy T is the integral of this quantity down to zero energy

$$R(T) = \int_0^t (-dE/dx)^{-1} dE$$

where E = energy

and x = distance

When a swift heavy ions traverses through matter it exerts electromagnetic forces on the atomic electrons and delivers a part of its energy to the electrons. The imparted energy may be sufficient to knock an electron out thus ionizing it or it may only cause the atom to be in an excited state. A Heavy charged particle may lose only a small part of its energy in collision and therefore travels in a straight path.

Along the energetic ion trajectory a cylindrical concentrated zone of defects called latent track is formed in insulating materials beyond certain threshold of electronic energy loss. The diameter and length of the track depend on the type of ion and its energy, as well as on the structure and chemical composition of the irradiated material. The latent track consists of atomic displacements, broken molecular chains, free radicals and chemical decomposition products [3,4]. If the irradiation dose is high such that the tracks overlap, then the physical and chemical properties of the material can be altered to such an extent that it can be considered a new material with new properties. Detailed studies on the track, its size, form, structure and composition will throw a great deal of information on the material which is exposed to the ion.

2.3 Track formation model :

The track formation due to energetic heavy ion in solid is often studied by two well known models,

(i) Thermal Spike model

(ii) Coulomb explosion model

Thermal Spike model :

This model explains how an energetic ion can produce an intense heating region of the lattice. The thermal spike model is a two step thermodynamic

process that describes the fate of the energy initially deposited on the target electrons by the swift heavy ion. The first step is the evolution of the energy within the target electron gas and the second is the energy transfer between electrons and lattice atoms which is proportional to the difference between the electrons and lattice temperature via the constant g(electron phonon coupling constant). This energy transfer leads to a local temperature increase that can reach the melting temperature thus creating the so called latent track, after rapid quenching of the molten matter.

The temperature T as a function of time 't' and radial distance 'r' from the axis of the ion path is given by [5],

$$T(r,t) = T_o + \frac{Q}{4\pi C\rho D_t \exp\left(-r^2 / 4D_t\right)}$$

T_o = initial temperature of the lattice

c = is the heat capacity of the medium

ρ = mass density

D = diffusivity (D = K/ cρ)

K = Thermal conductivity

Q = Energy deposited per unit length

at time t = o

The thermal spike model has been successfully applied in metals [6] as well as insulators [7].

Coulomb's explosion model:

Fleischer et.al [8] have proposed a model for track formation which has been much favored and successfully applied in insulators. According to this model when an energetic ion passes through a solid it leaves a narrow region containing a high concentration of positive ions along its path, provided that the time for electron-positive ion recombination is large compared to the lattice vibration time (~ 10^{-13} sec). Therefore the long cylindrical channel of charged ions will produce and explode radially due to the conversion of electrostatic energy to the radial movement of atoms under the Coulomb force. Positive ions are thus driven into the interstitial positions. The subsequent processes include neutralization of the positive ions and relaxation of the surrounding lattice that produces a long range strain field. Fig. 2.3a. illustrates a typical picture of the model.

2.4 Interaction of energetic ions with polymers:

The energy loss by energetic ions in polymers produces a high energy density with final products structurally different from those generated by low energy ions as the linear energy transfer for heavy energetic ions is much

higher [9]. The damage process in polymer due to heavy energetic ions is different from that arising from classical irradiation process as like those of α, gamma rays and electrons. This is due to the fact that the deposition of energy or the electronic stopping power $(dE/dx)_e$ that is transferred to the polymer by energetic ions is very high. For typical energy of a few Mev/amu the $(dE/dx)_e$ range from C to Xe irradiations is 0.5 -10 keV/nm [10]. Further, though its energy is spread out by the δ- electrons radially from the core, half of the energy is well confined to a radius of a few nm.

At a low fluence a significant destruction of bonds takes place, which leads to rapid dissociation of the polymer giving rise to unsaturated fragments called "free radicals". Some of them which forms volatile species and degasses from the track [11]. Eventually when tracks overlap the dissociated polymer leads to a predominantly carbon containing film [10]

Polymers which are very sensitive to ionization radiation are a class of covalent insulators which are of high technological importance. Due to the high deposition of energy along the ion track by electronic processes, ion beams induce large modification on the molecular structure and hence properties of the polymer. The induced modifications of the polymer are found to be confined mainly in the ion tracks, whose sizes show characteristics related to the energy dissipating process. Such changes in the polymer properties have been determined by the ion fluence [12].

Crosslinking and carbonization is another LET effect that leads to dramatic modifications of polymer properties. For irradiation of polymers where the carbon atoms of the main chain are bound to the hydrogen atom, the scission of the CH bond results mostly in cross-linking and formation of double bonds, as has been reported for Polystyrene [13], in the formation of Phenyl groups into cyclodihexadienyl crosslinking. and Molecular fragmentation also induce large modifications of molecular weight distribution. The modification of electrical, electronic and optical properties of polymers have been achieved by ion beams. In some polymers enhanced electrical conductivity with increase in optical absorption [14-24] have been found. The changes in these properties have been achieved due to changes in the chemical structures caused by modification of the chemical bonding as the incoming ions scissors the polymer chains, break covalent bonds and promoting crosslinking to liberate certain volatile species. Liberation of gas during irradiation of Polymers has been reported and found to lead to irreversible changes in the molecular structure [11]. It is found that large amount of hydrogen gas gets evolved with a lower evolution of heavy molecules.

Heavy charged particle on passing through a polymer induces along its path the recombination of the degraded products through a complex process. Released electrons (δ - rays) trigger a number of ionizations. The Primary ionization and excitations occurs close to the ion trajectory in the track core

which is of a few nanometers. The energy deposited in this region can reach to several hundred eV/Å. This high energy deposition is capable of breaking any bond in the track as energy of carbon bonds are only a few eV. The 'track halo' caused by the secondary electrons through ionization and excitation can reach about 1mm from the core depending on the energy of projectile.

Thus heavy ion irradiation lead to atomic displacements, broken molecular chains, formation of free radicals, excited species and a series of secondary chemicals processes which gradually modify the polymer structure and its physical properties [25-32].

The nature of the damage depends on the type of polymer and its properties such as composition, molecular weight, mass and the energy of the ion and also on the environmental conditions during irradiation.

2.5 Interaction of energetic ions with Fullerene (C_{60})

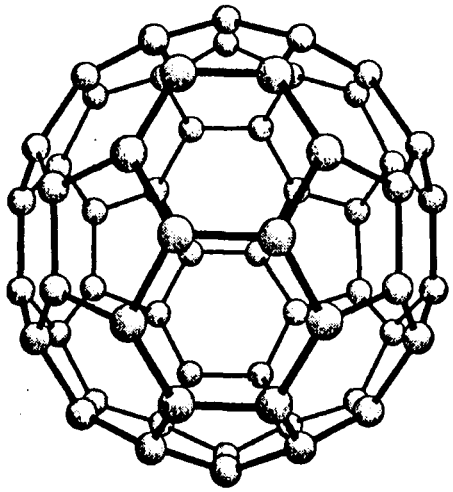

After the discovery of Buckminsterfullerene and its production in the laboratory, several workers have investigated on the modification on the material by the interaction of various energetic particles with different experimental parameters. It is observed that small changes in the fullerene charge distribution can destroy the molecule and once a fullerene molecule is destroyed it does not anneal back from the defects [33]. This makes the molecule different from other materials.

Fullerene destruction can take place by chemical attack [34], by thermal dissociation [35], by electronic photo excitation [36] or by energetic electrons or ions [37,38]. R. G. Musket et al. [39] have reported that for 100-200 keV proton irradiation a decrease in the IR absorption peaks with fluence was

observed. They have suggested the change of C_{60} to amorphous carbon, where C_{60} molecules explode in a kind of catastrophic event, instead of in a gradual process of destruction.

Electrical studies on 320 keV Xenon ions implantation are reported by Kalish et al.[40] who have also suggested a catastrophic model where each C_{60} cluster gets completely disintegrated by one ion impact to form 60 carbon atoms. The formation of amorphous carbon in C_{60} have also been observed by 30 keV K^+ implantation in C_{60} by Kastner et al.[41]. Steven Hobday et al. [42] investigated the interaction of 300-1000 eV Ar ions with C_{60} films and observed that the surface damage was more dominant in the film.

They also suggested that some C_{60} molecules escape from the surface owing to energy transfer from the collision of carbon atoms. The damage induced to the lattice of C_{60} causes polymerization of C_{60}. Bombardment of C_{60} thin films by H, He , C, and Ar ions at energies 160 -300 keV with doses ranging from $1x10^{12}$ to $5x10^{16}$ ions/cm^2 have been reported by L. Palmetshofer et al. [43]. Raman scattering studies suggested that destruction of C_{60} was mainly due to nuclear energy loss. Electronic energy loss contributed only to polymerization of fullerene.

So far there have been only a few studies reported on the interaction of heavy energetic ions on C_{60}. The process of energy transfer in the case of

heavy ions to the material is mainly through electronic rather than nuclear energy loss. Therefore the process of interaction leading to its modification is assumed to be different.

From the few published works done on MeV ion irradiation, it is reported that [44, 45] some C_{60} and other carbon clusters gets disrobed from the film due to electronic sputtering. The formation of clusters of carbon atoms have also been detected by the Swedish group [45,47] using plasma desorption mass spectroscopy (PDMS) set up. Papaleo et al. [48] investigated 55 MeV ion irradiation on C_{60} using Raman and PDMS. They observed that the modification starts around $4x10^{11}$ ions/cm^2 and saturates at around $3x10^{12}$ ions/cm^2. Fragmentation and destruction of C_{60} was found to be accompanied by cross-linking between the C_{60} molecules. The damage of fullerene by energetic ions leading to C_{60} desorbtion and destruction has been proposed by Fink et al.[49, 50] to be due to nuclear energy loss which dominates even if the electronic energy loss value is more than a hundred fold of that of nuclear loss. It is proposed that the destruction by electronic loss can be dominant at only in the specific case of high energy heavy ions.

Referenes:

1. D. K. Avasthi, Vacuum /Vacuum 47/ number 11/ (1996) 1249.
2. S. Klaumiinza and A. Gutzmann, Nuleonika 39 no 1-2 (1994) 125.
3. T. Steckenreiter, H. Fuess, M. Stamn and C. Trautmann. Nucl. Instr. Meth. B105 (1995) 200.
4. T. Venkatesan, L. Calgano, B. S. Elman and G. Foli, in: Ion Beam Modification of Insulators, eds. P. Mazzaldi, G. W. Arnold (Elsevier 1987) 309.
5. K. Izui, J. Phys. Soc, Jpn. 20 (1965) 915.
6. Z. G. Wang, Ch. Dufour, E. Paumir and M. Toulemonde. J. Phys. Cond. Matt. 6(1994) 6733; 7(1995)2525.
7. A. Meftah, F. Brisard, J. M. Costantini, E. Dooryhee, m. Hague-Ali, M. Y. Hervieu, J. P. Stoquert, F. Studer and M. Toulemonde, Phy. Rev. B 49(1992) 12457.
8. R. L. Fleischer, P. B. Price and R. M. Walker. The ion explosion spike mechanism for formation of charged particle tracks in solids: J. App. Phys. (1965) 3645.
9. L. Calcagno and G. Foti: Nucl. Instr. Meth. B 59/60 (1991) 1153.
10. E. Balanzai, S. Bouffard, A. Le Moel and N. Betz. Nucl. Instr.Meth. B91(1994) 140.
11. A. Schmoldt, L. T. Chaddertn and D. Fink, Rad. Eff. Def. Solids 128(1994) 277.

12. T. Venkatesan, L. Calcagno, B. S. Elman and G. Foti in Ion Beam Modification of Materials 2, eds. P. Mazzaldi and G. W. Arnold (Elseveir, Amsterdam, 1987) 312.

13. L. Wall and D. Brown, J. Phys. Chem. 61(1957) 129.

14. A. L. Evelyn, D. Ila, R. L. Zimmerman, K. Bhat, D. B. Porker, D. K. Hensley. Nucl. Instr. and Meth. B 127/128 (1997) 694.

15. D. Ila, A. L. Evelyn and G. M. Jenkins, Nucl. Instr. and Meth. B. 91 (1994) 580.

16. D. Ila, A. L. Evelyn and G. M. Jenkins, Mat. Res. Soc. Symp Proc. 321 (1994) 441.

17. A. L. Evelyn, D. Ila and G. M. Jenkins, Nucl. Instr. and Meth. B 85 (1994) 861.

18. T. Vekatesan, R. Levi, T. C. Banwell, T. Tombrello, M. Nicolet, R. Hamm and A. E. Meixner, in Ion Beam process in Advanced Elecronic Materials and Device Technology, eds. F. H. Elsen, T. W. Sigmon and B. R. Appleton (Mat. Res, Soc. Symp. Proc) 45, Pittsburg, PA (1985) 189.

19. C. J. Sofield, S. Sugden, C. J. Bedell, P. R. Graves and L. B. Bridwell, Nucl. Instr. and Meth. B 67 (1992) 432.

20. Y. Q. Wang, R. E. Giedd and L. B. Bridwell, Nudl. Instr. and Meth. B 79 (1993) 659.

21. M. S. Dresselhaus, B. Wasserman and G. E. Wnek, Mat. Res. Soc. Symp. Proc. 27 (1983) 413.

22. L. Calcagno and G. Foti, Nucl. Instr and Meth. B 59/60 (1991) 1153.

23. Y. Wang, S. S. Mohite, L. B. Bridewell, R. E. Giedd and C. J. Schofield, J. Mat. Res. 8 (1993) 388.

24. G. M. Jenkins, D. Ila and E. K. Williams, in Polymer/Inorganic interfaces, eds. R. L. Opia, F. J. Boerio and A. W. Czanderna, Mat. Res. Soc. Symp. Proc. 304. Pittsburg, PA, (1993)173.

25. P. Mazzaldi and G. W. Arnold(eds), Ion Beam Modification of Insulators, vol 2 (Elsevier, Amsterdam, 1987).

26. L. Calcagno, G. Canpagini and G. Foti, Nucl. Inst. and Meth. B65 (1992) 413.

27. L. Calcogno, P. Musumeci, R. Percolla, G. Foti, Nucl. Instr. and Meth. B91 (1994) 461.

28. T. Vankatesan, L. Calcagno, B. S. Elman and G. Foti in Ion beam Modification of insulators, eds P. Mazzaldi and G. W. Arnold(Elsevier, Amsterdam 1987).

29. L. Calcagno, G. Compagnini, G. Foti, Nucl. Instr. and Meth. B65(1992) 413.

30. E. Balanzal, N. Betz, S. Bouffand, Nucl. Instr. and Meth. B105(1995) 46.

31. N. Betz, A. Le Mod, E. Balanzat, J. M. Ramillon, J. Lamotte, J. F. Gallas, G. Jaskierowitez, J. Polymer sci. Polym. Phys. Ed. B32(1994) 1493.

32. T. Steckenreiter, E. Balanzat, H. Fuess, and C. Trautmann, Nucl. Instr. and Meth. B131 (1997) 159.

33. D. Fink ,W. H.Chung, K. K. Dweivedi, S. Ghosh, R. Klett, B. Stritzker, A. Richter, and L. T. Chadderton, Rad. Eff. Def. in Solids, 143 (1998) 311.

34. Y. Matsuo, T. Nakajima, and B. Kasamatsu, J. Flourine Chem. 78 (1996) 7.

35. S. Henke, B. Rauschenback, and B. Strizker, Mat. Res. Soc. Symp. Proc.359 (1995)405.

36. P. Milani, M. Manfredini, and Bottani, Synthetic Metals 77 (1996)81.

37. D. Fink, R. Klett, P. Szimkoviak, J. Kastner, L. Palmetshofer, L. T. Chadderton, L.Wang, and H. Kuzmany, Nucl. Inst. and Meth. B 108 (1996) 114.

38. R. M. Papaleo, R. Herino, A. Hallen, P. Demirev and B. U. R.Sundquist, Nucl. Instr. Meth. B 116 (1996) 274.

39. R. G. Musket, R. A. Hawley-Fedder, W. L. Bell, Rad. Eff and defects in Solids (1991) 118.

40. R. Kalish, A. Samoiloff, A..Haffman, C. Uzan-Saguy, Phys. Rev. B48 (1993) 18235.

41. J. Kastner, H. Kuzmany, L. Palmetshofer and P. Baur, Nucl. Instr. Meth. B 80/81(1993)1456.

42. S. Hobday, R. Smith, U. Gibson, and A. Richter. Radiat. Effects and Defects in Solids, Vol. 142 (1997) 301.

43. L. Palmetshofer, J. Kastner, nucl. Instr. and Meth., B 96 (1996) 343

44. D. K. Avasthi, Vacuum, Volume 47 (1996) 1249.

45. R. E. Johnson, B. U. Sundquist, Phys Today, 45 (1992) 28.

46. P. Demirer, G. Brimkmasna, D. Fenjo, P. Hakansson and B. U. R. Sundqust, Int. J. Mass Spectrum Ion process, 41 (1991) 111.

47. G. Brinkmalm, P. Hakansson, J. Kjellberg, P. Demirev, B. U. R. Sundquist and W. Entt. Int. J. Mass Spectrum Ion Process, 114 (1992) 183.

48. R. M. Papaleo, A. Hallen, J. Eriksson, G. Brinkmalm, P. Demirev, P. H. Kansson, B. U. R. Sundquist, Nucl. Instr. Meth. B 124 (1994) 1391.

49. D. Fink, L. T. Chadderton, J. Vacik, V. Hnatowiez, F. C. Zawislak, M. Behar and P. L. Grande, Nucl. Instr and Meth. B 113 (1996) 244.

50. D. Fink, R. Klett, P. Szimkoviak, J. Kastner, L. Palmetshofer, L. T. Chadderton, L. Wang and H. Kuzmany, Nucl. Instr and Meth B108 (1996)114.

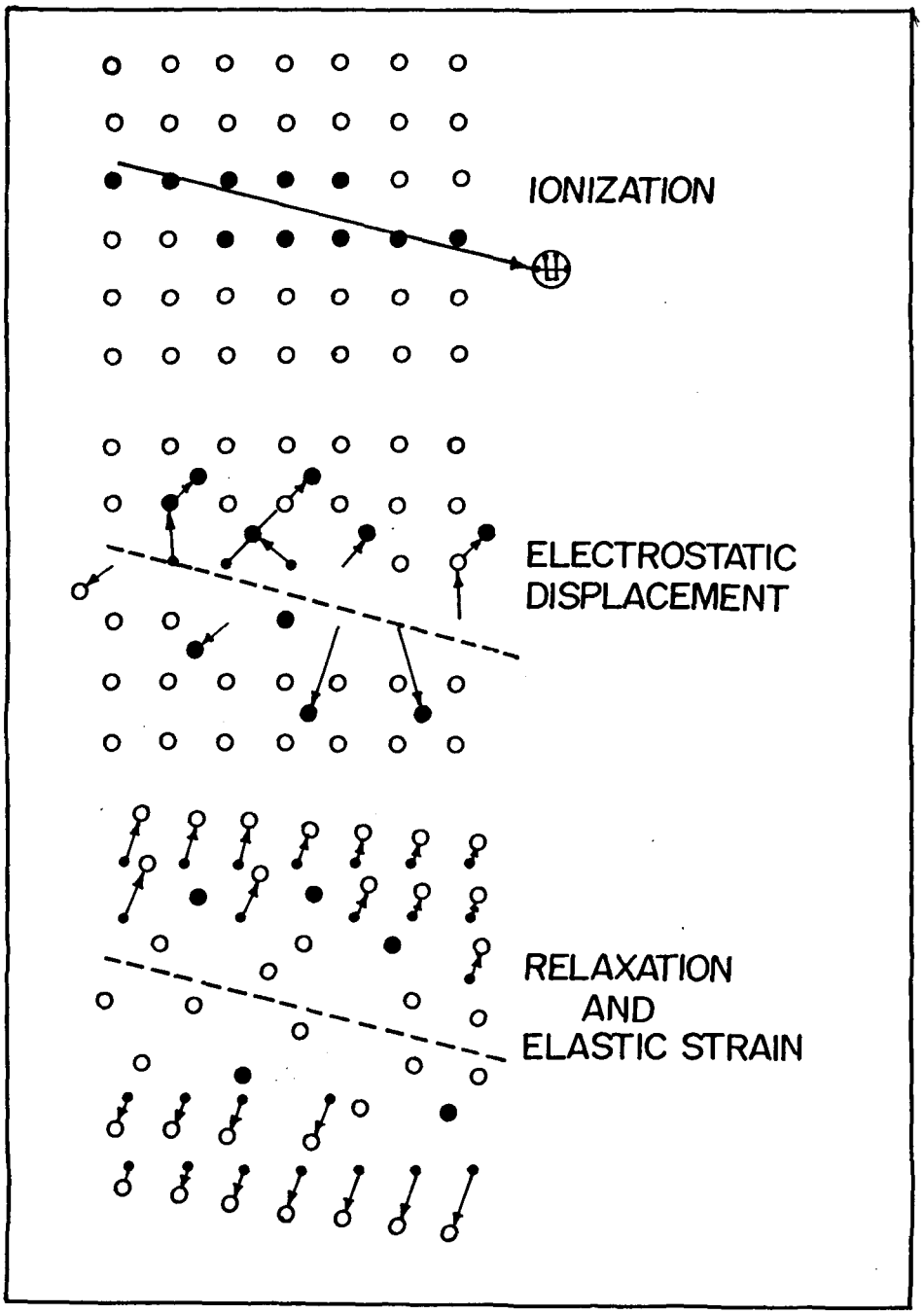

Fig. 2.3a. The ion explosion spike mechanism for track formation

CHAPTER - III

3.0 IRRADIATION PARAMETERS AND EXPERIMENTAL TECHNIQUES

In this chapter we present a brief discussion of the heavy ion beam accelerator which was utilized to irradiate the samples, using various ions at different energies. Sample preparation, characterization and measurement techniques have also been presented.

3.1 Operation of Pelletron Accelerator:

The accelerator installed at NSC New Delhi is a 15UD pelletron, which is a 15 MV Tandem Van De Graff machine. It provides ion beams of almost all elements across the periodic table providing energies in the range of ~ 50 MeV to 250 MeV.

The Accelerator is installed with a vertical configuration in a stain less steel tank which is 26.5m long and 5.5m in diameter. It is filled with an insulating gas of SF_6 at high pressure (6-7 atmosphere). The high voltage terminal which is inside the tank can be varied from 4 MV to 15 MV. A potential gradient is maintained through the accelerating tubes from the high voltage to ground at the top and bottom of the tank. The negative ions which are

produced in the ion source are injected into the accelerator and accelerated towards the high voltage terminal. Inside the terminal the electrons are stripped off from the negative ions, to become positive ions. The positive ions are then further accelerated to the bottom of the tank at ground potential by repulsive force. As a result, the ions emerges out with an energy given by

$$E = V (q+1) MeV + E_{inj}.$$

where V is the terminal potential (in MV) and q is the number of positive charges on the ion after stripping, E_{inj} is the energy of the ion from the ion source bench in the pre-acceleration region. E_{inj} can have maximum energy upto 400 keV. The high energy ions are then analyzed to the required energy by selecting a charge state of the ions with the help of a 90° bending magnet known as analyzer magnet. Depending on the mass, energy and charge of the ion, the magnetic field of this magnet can be set to select that particular ion of required energy. For ion beam having mass M, energy E and charge state q the analyzing magnetic field required for selection of the beam is governed by the relation $B = K(M E)/q^2$, where K is constant. Thus depending on the mass, energy and charge of the ion, the magnetic field of this magnet can be set to select ions of required energy. The selected ions are then directed to the desired experimental area with the help of the switching magnet which can deflect the beam into any of the beam lines in the beam Hall. Fig 3.1.1a shows the basic principle of a Tandem Accelerator. Fig. 3.1.1b shows the schematic of the pelletron at NSC, New Delhi. The accelerator is controlled by computer and is operated from the control room.

3.1. 2 The Vacuum System:

A high vacuum is very much necessary along its entire path, for the ions to have the least possible encounter with air molecules, so that it avoids scattering and energy loss or recombination. The Pelletron at NSC has different types of vacuum pumps which are used at different locations to give high vacuum from the source to the experimental area. The pressure is maintained at 10^{-8} torr or below in the entire accelerator.

The Pelletron at NSC uses turbo molecular pumps at the ion source for obtaining vacuum of 10^{-8} torr. In the beam line and most of the places the ion pump-getter pump combination is used. In the experimental areas where the present work is performed, it requires usually vacuum of 10^{-6} to 10^{-7} torr. Diffusion pumps with liquid nitrogen traps are employed, at the high vacuum chamber used for the experiment.

3.1. 3 Vacuum Chambers For Experiment:

The targets of C_{60} thin films and some of the polymer samples which were used in our study were irradiated in the material science high vacuum chamber, which is installed at +15° of the Pelletron accelerator. The polymer samples which were used to study Hydrogen loss on irradiation were performed using the General Scattering Chamber (GPSC).

3.1.3a General Scattering Chamber:

The general scattering chamber is of 1.5m in diameter and of 0.6m in height. It is equipped with a target ladder and viewing ports at -90° , -150° , 60° and 120° . It has two detector arms with provision for mounting five detectors at the spacing of 6° on each arm. The detector arm and the target ladder which has a provision for accommodating six targets can be controlled by remote. The sample mounting ladder can be moved up, down and rotated, and the detector mounting tables can be rotated around the ladder with 0.05° precision. The vacuum inside the chamber during the experiment was $1x10^{-6}$ mbar using a Difstack pump having a speed of 2000 l/s.

3.1.3b Material Science Target Chamber:

The high vacuum chamber (38cm diameter) has a facility for temperature controlled liquid nitrogen cooled multiple sample holders having provision for linear movement of 120mm and a rotation of 360°. A vacuum of 10^{-7} mbar is maintained by using a diffusion pumping system fitted with a LN_2 trap. A remote controlled target holder can be positioned perpendicular to the beam line for irradiation. Various samples can be irradiated in an experiment using bellow sealed linear movement of the holder by 140mm. The sample holder can also be rotated by 360° without breaking the vacuum. It is also equipped with electrical and optical feed through for on-line or in-situ studies.

3.2 Sample Preparation Of C_{60} Thin Films:

Thin films of C_{60} (350 -500nm) for irradiation were prepared by resistive heating method at NSC.. The C_{60} powder(99.9%) were obtained from Sterm chemicals INC, U.S. First Weighed C_{60} powder of 40 -50mg was made into a pellet. The pellet was put into a Tantalum boat and placed inside the evaporating vacuum chamber. The metal boat was kept attached to copper stripes which are connected for current supply through electrical feedthroughs. Before supplying current for evaporation, the evaporating chamber was made to achieve to a vacuum of 10^{-6} torr with the help of diffusion pump and LN_2 trap rotary pump. On reaching the desired vacuum which is observed by the penning gauge, current was supplied and the temperature was raised to 400 500 °C for evaporation. The sublimated C_{60} vapors were then made to condense on float glasses (1x1cm^2) substrates which were kept at ~20cm from the sublimation source. The thickness of the films were measured with the help of quartz crystal thickness monitor arrangement from outside. The block diagram of the evaporator is shown in Fig 3.2a.

3.3. CHARACTERIZATION TECHNIQUES.

3.3.1. Elastic Recoil Detection Analysis (ERDA):

ERDA is a technique for detecting the recoils of light elements from the target on bombardment using heavy ions. The H release as a result of irradiation of 100 MeV Ag ions on Polyvinylidene fluoride (PVDF), 110 MeV Ni ions on Polystyrene (PS), Polymethyl methacrylate (PMMA) and Polyvinylidene fluoride (PVDF), 85 MeV Ni ions on polypropylene (PP) and Polymide (PI) and 50 MeV Ni ions on Polypropylene and Polymide were studied using the non-destructive analytical nuclear technique (ERDA). This technique works on the principle as given below.

When an incident projectile ion strikes a target atom which is at rest, the incident ion imparts energy to the target atom and the target atom gets scattered at an angle θ. The target atom then recoils with an energy E_r. The energy E_r is given by the expression using the law of conservation of energy and momentum

$$E_r = \frac{4 m_p m_t E_p \cos^2 \phi}{\left(m_p + m_t\right)^2}$$

Where m_p = mass of the incident ion

m_t = mass of the target ion

E_p = energy of the incident

and ϕ = Recoil angle of the target atoms

Under given experimental conditions the mass m_p and its energy E_p and recoil angles remain fixed. Atoms having different masses will have different recoil energies. Thus the masses of different atoms can be identified from the energy spectrum.

The quantitative estimate of an element in the sample can be made by measuring the number of recoils Y detected for a given dose of projectiles. The number of atoms/cm^2 of an element is given by the relation

$$N_t = \frac{Y \sin\alpha}{N_p (d\sigma / d\Omega)\Omega}$$

Where N_p = no of incident ions on the sample

Ω = solid angle substented by the detector

α = Tilt of the sample with respect to the beam direction.

$d\sigma/d\Omega$ = Rutherford recoil cross-section given by

$$(d\sigma / d\Omega) = \left[\frac{Z_p Z_t e^2 (m_p + m_t)}{2 E_p m_t} \right]^2 \frac{1}{\cos^3 \phi}$$

where Z_p = atomic number of the projectile

Z_t = atomic number of the target atoms.

All the experiments were performed using the 15UD NSC pelletron. Ion beams of 100 MeV ^{107}Ag, 100 and 85 MeV ^{58}Ni and 50 MeV ^{28}Si were used. The beam current in all the experiments were less than one particle nanoampere (equivalent to 6.25×10^9 ions/s). The schematic of the experimental set up used in the present study is shown in Fig. 3.3.1a. The recoils from the film were detected in a silicon surface barrier detector with a depletion depth of 1 mm and kept at 45° with respect to the beam direction. A polypropylene stopper of 60 μm was kept before the detector to stop all the recoils except for hydrogen. The polymer foils used in the present experiment had thickness between 20 and 30 μm. The ion range in each case was always larger than the thickness of the film used. All the irradiations were carried out at room temperature. The energy resolution of the surface barrier detector used was about 30 keV for 5.48 MeV alpha particles.

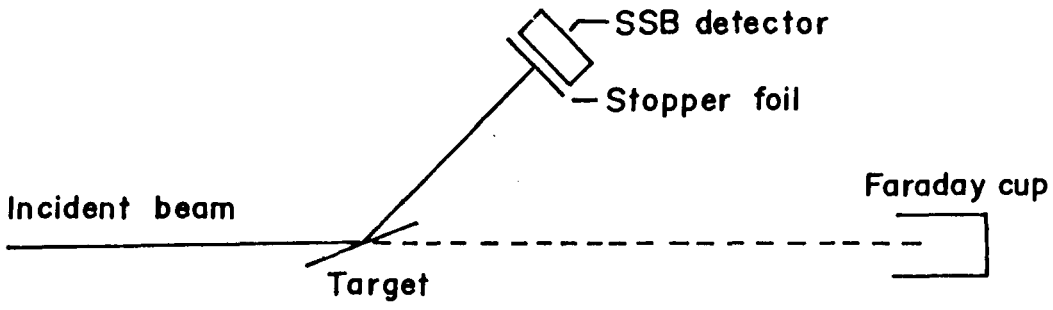

Fig. 3.3.1a. Experiment set up used in the present work

3.3.2 Differential Scanning Calorimeter (DSC).

The thermal analysis on the melting behavior and change in crystallinity of a polymer polyethylene terephthalate(PET) of thickness 13μm irradiated with 180 MeV Ag ion with ion fluence ranging from 1×10^{11} to 1×10^{12} ions/cm^2 was examined using Differential Scanning Calorimetry (DSC) Dupont modulated calorimeter (DSC 2910) at the Inter University Consortium IUC, Indore. This technique works on enthalpy change method in which the difference in energy absorbed by the sample and that by the reference material is measured as a function of temperature while both are subjected to a controlled temperature program for heating thin film of PET of mass (.5mg) was crimped in an aluminum pan and placed in the DSC cell along with an empty aluminum crimped pan as the reference. The thermographs showing heat flow (mW) versus temperature T, were recorded in the temperature range 230 -270 ^{0}C at a heating rate of 40 ^{0}C/min. The melting temperature of the pristine and the irradiated samples were then recorded.

3.3.3 X - Ray Diffraction.

Modification induced in the sample due to irradiation triggers a complex state which presents new bulk properties. It is observed that irradiation has a

large effect on the crystallinity which finally leads to carbonization and graphitization along the track of the ions. The XRD technique can give vital information about the modification of the structure. Therefore XRD investigation has been employed in our work to study the percentage loss of the initial crystallinity before and after irradiation.

The wavelength of x - rays is typically of the order of 0.1 nm, and so they will be diffracted or scattered by the crystals which have geometrically periodic arrangements of atoms, separated by distance comparable to the x - ray wavelengths. X-rays scattered from the atoms or molecules interfere constructively or destructively. For constructive interference it must satisfy the Brag's equation

$2d \sin\theta = n\lambda$

where n = 1, 2, 3-----

d = interplanar spacing

θ = x-ray incident angle

The X-ray beam incident at a glancing angle θ is scattered in random directions. Constructive interference takes place only between the scattered waves which are parallel and have a path difference of $n\lambda$, where λ is the x-ray wavelength. From the diffraction pattern the crystal parameters as well as the structure of the crystals can be deduced.

In our present work C_{60} powder, pellet and thin films of ~500nm were characterized using x-ray diffraction. X-ray diffraction patterns were recorded using Cu-K_α (wavelength λ = 1.54Å) from Semen's diffractometer D 5000 at IUC Indore. The entrance slit was of 0.2mm and the step time and step size was set at 3s and .020mm respectively. The 2θ values for all the samples were recorded from 5° to 90°.

3.3.4. Fourier Transformed Infra-red Spectroscopy (FTIR):

The frequencies of vibration of atoms and molecules fall in the infra-red range (5000-400cm^{-1}). Therefore investigation of the sample by IR absorption technique can provide enough information on the molecules under study. When IR radiation is passed through a sample certain frequencies of the IR are absorbed by the sample which correspond to vibrational changes in the molecule. This occurs for the simple reason that the incident radiation induces an oscillating dipole moment in the molecule with frequency equal to the frequency of the radiation. The secondary radiation emitted by the oscillating dipole then interacts with the oscillating electric field of the electromagnetic radiation resulting an absorption on resonance. Thus the absorption IR spectra of the molecule gives information on the chemical composition, chain structure, degree of branching and type of end groups. Fig. 3.3.4a. shows a diagram of a Fourier transform spectrometer.

In the present work, heavy ion irradiated and unirradiated polymers and C_{60} thin films have been investigated using IR technique to identify the

vibrational bands of chemical modification that may have been formed by the interaction with energetic ions. Commercial polymer films of i) Polyethylene-terephthalate (PET) 13μm, ii) Polyvinylydene diflouride (PVDF) 9μm, produced by Good-Fellow Industries, UK were used for the study.

The polymer samples were irradiated at the 15 UD pelletron at NSC, New Delhi. The thin films of PVDF were irradiated with 180 MeV Ag and 95 MeV Ni ions. The applied fluence was in the range from 1×10^{10} to 5×10^{11}ions/cm^2 for 180 MeV Ag ions and 1×10^{11} to 5×10^{13}ions/cm^2 for 95 MeV Ni ions. PET samples were irradiated by 180 MeV Ag ion with ion fluence ranging from 1×10^{11} to 1×10^{12} ions/cm^2.

Thin films (350 -500nm) of C_{60} evaporated on silicon(100) wafer of 0.5mm were also irradiated using 180 MeV Ag ions of fluence 10^9 -10^{12} ions/cm^2. All the FT - IR spectra of the samples were recorded in the transmission mode using model NICOLET, IMPACT 410, at NEHU Shillong.

3.3.5. Raman Scattering:

Inelastic scattering of photons by matter is known as Raman scattering. When a visible light of low energy interacts with a molecule, it can be scattered in one of three ways. It can be scattered elastically from the matter retaining its energy or it can be inelastically scattered by either giving or taking energy from the molecule. Photons which undergoes elastic collision

energy give rise to Stokes scattering, while photons which undergoes inelastic collision can give rise to anti-Stokes scattering. Anti-Stokes emission is weaker than Stokes emission due to population difference between the ground state and the excited energy levels.

In Raman spectroscopy the electric field of the intense incident light polarizes the molecule. This induces a dipole moment in the molecule which then interacts with the light. This may occur irrespective of whether a molecule has a permanent dipole moment or not. The magnitude of this effect is determined by how easily the sample is polarized and occurs for those molecules with an anisotropic polarizability.

When a system in a ground state interacts with an incident light of frequency n , it makes an upward transition from its lower energy E_i to an upper level E_f [Fig. 3.3.5a] by gaining energy difference of $\Delta E = E_f - E_i$ from the incident radiation. In the process a small proportion of the incident light is scattered with decreased frequency ν_s (Stokes radiation). On the other hand the interaction of incident radiation with the system in the excited state may cause a downward transition emitting light of increased frequency ν_a (anti-stokes radiation). The transition may be considered to occur in two stages, from the initial state to a " Virtual state " denoted by V which is not a true stationary state, and then to a different state.

In a typical experiment a monochromatic light in the visible region is allowed to be incident on the sample. The irradiation that is scattered

perpendicular to the beam is then gathered by collecting optics and is directed to a dispersing system (usually a double monochromator), which selects the scattered light of particular frequency range. At the exit port of the monochromator, the Raman spectrum displays in the form of a series of faint lines. These signals are detected by a photomultiplier tube and recorded after electronic processing in a chart recorder. Fig. 3.3.5b shows schematic diagram of a Raman instrument. The shifts in frequency of the scattered radiation from the incident radiation are small, and the intensity is also low. Therefore the incident radiation must be very monochromatic for the shifts to be observed. Lasers are ideal for both respects and have entirely displaced the mercury arc used originally.

In our work, thin films of C_{60} of thickness 500nm were deposited on float glass, substrates by evaporation using resistive heating set up in a vacuum better than $1x10^{-6}$ torr. The samples were irradiated by 189 MeV Ag, 110 MeV Ni, and 50 MeV Si ions with fluence ranging from $9x10^{10}$ to $1.8x10^{12}$ ions/cm^2 from the 15 UD Pelletron at NSC. Areas of 1cm^2 of the targets were bombarded to the desired fluences with a beam current less than 2pnA. The vacuum in the experimental chamber was better than $2x10^{-6}$ torr. Raman and Photoluminescence(PL) measurements were done at ambient and also in vacuum (10^{-3} mbar) where ever required in backscattering geometry at room temperature. The backscattered light was passed through the double monochromator U1000 (Jobin Yvon) with R943-002 photomultiplier tube (Hamamatsu) in photon counting mode. Raman spectra obtained over the range 1450 -1500 cm^{-1} by using 5145 Å excitation of Argon ion laser with

line focus of 2.5mm x 50μ. The laser power used for Raman scattering and PL was 1mW and 5mW (4880Å) respectively. Rutherford back scattering(RBS) measurements with 2 MeV α- particles using Van de graff accelerator at I.T.T Kanpur, has been performed for determination of oxygen content in the pristine thin films of C_{60}

3.3.6 Photoluminescence:

When a molecule is raised to an excited state by a radiation of a certain frequency, the molecule may come back to its initial state with an emission of radiation of a lower frequency than that of the incident. This phenomenon is known as "LUMINESCENCE". In fluorescence the emission of the radiation stops as the incident light is removed, whereas in phosphorescence emission persists longer time after the incident is removed. If a molecule in a ground state (E_o) absorbs an energy hν which leads to the promotion of one electron from the ground state to one of the vibrational sub levels of the first excited state (singlet state) it rapidly decays by a radiationless process to the lowest vibrational sublevels of E_1. The electron then decays to the ground state by emission of radiation ($h\nu_f$) which is of lower energy.

An alternative path involves the loss of energy from the singlet state (E_1) to the triplet state (T_1) by non radiative mechanism. From this level it can return to the ground state (E_o) by emitting the radiation $h\nu_p$, the phosphorescent radiation. Phosphorescence has always longer wavelength than fluorescence.

Since Triplet states being more stable than singlet states it is longer lived and thus survives even after the exciting radiation is removed.

In our work, photoluminescence study was utilized to analyze the emission of radiation from the decay of defects that have been excited. From the defects introduced by irradiation on the samples the emission of optical radiation and the wavelength dependence of the emitted radiation can be analyzed to determine the energy levels involved.

3.3.7 Atomic Force Microscopy (AFM):

To see the changes on the surface topology on irradiation of C_{60} thin films at different fluences by 180 MeV Ag ion, an atomic force microscope (AFM) was employed. The measurements were done at I. U. C (Indore) using the Digital Instruments, Nanoscope E, in the contact mode.

In AFM the cantilever or the microscopic force sensor is the most important element. The cantilever is formed by one or more beams of silicon nitride that is 100 to 50 μm long and about 0.5 to 5 μm thick. The sharp tip at the end of the cantilever is used to sense a force between the sample and the tip. For topographic imaging, the probe is brought into continuous or intermittent contact with the sample and raster-scanned over the surface. Piezoelectric scanners are used to generate the precision motion needed to generate topographic images.

Scanning the AFM cantilever over a sample surface and recording the deflection of the cantilever, the local height of the sample is measured. Three dimensional topographical maps of the surface are then constructed by plotting the local height versus horizontal probe tip position. A well built scanner motion can generate stable motion on a scale below one Angstrom. Fig 3.3.7a. shows a schematic diagram of an AFM instrument.

References

1. G. K. Mehta and A. P. Patro, Nucl. Instr. Meth. A268 (1998) 334.

2. The 16-MV Pelletron Accelerator at NSC, Physics Education, october-December 1994.

3. D. K. Avasthi, A. Tripathi, D. Kabiraj, S. Venkataramanan and S. K. Datta, Internal report NSC/TR/DKA/ 92/16.

4. D. K. Avasthi, Bull Mater. Sci. Vol. 19. No. 1, February (1996) 3.

5. Crystals X-rays and proteins, D. Sherwood, IBM Press Roman (1976).

6. Raman spectroscopy, Herman A. Szymanski, Plenum Press, New York, London(1970).

7. Fundamentals of molecular spectroscopy, C. N. Banwell and E. M.cash, Tata Mcgraw -Hill (1995)

8. Physical Chemistry, P. W. Atkins, Oxford University Press (1994).

9. Atomic Force Microscope. From M/S Digital Instruments USA. (Model Nano-scope E).

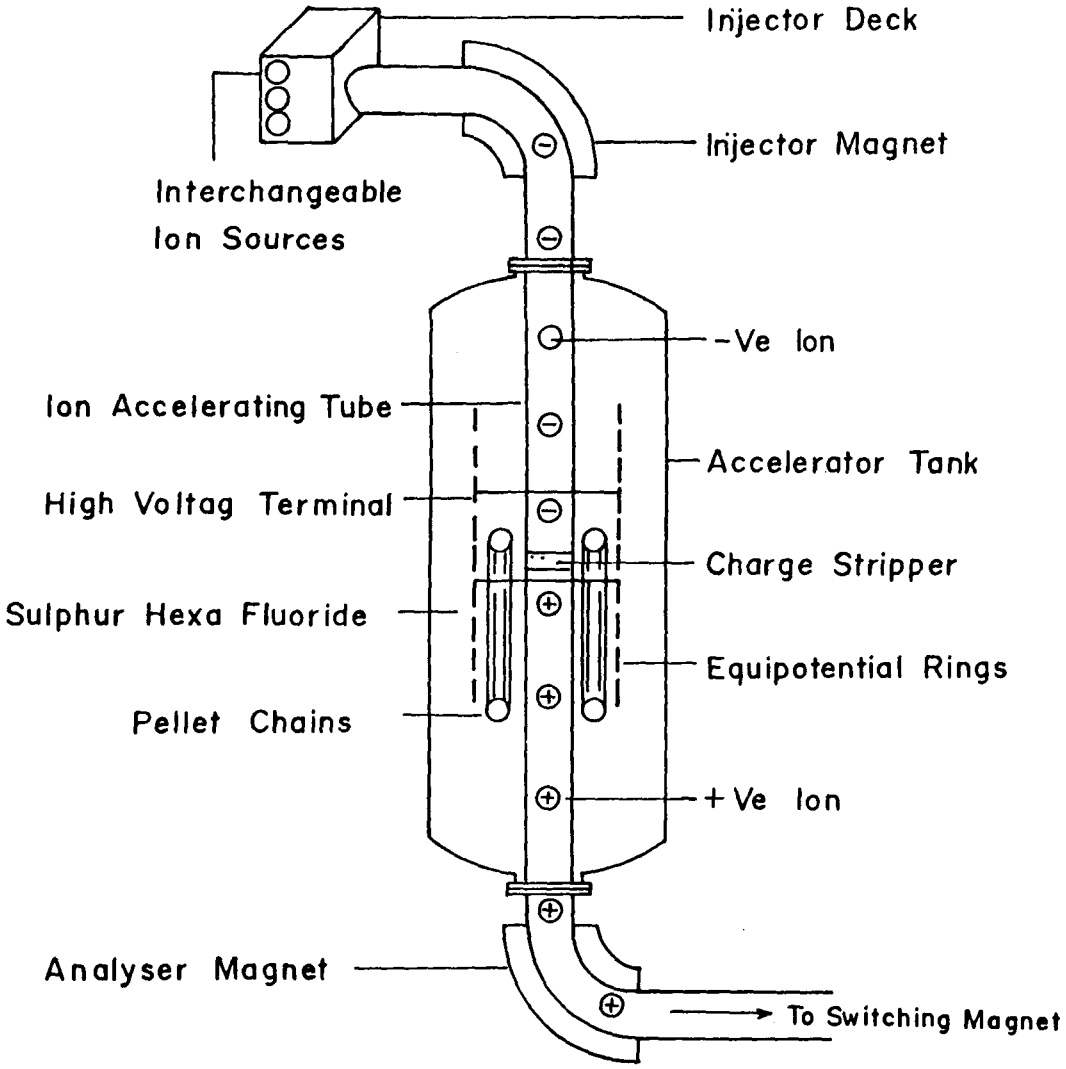

Fig. 3.1.1a. A schematic diagram showing the basic principle of acceleration in Pelletron.

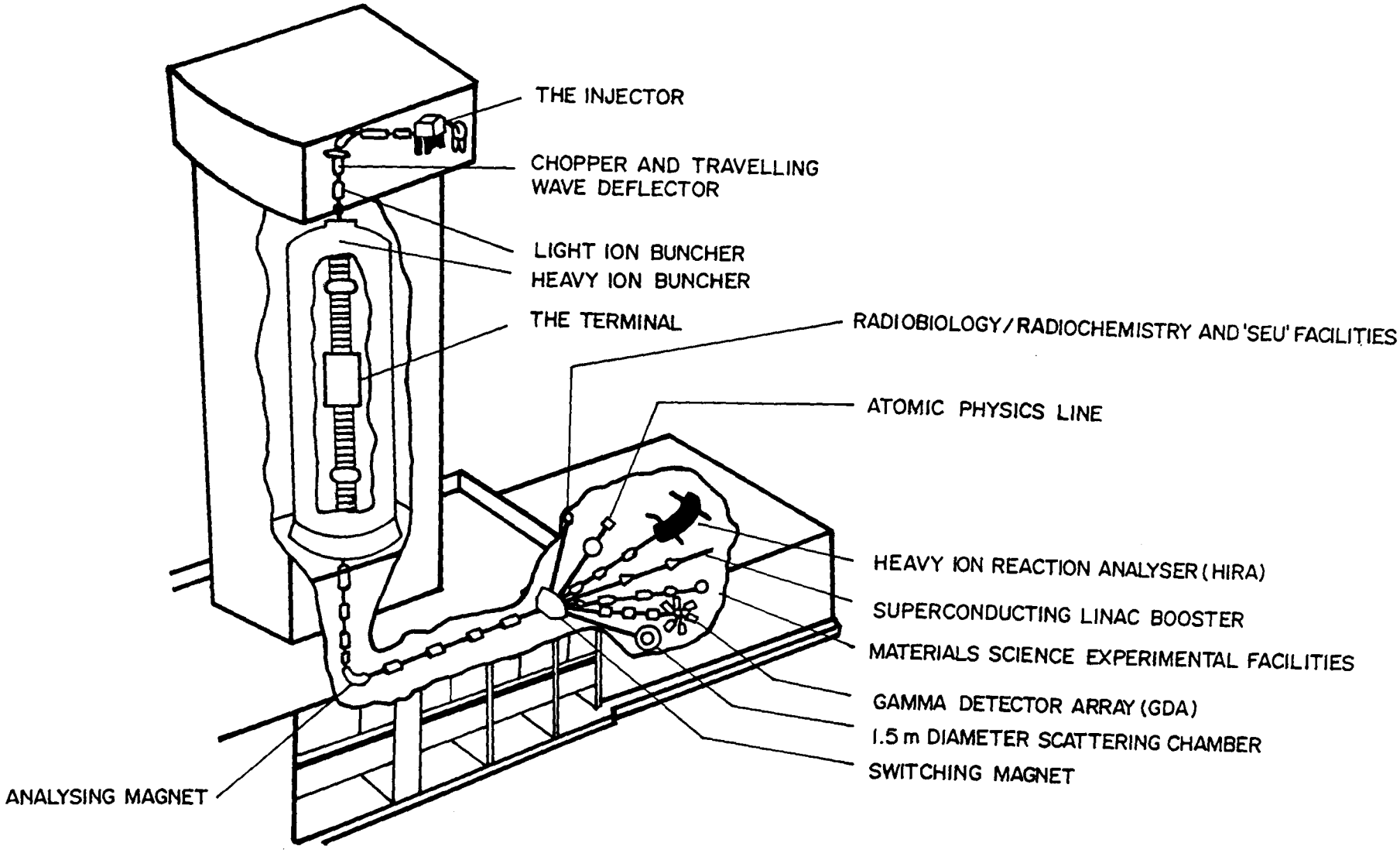

Fig. 3.1.1b A schematic diagram of the accelerator facilities at NSC.

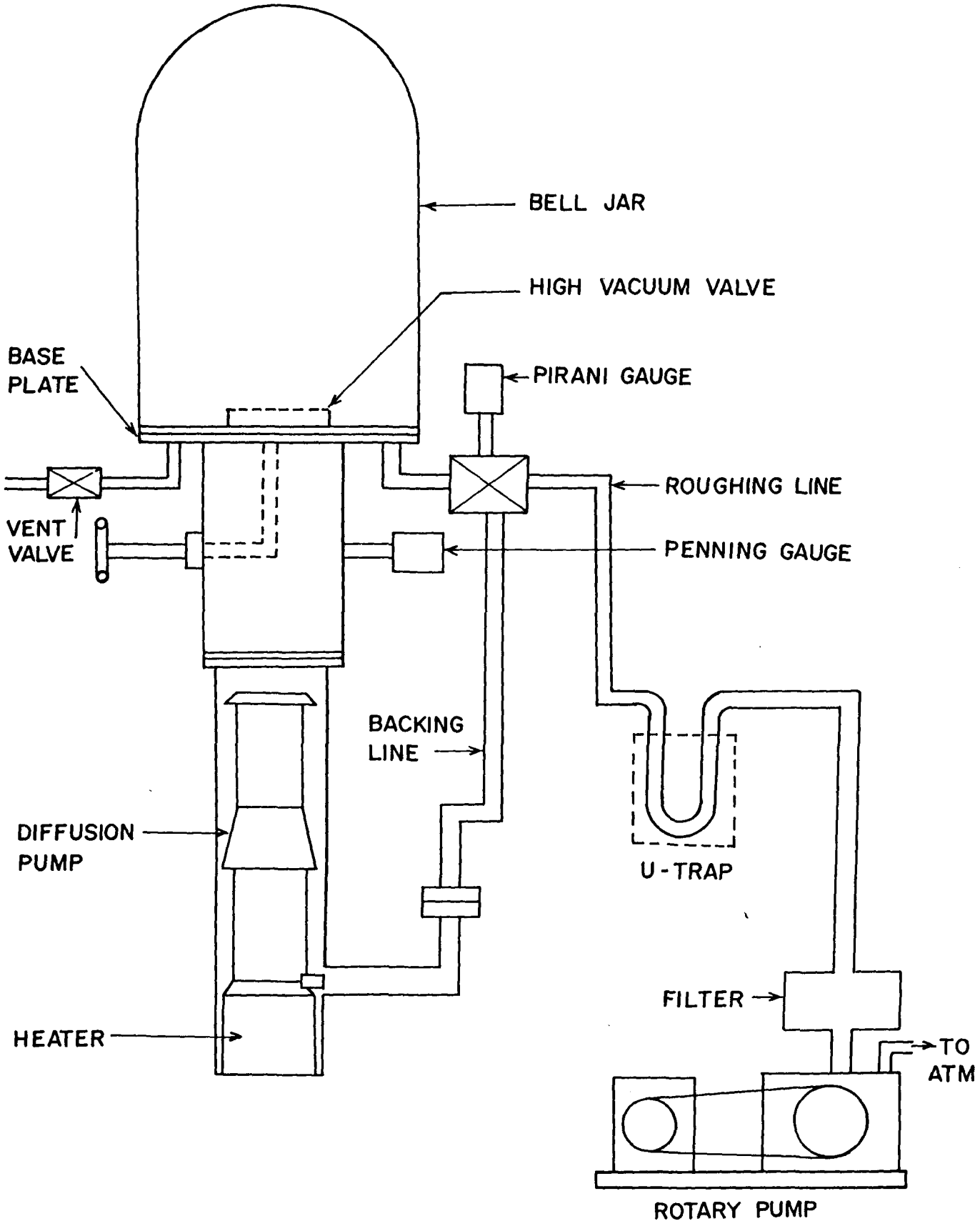

Fig. 3.2a Block diagram of the vacuum system of the evaporator.

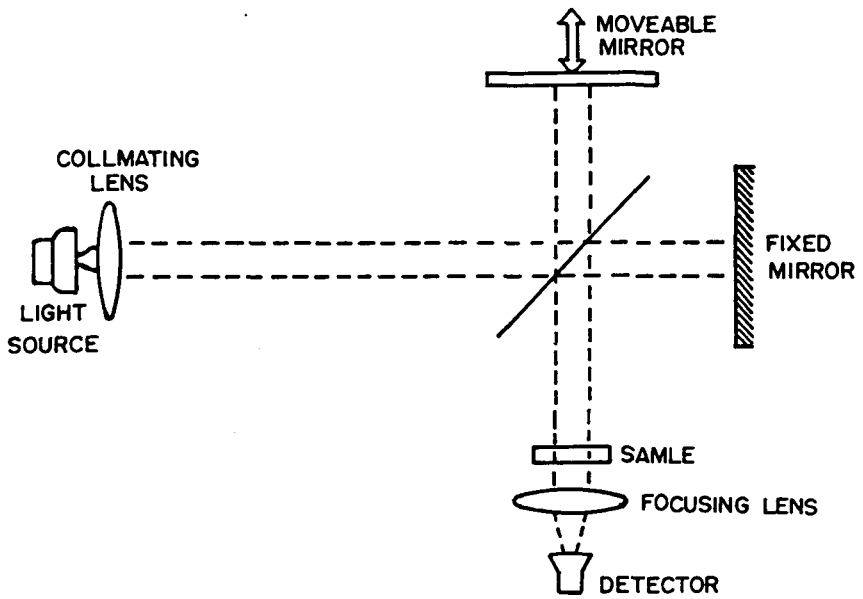

Fig. 3.3.4a Diagram of a Fourice Transform Spectrometer

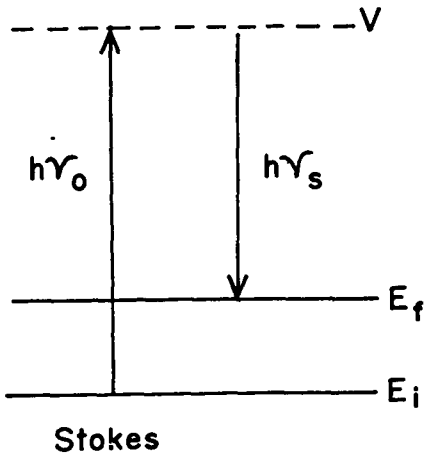

$$h\nu_s = h\nu_o - (E_f - E_i)$$

$$h\nu_o - h\nu_s = E_f - E_i$$

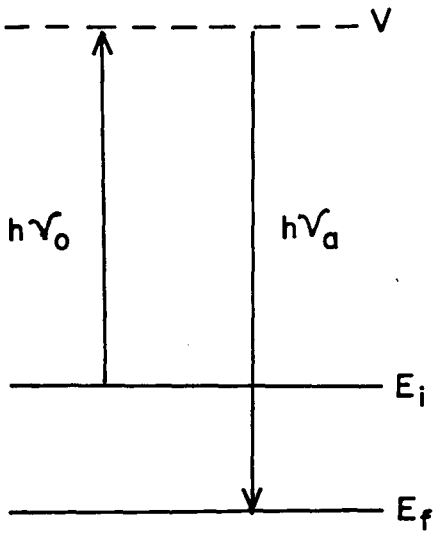

$$h\nu_a = h\nu_o + (E_i - E_f)$$

$$h\nu_o - h\nu_a = E_i - E_f$$

Fig. 3.3.5a Idealised model of Stokes and anti-Stokes Raman Scattering

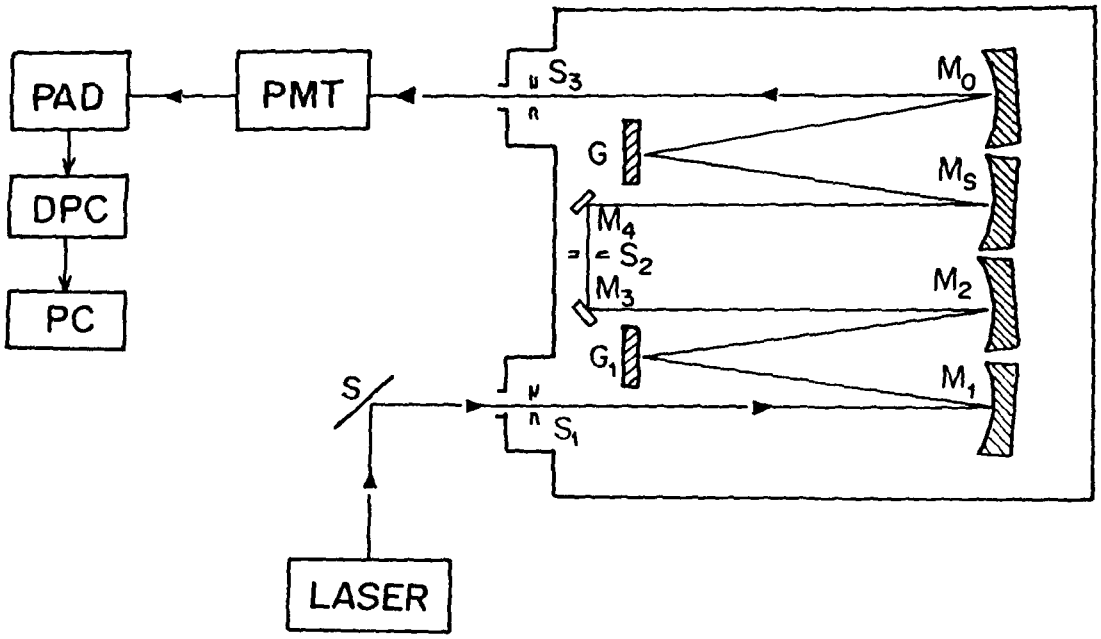

Fig. 3.3.5b Schematic diagram of Raman spectrometer equipped with a photomultiplier tube.

G1, G2- gratings, M1, M2, M5 and M6- plano-concave mirrors, M3 and M4--plane mirrors. S1- entrance slit, S2- intermediate slit, S3- exit slit, PMT- photomultiplier tube, PAD - preamplifier and discriminator, DPC - digital photon counter and PC - personal computer.

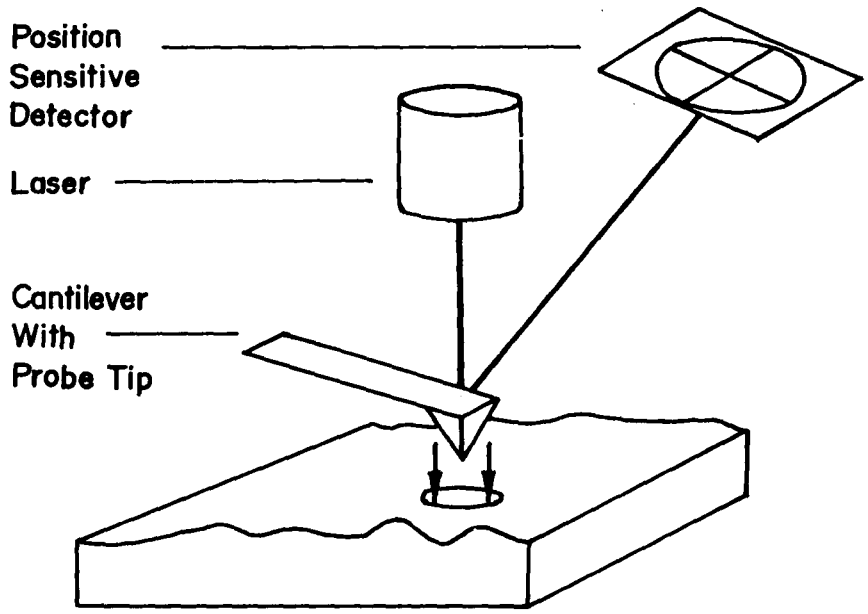

Fig. 3.3.7a Schematic of an atomic force microscope (AFM) showing the force sensing cantilever.

CHAPTER - IV

4.0 HYDROGEN LOSS IN POLYMERS UNDER HEAVY ION IRRADIATION

4.1. Introduction:

Polymers which form a class of covalent insulators are of technological importance. They are highly sensitive to ionizing radiations. Ion beam irradiation induces modifications of the molecular structure in polymers, which leads to substantial changes in their chemical, optical, electrical, mechanical and other properties [1-4]. For example, it was found that ion irradiation causes the decrease in the resistivity by many orders of magnitudes in some polymers [5]. Modification of polymers under ion irradiation is an expanding field of research. When charged particles pass through polymers, they lose energy and induce a continuous trail of excited and ionized atoms. For example, at low fluences, scission and cross-linking of bonds take place, and the polymer begins to desorb small molecules like hydrogen, etc. For higher fluences, graphitization and carbonization occur which lead to the formation of inorganic compounds [6].

It is known that hydrogen affects the properties of materials. It is also known that the hydrogen content of hydrogenous materials decreases with

incident ion fluence. It is therefore possible to tailor the properties of materials by altering the hydrogen content. The present work investigates the hydrogen loss behavior in different polymers with the objective of studying the dependence of hydrogen loss on

(i) Electronic stopping power

(ii) Chemical composition by way of a the different bonding

Hydrogen is the most difficult atomic species to analyze by traditional methods. Because of its low atomic Z, methods based on X-ray or Auger emission do not work and because of its light mass, the Rutherford backscattering (RBS) method cannot be used. Methods based on the fact that the presence of hydrogen alters the spectroscopic properties of materials such as Raman spectroscopy, IR spectroscopy, etc., require a standard calibrator which is used as a reference to quantify hydrogen. These methods also suffer from the drawback that they are not dynamical, i.e. we cannot get an idea as to what is happening during ion bombardment. Partial pressure study by residual gas analysis (RGA), or nuclear reaction analysis (NRA) using a 15N beam at a resonance energy of 6.385 MeV and elastic recoil detection analysis (ERDA) are the techniques which can be normally employed to monitor the changes in hydrogen concentration during ion irradiation. In the present work, ERDA has

been used to monitor the changes in hydrogen concentration under ion irradiation.

A report is given here of the study of the release of hydrogen from different polymers as a result of bombardment of 100 MeV ^{107}Ag ions on polyvinylidene fluoride (PVDF): 110 MeV ^{58}Ni ions on polystyrene (PS), polymethyl methacrylate (PMMA), and polyvinylidene fluoride (PVDF); 85 MeV ^{58}Ni on polypropylene (PP) and polymide (PI); and 50 MeV ^{28}Si on polypropylene (PP) and polymide (PI).

4.2 Result and Discussion:

The loss of hydrogen as a function of ion fluence from different polymers for irradiation by 100 MeV ^{107}Ag, 110 and 85 MeV ^{58}Ni and 50 MeV ^{28}Si are shown in Figs. 4.2.1 - 4.2.4., respectively. The electronic energy loss (S_e) of these ions in different polymers and other parameters as calculated by TRIM 95 [7] are shown in Table 4.2.5. At these energies, the nuclear energy losses are negligible as compared to the electronic stopping power.

4.3 *Possible Correlation with ion Track Diameters:*

The hydrogen loss data as shown in Figs. 4.2.1. - 4.2.4., were fitted using two equations in two different regimes:

$$N_1 = N_{1,0} \exp(-\sigma_1 \phi) \qquad (1a)$$

$$N_2 = N_{2,0} \exp(-\sigma_2 \phi) \qquad (1b)$$

Here ϕ is the ion fluence in ions/cm^2, σ_1 and σ_2 are the hydrogen release cross sections in cm^2 and $N_{1,0}$ and $N_{2,0}$ are constants. The sum of $N_{1,0}$ and $N_{2,0}$ is the initial hydrogen content in the sample at ϕ = 0. This fitting is shown in Figs.4.2.1. - 4.2.4., as solid lines. It indicates two types of hydrogen release mechanism in ion-polymer interaction.

The equation of the first line (1a) is given by

$$N_1 = N_{1,0}\, e^{-\sigma 1 \phi}$$

or $$\ln N_1 = \ln N_{1,0} - \sigma_1 \phi \quad \text{----------(1)}$$

let $Y = \ln N_1$

$A = \ln N_{1,0}$

$B = \sigma_1$

$X = \phi$

The equation (1) then reduces to the form

$$Y = A + BX \text{ ----------(2)}$$

The above equation then gives:

$$\Sigma Y = nA + B\Sigma X \text{----------(3)}$$

and $$\Sigma XY = A\Sigma X + B\Sigma X^2 \text{ --------(4)}$$

Solving the above equations for A and B, we have

$$A = \frac{\Sigma Y \Sigma X^2 - \Sigma XY \Sigma X}{n\Sigma X^2 - (\Sigma X)^2} \quad , \quad B = \frac{n\Sigma XY - \Sigma X \Sigma Y}{n\Sigma X^2 - (\Sigma X)^2}$$

Now; $A = \ln N_{1,0}$ or $N_{1,0} = e^A$

and $B = -\sigma_1$, therefore $\sigma_1 = -B$

Table 4.3.1 (a) and (b) gives the values of dose and the corresponding loss in H for the case of PS and PVDF respectively. The calculated values of $N_{1,0}$, σ_1, $N_{2,0}$ and σ_2 for different cases are shown in Table 4.3.2.

From the measured hydrogen release Cross sections σ_1, the effective ion track radius is derived. If r_{track} is the radius of the ion track formed, then

$$r_{track} = (\sigma_1 / \pi)^{1/2}$$

where σ_1 is always larger than σ_2 as we deal with ion-overlapping tracks.

The track radii calculated in the present work for the different ion-polymer combinations are shown in the 7th column of Table 4.3.2.

The effective track radius varies from 2.5 to 5.0 nm, which is consistent with the finding of Trautmann [8] where the track radius was measured by scanning force microscopy of the chemically etched tracks. The track radii measured by neutron diffraction [9,10] are also consistent with the present work. The average amount of hydrogen released per incident ion can be calculated by multiplying the hydrogen release cross section σ_1 with the hydrogen concentration $N_{1,0}$. These numbers are shown in the last column of Table 4.3.2. Typically about 10^6 hydrogen atoms are lost from the polymers (within about 1 μm thickness) per incident ion.

4.4 Dependence on chemical Bonds:

It has been suggested by Fujimoto et al. [11] that the CH_3 bond is more prone to breakage than CH and CH_2. When hydrogen is released as H_2 molecule, it does not combine with dangling bonds of carbon. However if bonds of CH or CH_2 type break, the chances that hydrogen is released as H^+ ion are higher and there is a finite probability for H^+ to recombine with dangling carbon bonds. Therefore in a polymer, where CH_3 type bonds are present, the rate of

hydrogen loss should be higher. This observation is supported by the present investigations as is evident from Tables 4.2.5. and 4.3.2. For example, PMMA has two CH_3 bonds and PP has one CH_3 bond. In these two cases the hydrogen released per incident ion is higher compared to the other polymers. In case of 110 MeV ^{58}Ni, the electronic energy loss and the initial hydrogen content are almost the same for PS and PMMA, but the average hydrogen loss is much higher in case of PMMA than PS due to the presence of CH_3 type bonds in PMMA.

4.5 Nature of the Hydrogen Loss Curve:

Another important feature which is evident from Figs. 4.2.1 - 4.2.4. is that after some ion fluence, the hydrogen loss diminishes and hence the hydrogen loss curve tends to flatten. This behavior can be explained by ion track overlapping. From Table 4.3.2., we can take the track radius to be around 4nm. So the total number of tracks for the onset of overlapping in 1 cm^2 will be of the order of $1/(8 \times 10^{-7})^2 = 1.5 \times 10^{12}$ tracks. This number is clearly supported by the present experiment, where the hydrogen loss curve tends to flatten at a fluence of ~ 10^{12} ions/cm^2 if plotted on a linear-log scale.

4.6 Dependence of Electronic Energy Deposition:

The release rate of H after 100 MeV ^{107}Ag irradiation of PVDF was found to be higher by a factor of about 1.2 as compared with 110 MeV ^{58}Ni ions. The ratio of electronic energy loss (S_e) for these two ions in PVDF is about 1.5. Similarly the ratio of H release for 85 MeV ^{58}Ni and 50 MeV ^{28}Si in PP is 2.4, whereas the ratio of the S_e is 2.6, respectively. The ratio of H release for 85 MeV ^{58}Ni and 50 MeV ^{28}Si in PI is 2.3 and the ratio of S_e is 1.9. Thus there is a reasonable agreement in the ratio of their electronic energy losses in that polymer. It is clearly evident that the hydrogen release is dependent on electronic energy deposition. In Fig.4.6.1 (a). we have plotted the hydrogen release cross section versus the electronic energy loss (S_e) and in Fig. 4.6.1 (b). the ion track radius versus the electronic energy loss S_e. is plotted. These figures show that σ_1 and r_{track} correlate with S_e. Correlation between ϕSe^2 and the track radius was not found as observed by Klett et al. [12],

References

1. T. Venkatesan, L. Calcagno, B. S. Elman and G. Foti, In: Ion Beam Modifications of Insulators, Eds. P. Mazzoldi and G. W. Arnold (Elsevier Amsterdam 1987) p. 301.
2. I. Adesida, Nucl. Instr. Meth. 209/210 (1993) 79.
3. B. S. Elman, M. K. Thakur, D. J. Sandman and M. A. Newkirk, J. Appl. Phys. 57 (1985) 4996.
4. J. Davens, X. L. Xu, G. Boiteux and D. Sage, Nucl. Instr. Meth.B39 (1989)754.
5. S. R. Forrest, M. L. Kaplan, P. H. Schmidt, T. Venkatesan and A. Lovinger, Appl. Phys. Lett. 41 (1982) 706.
6. J. P. Durand and A. Lemoel, Nucl. Instr. Meth.s B105 (1995) 71.
7. J. F. Ziegler, J. P. Biersack and U. Litmark, The stopping and Range of Ions in Solids, Pergamann Press, New York (1985).
8. C. Trautmann, Nucl. Instr. Meth. B105 (1995) 81.
9. D. Alnrecht, P. Armbuster, R. Spohr, M. Roth, K. Schaupert and H. Stuhrmann. Appl. Phys. A37 (1985) 37.
10. R. Spohr, P. Armbuster and K. Schaupert, Radiat. Eff. and Def. in Solids 110 (1985) 27.
11. F. Fujimoto, M. Tanaka, Y. Iwata, A. Ootuka, K. Komaki, M. Haba and K. Kobayashi, Nucl. Instr. Meth. B33 (1988) 792.
12. R. Klett, D. Fink, A. Schmoldt, and L. T. Chadderton, Radiation measurements 28 (1997) 55.

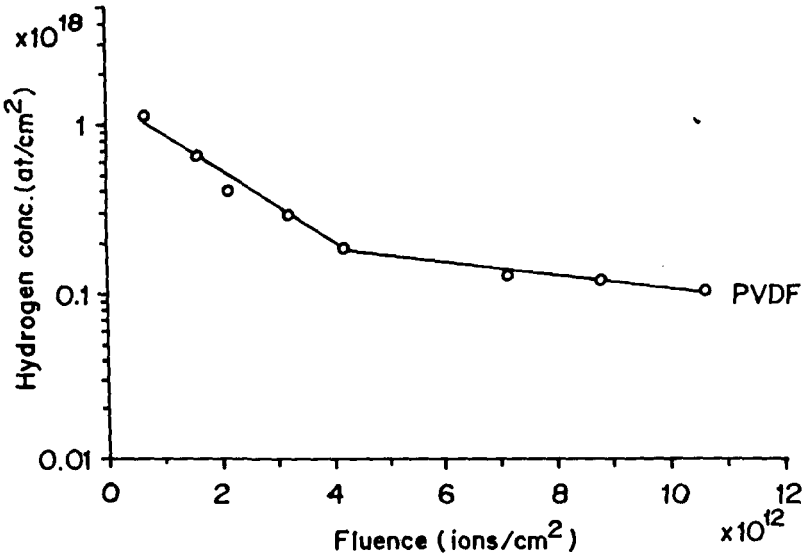

Fig.4.2.1.Hydrogen loss versus fluence curve for 100 MeV ^{107}Ag bombarded on PVDF

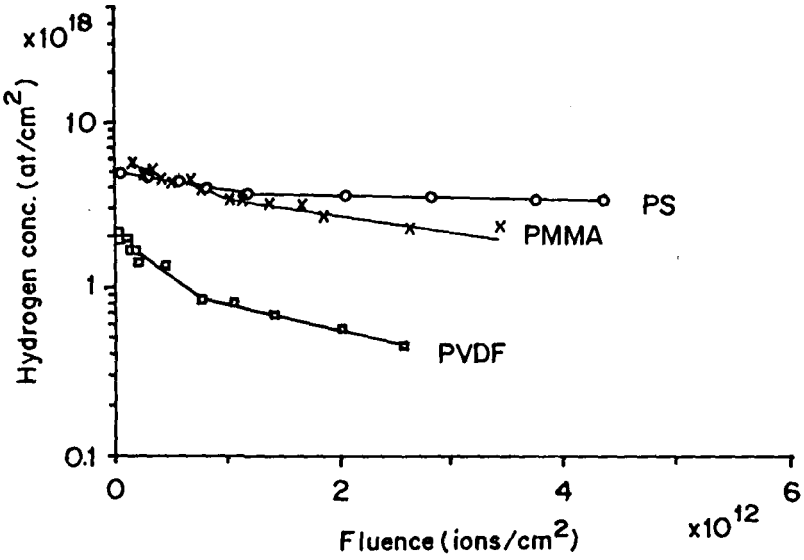

Fig. 4.2.2. Hydrogen loss versus fluence curve for 110 MeV ^{58}Ni bombarded on PS, PMMA and PVDF

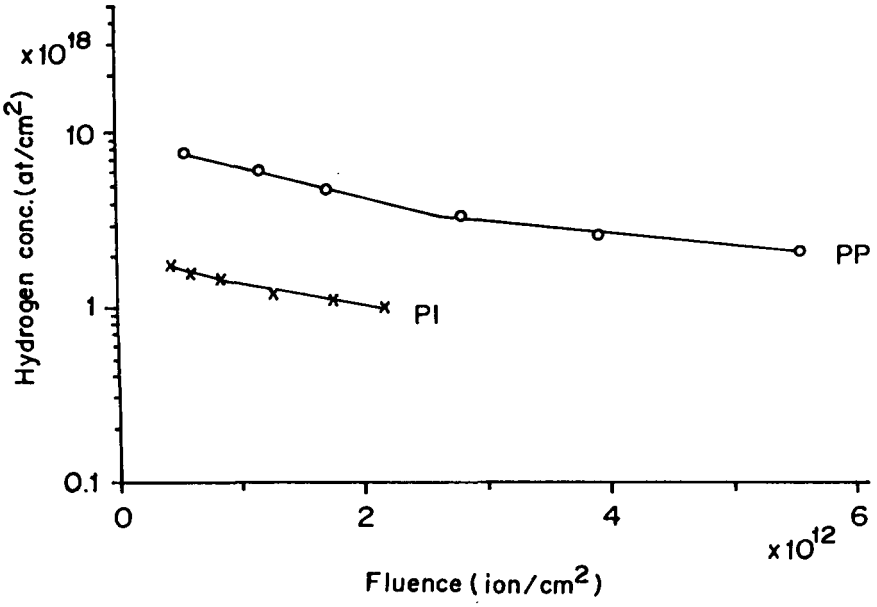

Fig. 4.2.3. Hydrogen loss versus fluence curve 85 MeV ^{58}Ni bombarded on PP and PI

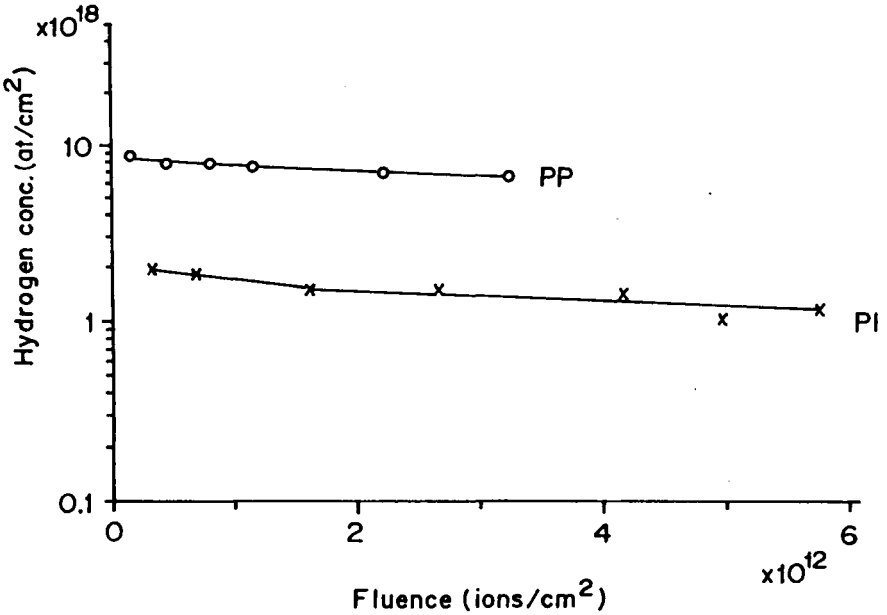

Fig. 4.2.4. Hydrogen loss versus fluence curve for 50 MeV ^{28}Si bombarded on PP and PI

Table 4.2.5

Electronic energy loss Se for ion-polymer combination used in the present work. These values are taken from TRIM 95 [7]. In the last three columns are the number of CH, CH_2 and CH_3 type bonds present in the polymer.

Ion energy	*Polymer*	S_e	*Percentage hydrogen*	*No of different type of bonds*		
				CH	CH_2	CH_3
^{107}Ag (100 MeV)	PVDF	1084	33	Nil	1	Nil
^{58}Ni (110 MeV	PS	513.4	50	6	1	Nil
	PMMA	516.5	53	Nil	1	2
	PVDF	727.9	33	Nil	1	Nil
^{58}Ni (85 MeV)	PP	424.8	66	1	1	1
	PI	723.2	25	10	Nil	Nil
^{28}Si (50 MeV)	PP	166.1	66	1	1	1
	PI	285.5	25	10	Nil	Nil

Table. 4.3.1.
(a) Hydrogen loss with dose for 110 MeV ^{58}Ni on PS

dose (ions/cm^2)	H loss	ln (H loss)
4.00×10^{10}	4.85×10^{18}	43.025510
2.80×10^{11}	4.60×10^{18}	42.972590
5.60×10^{11}	4.40×10^{18}	42.928150
8.00×10^{11}	4.00×10^{18}	42.832820
1.16×10^{12}	3.70×10^{18}	42.754860
1.16×10^{12}	3.70×10^{18}	42.754860
2.04×10^{12}	3.60×10^{18}	42.727470
2.82×10^{12}	3.60×10^{18}	42.727470
3.76×10^{12}	3.50×10^{18}	42.699300
4.36×10^{12}	3.49×10^{18}	42.696430

$N_{1,0} = 4.45 \times 10^{18}\ cm^{-2}$ $N_{2,0} = 3.70 \times 10^{18}\ cm^{-2}$

$\sigma_1 = 2.57 \times 10^{-13}\ cm^2$ $\sigma_2 = 0.13 \times 10^{-13}\ cm^2$

(b) Hydrogen loss with dose for 100 MeV ^{107}Ag on PVDF

dose (ions/cm^2)	H loss	ln (H loss)
.7x10^{12}	1.15x10^{18}	41.5862
1.6x10^{12}	0.66x10^{18}	41.0310
2.15x10^{12}	0.410x10^{18}	40.5549
3.22x10^{12}	0.290x10^{18}	40.2086
4.2x10^{12}	0.180.x10^{18}	39.7317
4.2x10^{12}	0.180x10^{18}	39.7317
7.15x10^{12}	0.128x10^{18}	39.3908
8.8x10^{12}	0.120x10^{18}	39.3263
10.65x10^{12}	0.104x10^{18}	39.1832

$N_{1,0} = 2.46 \times 10^{18}\ cm^{-2}$ $N_{2,0} = 0.27 \times 10^{18}\ cm^{-2}$

$\sigma_1 = 6.90 \times 10^{-13}\ cm^2$ $\sigma_2 = 0.89 \times 10^{-13}\ cm^2$

Table 4.3.2.

Hydrogen release cross sections σ_1 and σ_2: hydrogen concentration $N_{1,0}$, $N_{2,0}$ measured in the present work. The track radius and average hydrogen evolved are shown in the last two columns.

Ion energy	*Polymer*	*First curve*		*Second curve*		*track radius*	*Average H release*
		$\sigma_1(cm^2)$ $\times 10^{-13}$	$N_{1,0}(cm^{-2})$ $\times 10^{18}$	$\sigma_2(cm^2)$ $\times 10^{-13}$	$N_{2,0}(cm^{-2})$ $\times 10^{18}$	*(nm)*	$\times 10^6$
^{107}Ag	PVDF	6.90	2.46	0.89	0.27	4.0	1.71
100(MeV)							
	PS	2.57	4.45	0.13	3.70	2.9	1.17
^{58}Ni	PMMA	5.12	5.80	2.29	4.38	4.0	2.97
110(MeV)	PVDF	7.70	1.81	3.48	1.15	6.1	1.39
^{58}Ni	PP	3.96	9.49	1.71	5.34	3.6	3.76
85(MeV)	PI	4.18	2.18	2.84	1.82	3.7	0.91
^{28}Si	PP	1.66	8.66	0.52	7.88	2.3	1.44
50(MeV)	PI	1.92	2.07	0.81	1.78	2.5	0.40

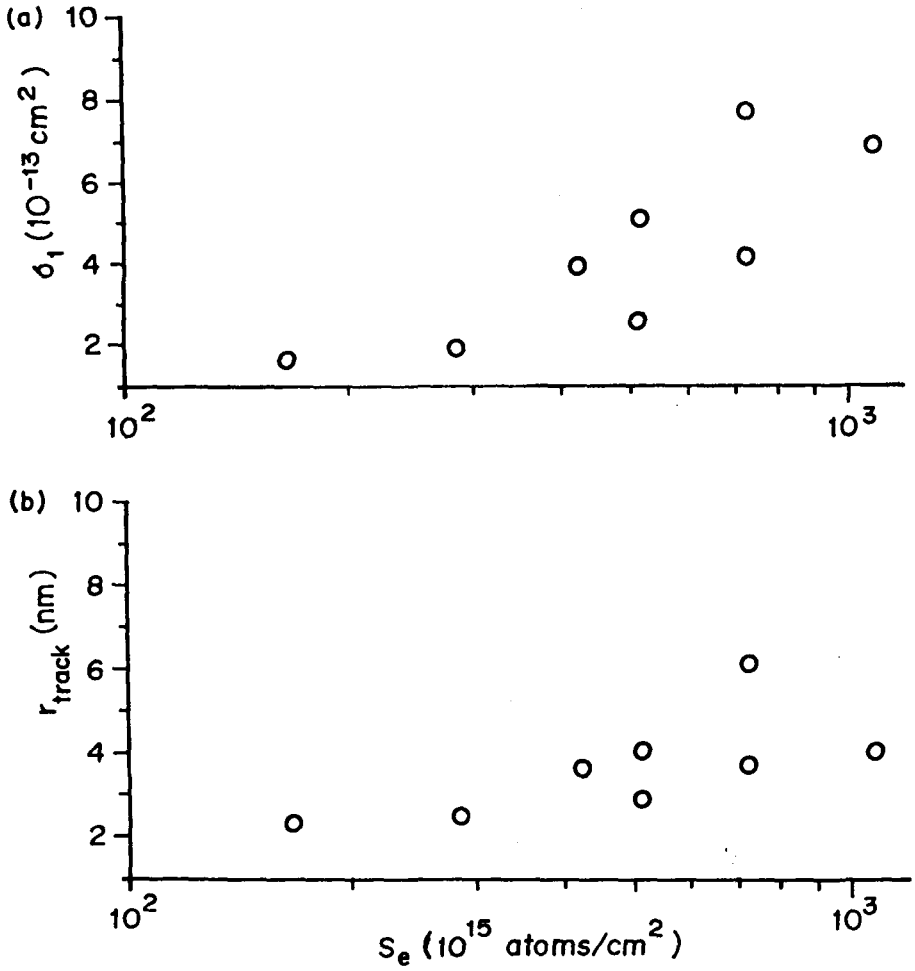

Fig. 4.6.1 Correlation of (a) hydrogen release cross section σ_1 and (b) ion track radius r_{track} with electronic stopping power

CHAPTER - V

5.0 ANALYSIS OF PHYSICAL AND CHEMICAL MODIFICATIONS OF IRRADIATED POLYMERS

5.1 The effects of swift heavy ion irradiation on the radiochemistry and melting characteristics of PET

5.1.1 Introduction:

When swift heavy ions pass through polymers, a considerable amount of energy is transferred by collisions with electrons of the target material, resulting in transient high local energy densities along the ion paths. The knocked out electrons, in turn, either dissipate their energy by collisions with other electrons or through electron-phonon coupling. High energy densities are known to be a prerequisite for phase transitions, which have occasionally been found to occur along swift heavy ion tracks. For example heavy ions in GeV range, impinging onto carbonaceous material (e. g. graphite, kapton, or sugar) give rise to formation of fullerenes [1]. Also, change of the molecular alignment after low fluence ion irradiation [2] and vice versa transitions from crystalline to amorphous [2-4] after high fluence ion impact have been reported. The ionization and electronic excitation processes in polymers are known to lead in to both chain scission and cross-linking, their ratio depending on the system under consideration. The first effect leads to decreasing molecular weight and the latter to its increase.

All the above mentioned effects cause changes in the polymer's phase and chemical structure, its crystallinity, its molecular weight and eventual chemical reactions of the material. The eventual introduction of impurities into the polymer and the sample's thermal pre-history (such as annealing time, cooling rate, and even the method by which the polymer's thermal behavior is determined) may influence the polymer's thermal parameters such as T_g (glass transition temperature) and T_m (the melting temperature) [5].

Earlier examinations [6] have shown that, after irradiation of polyethylene terephthalate (PET) with MeV heavy ions at fluences between 1×10^{11} and 6×10^{12} ions/cm^2, a significant loss of crystallinity is found, resulting from scission processes in the main chains of the trans configurations of the ethylene glycol residue. For contrast, other authors [7] rather interpret that the increase in amorphization during MeV heavy ion irradiation of PET is a function of degradation and cross-linking. Apel et al [8], have reported both chain rupture and cross-linking occurring simultaneously from swift heavy ion irradiation on PET. They have suggested that the chain rupture is shown to predominate inside the track core with a diameter of several nm, and cross-linking is found to take place in the vicinity of the core at larger radii [8,9].

There appears to exist only one thorough DSC examination on swift heavy ion irradiated PET. This is the work of Ciesla et al. [7] who irradiated 23μm

thick PET foils with 5.5 MeV/amu Ar ions at an ion fluence of 6×10^{11} ions/cm^2. They found a melting point of 251.9 °C after the first DSC measurement, and a double melting point at both 240.7 and 251.9 °C after the second DSC run (indicating premelting and melting as endothermic), corresponding to a total heat of fusion of 44 J/g and 40 J/g respectively. Ion irradiation led to a lowering of T_m to 204.8 °C after the first, and 195.4 °C after the second DSC run, with the total heat of fusion decreasing in this case to some 17.04 J/g. No recrystallization during cooling of the samples was found to occur.

From the several works that have been performed earlier on the radiochemical processes governing the thermal properties of ion-irradiated PET there is still much to be understood clearly. In our study of ion irradiated PET we have used used techniques of FTIR, DSC and X-ray diffraction analysis to get a more definitive picture and understanding of the concerned processes.

5.2 Analytical Results:

5.2.1 FTIR Results:

FTIR spectra of pristine and irradiated PET at various fluences were recorded as shown in Fig. 5.2.1a. In contrast to Ref. [6], we did not observe alkyne formation in our FTIR measurements; rather our results show different

trend of amorphisation. Table 5.2.1b (i) and (ii) gives the experimental parameters in the present work and the IR peak assignments of PET.

1]. No alkyne formation around 3294cm^{-1} as reported in Ref. [6] was observed. The spectra rather showed broad OH (aromatic) stretching at around 3300 cm^{-1}.

2]. Steckenreiter et. al [6] observed decrease on absorption of the band at 1504cm^{-1} with fluence from 1×10^{11} to 6×10^{12} ions/cm^2, suggesting amorphisation of the crystalline fraction and main chain scission at the para position of disubstituted benzene rings. We do not observe any change on irradiation even upto a dose of 1×10^{12} ions/cm^2.

3] An interesting result is the remarkable increase in the absorbance of the 730cm^{-1} vibration band, which corresponds to the bending vibration of the CH_2 group of crystal phase [10], at lower ion fluence (~10^{11}ions/cm^2), followed by its gradual decrease in the absorbance at higher ion fluence (~10^{12}ions/cm^2). This might be ascribed to the possible transient recrystallization upon swift heavy ion impact in our case, which eventually gets destroyed at higher ion fluences. The partial different trend of amorphisation in the present case is further evidenced by the increase in the absorbance of 873 cm^{-1} vibration band (crystal phase, Ref. [7] at lower ion fluence (~10^{11}ions/cm^2), in contrast to the findings of another group [7] at similar ion fluence. Further, the absorbance of the vibration

bands at 1132 cm^{-1} and 1286 cm^{-1} (amorphous phase, Ref. [11,12]) decrease at lower ion fluence, which support the possibility of the formation of polymer crystallites induced by high electronic excitation and ionization in the present work. At higher ion fluence (~10^{12} ions/cm^2) the absorbance peaks of the amorphous phase at 1132 cm^{-1} and 1286 cm^{-1} seem to increase drastically, denoting the destruction of newly formed polymer crystallites and leading to the advanced amorphisation.

4]. However, the absorbance of the bands at around 848 cm^{-1}, 972 cm^{-1} and 1471 cm^{-1}, which correspond to the crystalline phase [6,7] seem to decrease with the ion fluence and matches with the findings of Refs. [6,7]. This may be attributed to the destruction of crystalline lamella structure of the polymer in our case..

5]. Further, the absorbance bands at around 1044 cm^{-1} 1095 cm^{-1}, 1370 cm^{-1} and 1454 cm^{-1} (amorphous phase, Ref. [6,7]) are found to increase with the ion fluence, suggesting amorphisation with fluence.

5.2.2 **DSC Results:**

Fig. 5.2.2a. shows the DSC measurements of the unirradiated and irradiated PET films at different fluences ranging from 1×10^{11} to 1×10^{12} ions/cm^2. All the thermograms are normalized to the same sample amount of 0.5 mg.

The DSC curve of pristine sample shows that the melting transformation occurs in the temperature range 225-260 °C. The calorimeter curve gives the melting of the pristine PET at 246.19 °C. The melting enthalpy of pristine PET calculated by the integration of the DSC curve in the temperature range 225 -260 °C gives the value ΔH_o=17.54 J/gr. This value corresponds to the polymer crystalline fraction, which can be calculated by using the relation $\chi = \Delta H_o / \Delta H_{sc}$, where ΔH_{sc} is the melting enthalpy of a completely crystalline polymer, which is 104 J/gr [11]. Accordingly the crystalline fraction of our pristine sample gives the value of 0.16.

DSC curves of irradiated PET films at different ion fluences exhibit a significant change in the melting behavior. It appears from the DSC curves that the temperatures of the melting peaks first increase upto a critical ion fluence of 5×10^{11} ions/cm^2 and then shift towards pristine value at higher ion fluences. Sharp and intense melting peak of temperature 251.96 °C at ion fluence 5×10^{11} ions/cm^2 with respect to the pristine melting peak (246.19 °C) is observed.

5.2.3 XRD Results:

X-ray diffraction results of our pristine and irradiated PET at 5×10^{11} ions/cm^2, Fig. 5.2.3a, show the reduced and slightly shifted main peak at 2θ = 25.495^0 after irradiation along with the appearance of a small new peak at 2θ =

37.933^0. The observed changes in the X-ray diffraction spectra are thought to be due to the destruction and disordering of the original lamella (crystalline) structure of PET. The shift in the main peak maximum from $2\theta = 25.925^0$ (pristine) to $2\theta = 25.495^0$ along with a decrease in intensity might indicate a distortion of the crystal structure due to increasing strain, resulting from differences in density of the pristine and irradiated zones.

The appearance of a small new peak at $2\theta = 37.933^0$ after irradiation may have some correlation with the newly formed fine polymer crystallites in the amorphous zone of PET, not present earlier in the polymer.

5.3 Discussion:

From the FTIR results there is a general agreement in our findings and those ones obtained earlier in the literature, in spite of the different irradiation conditions. This suggests that the general picture which emerged before can be referred for our case of swift heavy ion irradiation. Low fluence irradiation results in stretching of the polymer bonds by energy transfer to the electronic system of the polymer, which subsequently leads to the release of characteristic functional groups as individual molecules. In conclusion, it appears that the FTIR spectra indicates some radiochemical degradation processes for both the low fluence and the high fluence cases which might be reasons to explain the observed changes of T_m.

Apart from the general similarity of all FTIR results on PET, there are, however marked differences in the behavior of individual peaks between our results and earlier results. Our result mainly show that the alkyne formation is not a general peculiarity of swift heavy ion radiochemistry of polymers. Our FTIR signals indicating amorphisation also partly show a different trend than those of earlier observations, which might support speculations of transient partial recrystallization upon heavy ion impact.

The unusual growth in the melting temperature by the DSC measurement can be correlated to the recently observed 'secondary radiation induced crystallization' processes (SRIC) in γ-ray irradiated Polypropylene [13], where they have verified radiation enhanced microcrystalline regions by transmission electron microscopy (TEM) ~~have been verified~~. The new microcrystalline regions were reported to be distributed inhomogeneously on the surfaces of the strongly stressed interlamella and interspherolite spaces, characterized by considerably high values of the mechanical surface energy. Thus the growth of the melting points at lower ion fluences (~10^{11} ions/cm^2) in our case, might be due to SRIC which supports the possibility of the transient formation of small size crystallites in the amorphous zone of irradiated PET.

Another possibility on the peculiar melting behavior may also be assigned to the two-step melting process. At the onset of melting of a polymeric material

the chains shift against each other in their positions, while maintaining their overall longitudinal orientation, i.e. the chain structure becomes nomadic(stage 1). In the second stage the overall chain orientation is lost [14]. The observation of a double melting point for PET in Ref. [7] at $T_{premelt}$ = 240.7 °C, and T_{melt} = 251.0 °C indicating premelting and melting, is thought to be explained by the two above melting stages. These two melting stages are also somewhat similar in value to the ones found in our study: $T_{m.prist}$ = 246.19 °C for the pristine sample, and $T_{m.irr}$ = 251.98 °C after irradiation at 5×10^{11} ions/cm^2. The melting peak of the pristine sample $T_{m.prist}$ is found to be so broad in our measurement that we might well regard it as a superposition of $T_{pre.melt}$ and T_{melt}, with $T_{premelt}$ dominating in our special sample. The latter would signify that for the pristine PET material used by us, the energy transfer required to initiate the oriented polymer chain shifts at $T_{premelt}$ exceeds somewhat the one required for subsequent orientation-free chain mobility at T_{melt}. With increasing interchain interaction due to irradiation induced radical formation, scissioning and cross-linking, the capability for oriented polymer shifts at $T_{premelt}$ will be lost so that at 5×10^{11} ions/cm^2 the peak at T_{melt} dominates.

Due to the largely absent contribution of the peak at $T_{premelt}$ the measured melting point distribution around $T_{m.irr}$ hence becomes narrower.

The observed changes in the X-ray diffraction pattern are thought to be due to the destruction and disordering of the original lamella (crystalline) structure of PET. The small new peak at 2θ = 37.93° after the irradiation may

have some correlation with the newly formed radiochemical reaction products in the amorphous zone of PET. The shift in the main peak might indicate a distortion of the crystal structure due to increasing strain, resulting from differences in density of the pristine and irradiated zones.

5.4 Infra-red Transmission studies on swift heavy ion irradiated Polyvinylidene Fluoride (PVDF)

5.4.1 Introduction:

Polyvinylédene fluoride (PVDF) is a semicrystalline polymer, having three phases α, β and γ, and the degree of its crystallinity is important for its piezoelectric and pyroelectric activites. Application of a high electric field produces the polarization of the PVDF film due to the alignment of the hydrogen and fluorine ions. The formation of these oriented dipoles give rise to its piezoelectric and pyroelectric behavior [15]. Its piezoelectric and pyroelectric activity accompanied together with its high elasticity and high processability has made it technological important. [16,17].

The disruption of the crystal structure or dipole orientation, or changes in chemical composition, may result in alterations of the PVDF piezoelectric and pyroelectric activity, as well as changes in its physical and chemical properties.

Using Fourier Transformed Infrared spectral features of irradiated PVDF films. we have tried to analyze the effects of high electronic excitation resulting from swift heavy ion ions.

The infrared was taken nearly a month after the irradiation, so that the results reported can be assumed to be free from metastable defects and incomplete radiation -enhanced oxidation. In both the cases the range of the ions exceeded the thickness of the film, so that the energy deposited in the films through electronic excitation is uniform throughout.

5.4.2 Results and Discussion:

The Fourier Transformed IR spectral features of the unirradiated and irradiated PVDF films at various fluences using 180MeV Ag ions are shown in Fig 5.4.2a. The IR spectra shows the appearance of two prominent vibrational features at 1715 and 1725 cm^{-1}. These bands correspond to a terminal vinyl group $=C=CF_2$ [18]. The intensity of these groups fall with the increase in ion fluence upto a limiting value of around 5×10^{11} ions/cm^2. The result indicates the dynamic characterization of the chemical evolution of the fluorpolymer which can be explained in terms of extensive electronic excitation caused by the energetic ions leading to breakage of the terminal vinyl bonds. The other features which

can sustain their structural identity are the C - H stretching modes which are observed to appear at 3019 and 2979 cm^{-1}.

To unreveal the extent of sensitivity of these modes PVDF was irradiated by 95 MeV Ni ions with energy approximately half of the energy of that of the Ag ions. The FTIR spectra of the unirradiated and irradiated are shown in Fig. 5.4.2b. The result indicates appearance of the terminal vinyl group at ion fluence of 5×10^{11} ions/cm^2. The disappearance of the peak at 1715 cm^{-1} at 5×10^{13} ions/cm^2 indicates substantial modification leading to a more disordered system. The result however reflects lower order of sensitivity towards the nature and energy of the irradiating ion within an ion fluence of 5×10^{11} to 7×10^{12} ions/cm^2. The C - H stretching modes, however losen their identity above the fluence limit of 5×10^{13} ions/cm^2. The disappearance of these bands indicates the formation of simpler structural units at the expense of the complex molecular system. Table 5.4.2c (i) and (ii) gives the experimental parameters and the IR peak assignments of PVDF respectively.

References:

1. L. T. Chadderton, D. Fink, H. Mocckel, and K. K. Dwivedi, Rad. Eff. Def. Sol. 127 (1993) 163.

2. R. Percolla, L. Calcagno, G. Foti, and G. Ciavola, Appl. Phys. Lett. 65 (1994) 2966.

3. L. Calcagno, P. Musumeci, R. Percolla and G. Foti, Nucl. Instr. and Meth. B 91 (1994) 461.

4. R. M. Papaleo, M. A. deArajuo and R. P. Livi, Nucl. Instr. and Meth. B 65 (1992) 442.

5. J. Brandrup and E. H. Immergut (eds), Polymer Handbook, 3rd ed., J. Wiley and Sons, New York, 1989.

6. T. Steckenreiter, E. Balanzat, H. Fuess, and C. Trautmann, Nucl. Instr. Meth. B 131 (1997) 156.

7. K. Ciesla and W. Starosta, Nucl. Instr. Meth. B 105 (1995) 115.

8. P. Yu. Apel, A. Yu. Didik, L. I. Kravets, and V. I. Kuzentsov, Report JINR-E-18-88--540 of the Joint Instr. For Nucl. Research, Dubna (USSR) 1998.

9. P. Yu. Apel, A. Yu. Didik, L. I. Kravets, V. I. Kuznetsov, and O. L. Orelovich, Report JINR-R-12-84-773 of thr Joint Instr. For Nucl. Research, Dubna (USSR) 1984 (in Russian).

10. S. Krim, C. Y. Liang and G. B. B. M. Sutherland, J. Chem. Phys. 25 (1956) 549.

11. Infrared Spectroscopy of high polymer by R. Zbinden, Academic Press, New York (1964) 11.

12. G. Cortili and G. Zerbi, Spectrochim, Acta 23 (1967) 285.

13. M. Mateev and S. Karageorgiev, accepted for publication in Rad. Eff. and Def. Sol. (1999).

14. H. G. Elias, Makromolekuele, Huethig and Wepf Verlag, Basel and Heidelberg, 1971 (in German).

15. M. G. Broaddhurst and G. T. Davies, Ferroeleclectrics 32 (1981) 1.

16. T. Venkatesan, S. R. Forrest, M. L. Kaplan, C. S. Murray, P. H. Schmidt and B. J. Wiekens, J. Appl. Phys. 54 (1983) 3150.

17. L. G. Banks, H. A. Resing, D. C. Weber, C. Carodella, G. R. Miller and P. Brant, J. Phys. Chem. Solids, 43 (1982) 351.

18. Infrared Characteristic group Frequencies (Wiley, New York, 1980).

19. D. Fink, F. Hosoi, H. Omichi, T. Sasuga and L. Amaral, Rad. Eff. and Def. in Solids 132 (1994) 313.

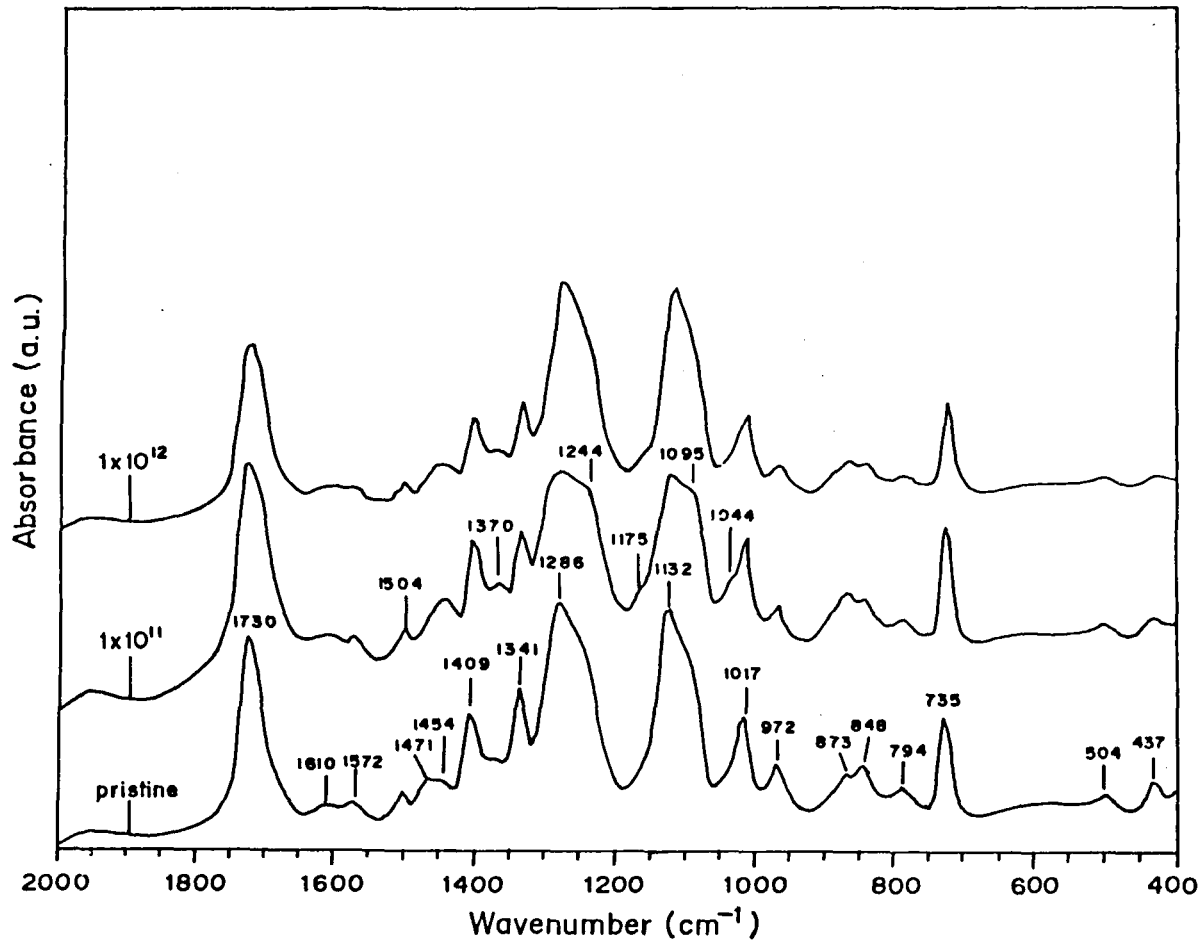

Fig.5.2.1a FTIR spectra for unirradiated and irradiated at various fluence with 180 MeV Ag, on PET

Table. 5.2.1b.

(i) Experimental Parameters of 180 MeV Ag ion irradiated on polyethylene terephthalate (PET).

Ion	Energy	Se(eV/Å)	Sn(eV/Å)	Range	Fluence ions/cm^2
Ag	180 MeV	1022	2.52	24μ	1×10^{11}
					5×10^{11}
					1×10^{12}

(ii)

IR peak assignments of PET

Wavenumber (cm^{-1})	Interpretation	Reference
730	Bending vibration of CH_2 group of crystal phase	[10]
848	C - H deformation of phenyl ring	[19]
972	C - H stretching (fundamental)	
1300 - 1000	C - O - C stretching of ester	[19]
1454	CH_2 (scissor)	
1730	C = O stretching from ester	

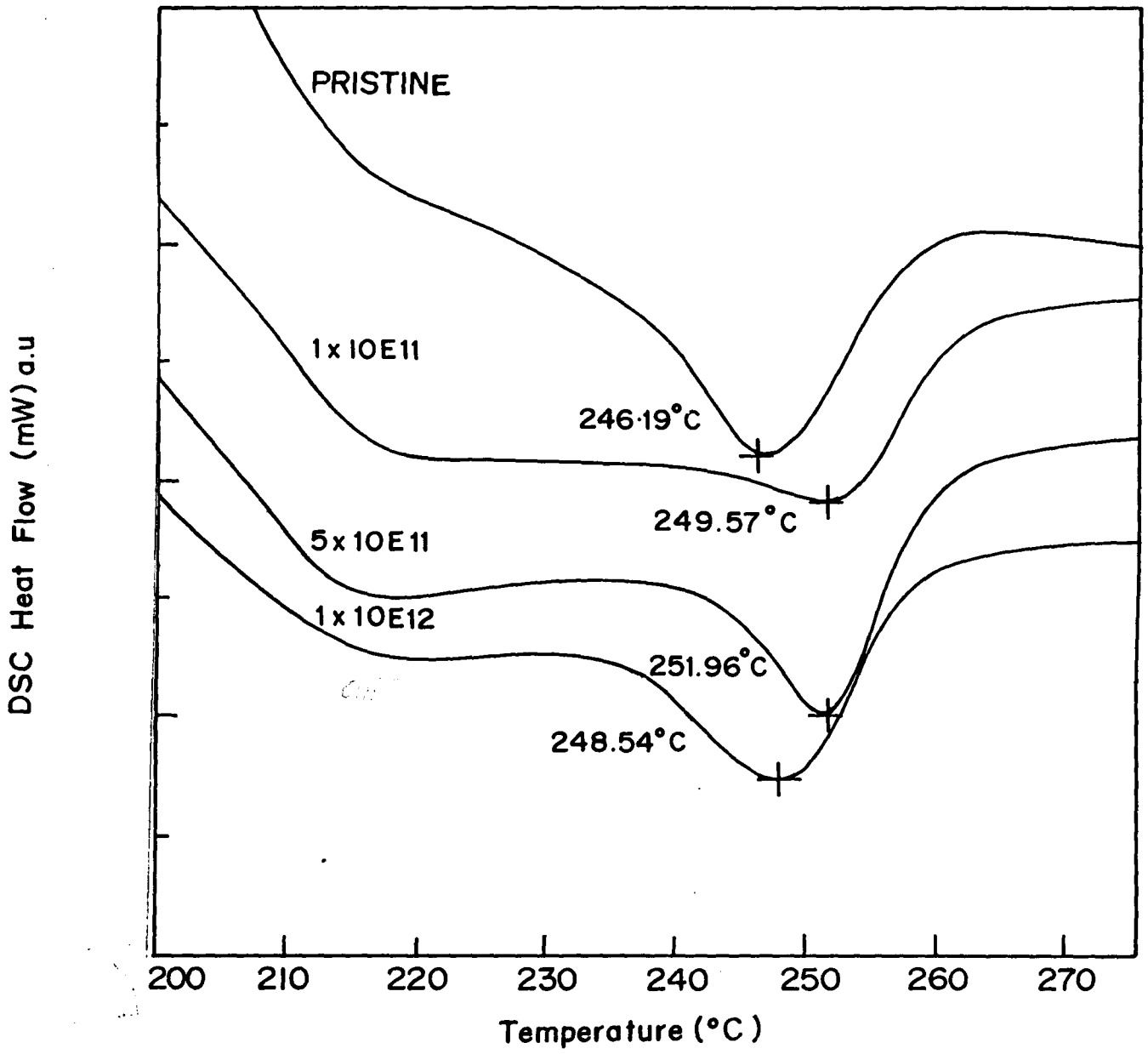

Fig.5.22a DSC curves of pristine and of energetic Ag ionsirradiated PET

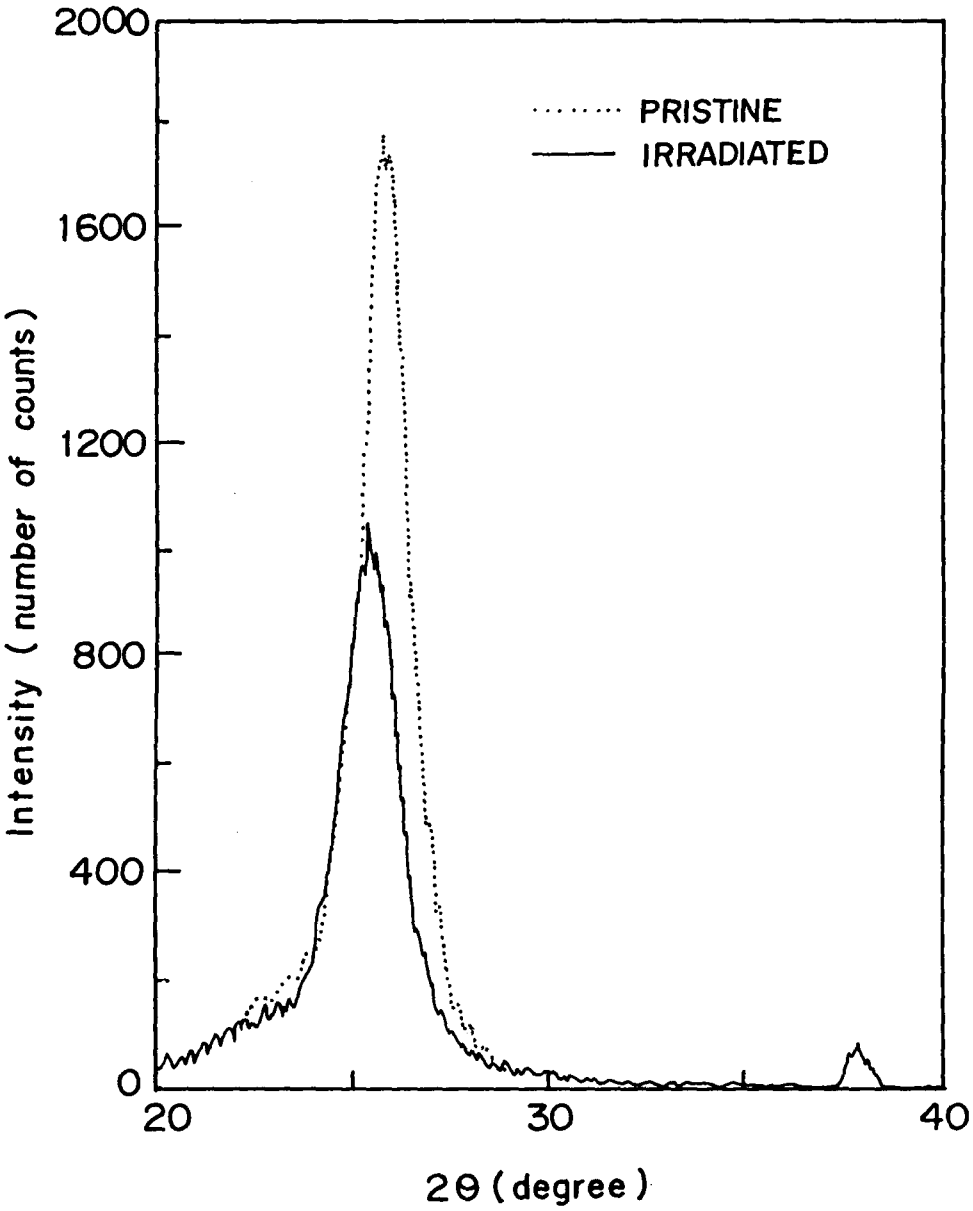

Fig.5.2.3a X-ray diffraction spectra of PET, pristine and irradiated at a fluence of 5×10^{11} ions/cm^2. The appearance of a new small peak at $2\theta = 37.933^\circ$ can be seen for the irradiated PET

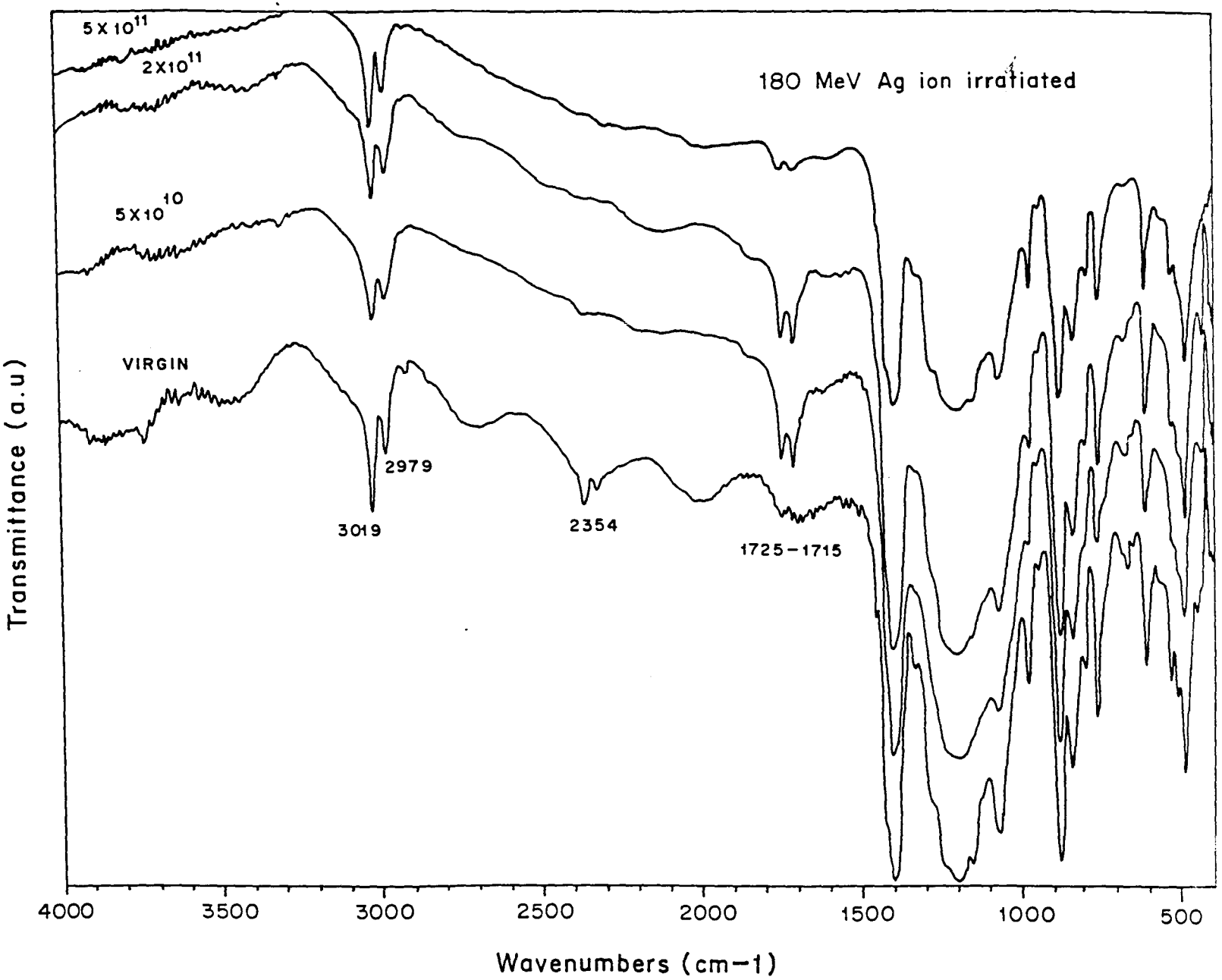

Fig.5.4.2a FTIR spectra of 180 MeV Ag ion irradiated ~~of~~ PVDF

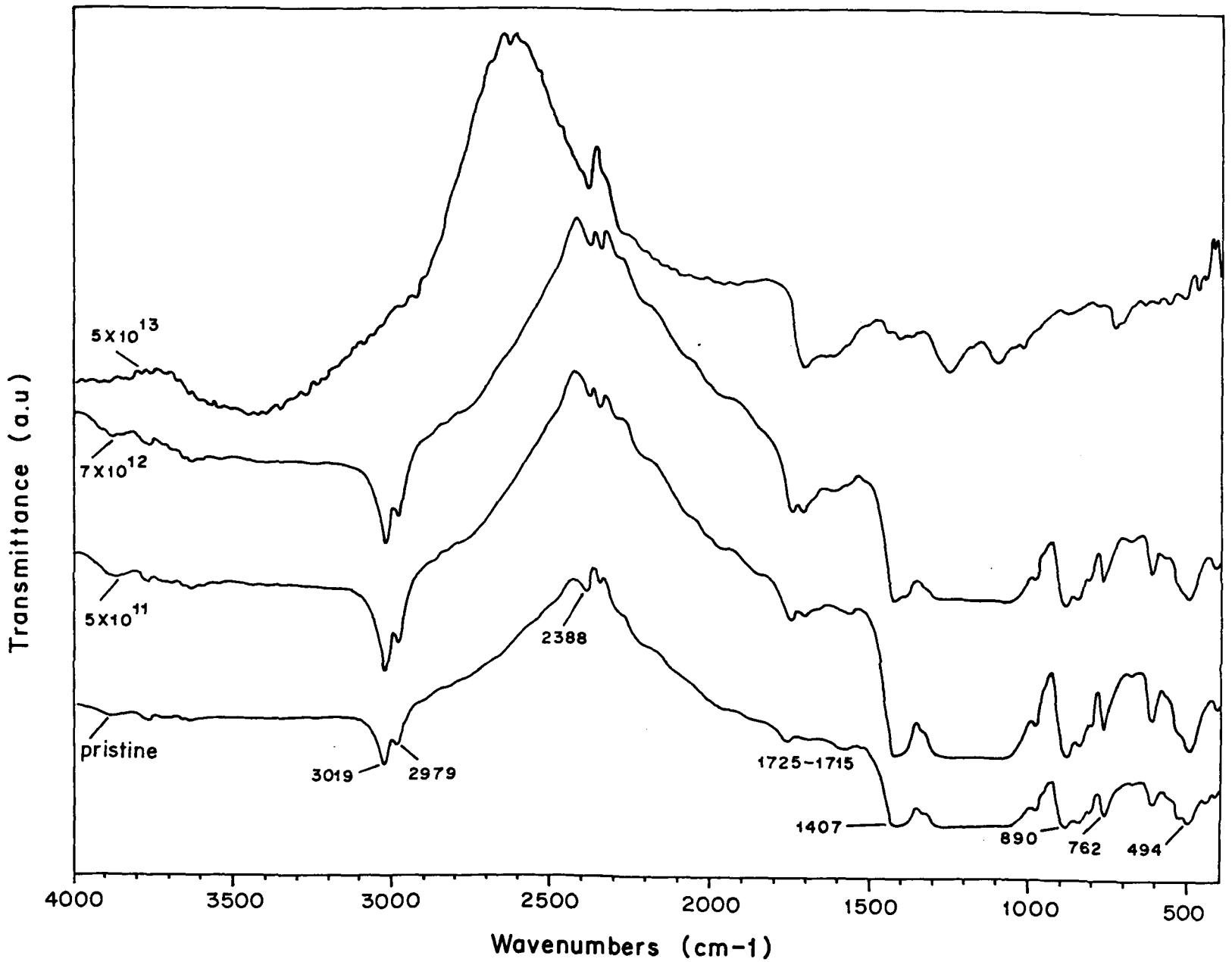

Fig.5.4.2b F TIR spectra of unirradiated and irradiated PVDF with 95 MeV Ni ion

Table. 5.4.2c.

(i) Experimental parameters of irradiated PVDF.

Ion	Energy	Target	Se (eV/Å)	Sn (eV/Å)	Range	Fluence (ions/cm^2)
$^{107}Ag^+$	180 MeV	PVDF	784	1.90	34μm	5×10^{10}
						5×10^{10}
						2×10^{11}
$^{58}Ni^+$	95MeV	PVDF	470	.78	25μm	5×10^{11}
						7×10^{12}
						5×10^{13}

(ii)

Assignments of IR peaks of PVDF.

Wavenumber (cm^{-1})	Interpretation	Reference
1715 - 1725	$= C = CF_2$	[18]
2979 - 3019	CH(stretching of CH_2)	[19]
2354	CO_2 (from air ?)	[19]

CHAPTER - VI

6.0. Effect of heavy ion irradiation on C_{60}

6.1. Introduction:

After the discovery of large quantities of C_{60} (fullerene) [1] and the demonstration of its superconducting properties after doping [2,3], the electronic and structural properties of C_{60} have become subjects of both scientific and potential technological importance. Several experimental and theoretical studies have been done to confirm the structure and physical properties of C_{60} clusters [4]. At room temperature C_{60} molecules are found to be centered on sites of a face-centered-cubic (f. c. c) [5], and held together only by weak Van der-Waals force. This ball shaped structure having volume of 694$Å^3$ is expected to trap atoms and molecules inside [6,7], which may have varying electronic structure, giving a new set of atom like units which could be used to make new materials as well as make small molecular devices.

There are 60 atoms in a C_{60} molecule. Therefore it has $3 \times 60 = 180$ degrees of freedom. Three degrees of freedom or modes are due to translation, three of them are due to rotation and the remaining 174 are vibrational degrees of freedom or vibrational modes. The symmetries of these modes can be found out

by using the character table for I_h point group which is given in Table 6.1a. and Table 6.1b. and using the relation

$$n(\gamma) = 1/g \sum g_i \chi_i^{\gamma *} \chi_i$$

where $n(\gamma)$ is the number of modes belonging to symmetry species γ,

'g' is the number of group elements (120 in this case)

'g_i' the number of elements in the i_{th} class.

'$\chi_i^{\gamma *}$ is the character for the i_{th} class belonging to symmetry species

and 'χ_i' is the character for i_{th} class of reducible representation.

g_i =1 for E, 12 for C_5, 12 for C_5^2, 20 for C_3, 15 for C_2, 1 for i, 12 for S_{10}, 12 for S_{10}^3, 20 for S_6 and 15 for σ.

The reducible representations for C_{60} molecule can be found out by considering the Table 6.1a. Under operation E all C_{60} carbon atoms remain unchanged therefore its character $\chi(E) = 3 \times 60 = 180$. For all operations except σ, all the carbon atoms are shifted and therefore contributions to their character are zero. Under the operation 'σ' four (4) carbon atoms remain unchanged, giving $\chi(\sigma) = 4 \times 1 = 4$.

The vibrational modes of C_{60} have been analyzed earlier [8]. Accordingly there are 174 modes distributed as follows.

$$\Gamma = 2A_g + 3T_{1g} + 4_{2g} + 6G_g + 8H_g + A_u + 4T_{1u} + 5T_{2u} + 6G_u + 7H_u$$

From the character table of I_h it is seen that $2A_g$ and $8H_g$ are Raman active and $4T_{1u}$ are IR active. Several workers have investigated the frequencies of the Raman active and the IR active modes. Palmetshofer et al. [9], have reported the $2A_g$ Raman modes at 1469 and 495 cm^{-1} and Negri et al.[10] at 1442 and 513cm^{-1} The strongest Ag mode of C_{60} have also been reported at 1467cm^{-1} [11] and 1468 cm^{-1} [12] . The 8Hg modes have been observed at 1644, 1465, 1265, 1154, 801, 440, and at 25cm^{-1} [10].

The $4T_{1u}$ IR active modes have been assigned to 1429, 1183, 576, and 526 cm^{-1} [13]. Negri et al. [10] from their work has reported the wave numbers at 1437, 1212 , 637, and at 544 cm^{-1}.

Methods have been now established on routine production of crystalline C_{60} films. A great interest has emerged on the of stability of C_{60} under ion beam irradiation and on whether the properties of the films can be changed by ion bombardment so as to be of a particular technological importance. For example it is possible to modify the films into a hard form of carbon by radiation induced damage [14-16]. Irradiation experiments with 100 keV B ions revealed that even a low dose of 3×10^{14} ions/cm^2 is sufficient to destroy the crystal structure of the

film [18]. Musket et al. [19], showed irradiation of 100 - 200 keV protons at a fluence of 6.1×10^{16} ions/cm^2 resulted the destruction of nearly all C_{60} molecules.

For ion bombardment energies in the energy range of MeV/amu, the energy loss mechanism in the target is predominantly through electronic excitations, as against nuclear collisions which dominate in the keV energy range. Thus the nature of associated damage at such energies is also expected to be different [20]. There are a few studies [21-24] on this aspect but much more needs to be understood on the process.

In this work we report the induced damage and polymerization on C_{60} films at large electronic excitation by MeV heavy ions at different doses. Since swift heavy ions are likely to produce ion tracks [25] in the materials with poor conductivity and high electron phonon coupling, we attempted to explore this aspect of generation of ion tracks in the film by ion beams. The damage on fullerene films depends on the ion dose and one can obtain the radii of the tracks from such information. Such an effect is totally different from that produced by low energy ions. When C_{60} crystallizes in the f.c.c lattice the C_{60} molecules occupy only 66 per cent of the apparent volume, leaving voids with octahedral symmetry of a dimension large enough to accommodate any element of the periodic table. It has been shown that molecular O_2 readily and spontaneously intercalate in the solid C_{60} [26,27] and oxygen is likely to react with the reactive

irradiated C_{60} films. We have therefore also attempted to see the formation of fullerene oxide using PL spectroscopy.

6.2. Results and Discussions:

When an energetic ion passes through a C_{60} film, it effects an area that is larger in diameter than its own due to electronic excitation and subsequent processes. The diameter of such a damage zone is estimated by Raman data. It is believed that the ion causes total damage resulting in fragmentation and amorphization. Around this damage zone, the effect of the ion is weaker where the cluster of C_{60} that have a few broken bonds combine with each other to cause polymerization. Thus the polymerization occurs in a region surrounding the damaged core. If the broken bonds of C_{60} combine with oxygen present in the film, it leads to the formation of oxide. The details of the damage, polymerization and oxidation are discussed in the following sections.

6.2.1. Damage:

For the investigation of C_{60} damage, the change in the intensity of the characteristic peak of C_{60} A_g mode ~1467cm^{-1} arising from the tangential breathing mode of the five carbon atoms around each of the 12 pentagons referred to as the pentagonal pinch mode [27] was examined. The recorded Raman data on the thin films for all the three ions showed small broad structure

around 1459cm^{-1} in addition to the pentagonal pinch A_g mode peak at ~1467cm^{-1}. The characteristic band at ~1467cm^{-1} is seen to decrease in intensity as a function of fluence. Fig.6.2.1a. and Fig.6.2.1b. show such decrease in the intensity of the pentagonal pinch mode (A_g) ~1467cm^{-1} for 50 MeV Si ion and 180 MeV Ag ion at various fluence. Comparing the oscillator strength of the A_g mode in unirradiated sample with that of the irradiated the percentage of damage of C_{60} is obtained, and plotted for various doses. Fig.6.2.1c. shows such plots for 50 MeV Si.

It has been shown by Dufour et al [22] that the extent of ion track damage is related to the electron-phonon coupling (g) and the melting energy (ΔH) of the material. The track formation in C_{60} is therefore expected with radius whose value is electronic energy loss dependent since it has a high electron-phonon coupling ($g = 10^{14}$ Wcm^{-3} k^{-1}) and a high melting energy (ΔH =1.15 eV/atom).

From the Raman spectra It is thus observed that the Intensity of the characteristic peak ~1467cm^{-1} decreases exponentially with fluence. The experimental data thus can be fitted to an exponential relation given below

$$I_{irr} = I_{unirr} \exp(-\sigma\phi)$$

taking ln on both sides

$$\ln I_{irr} = \ln[I_{unirr} \exp(-\sigma\phi)]$$

$$\text{or } \ln I_{irr} = \ln I_{unirr} - \sigma\phi$$

$$\text{Therefore } \ln(I_{irr} / I_{unirr}) = -\sigma\phi$$

where

I_{unirr} = intensity of the pristine C_{60} at ~1467cm^{-1}

I_{irr} = intensity of the peak (~1467cm^{-1}) on irradiation

ϕ = fluence

σ = damage cross section

By plotting Intensity of $\ln(I_{irr}1467/I_{unirr}1467)$ which is obtained from Lorentzian fitting of the Raman mode versus the fluence, the damage cross section was obtained. Fig.6.2.1d and Fig.6.2.1e shows such a plot for the case of 189 MeV Ag ion and 110 MeV Ni ion. The damage area cross section is interpreted as the mean circular area around the ion path over which a certain chemical species is modified, destroyed or damaged by the incoming ion [21].

The damage cross section thus obtained for Ag^{13+} ,Ni^{7+} and Si^{5+} on C_{60} are found to be 1.14×10^{-12} cm^2, 8.35×10^{-13} cm^2 and 7.39×10^{-13} cm^2, respectively. From the cross section thus obtained the mean ion track radii are calculated from the relation; $T_{rd.} = (\sigma / \pi)^{1/2}$.

6.2.2. Polymerization:

The region around 1459cm^{-1} in Raman spectrum has been observed on ion bombardment of C_{60} films, suggesting damage induced polymerization of C_{60} molecules [9,12,17]. In their Raman scattering study of C_{60} using high laser flux,

Zhou et al. [13] assigned the 1458cm^{-1} line to a phototransformation phase of C_{60}. This region in Raman spectrum has also been attributed to a dimer of C_{60}, where the C_{60} molecules are linked by covalent bonds on photoinduced polymerization [28]. A similar phenomenon can take place at high electronic excitation, where the highly excited C_{60} molecules can react by linking with each other from the lone pair electrons on breaking the parallel double bonds on adjacent molecules forming "2+2 cycloaddition" [29]. This suggests that the 1459cm^{-1} peak which increases at low dose and starts decreasing at higher doses in the present work is due to polymerization or crosslinking of C_{60} molecules.

The percentage of polymerization of C_{60} molecules is obtained by comparing the intensity of the polymer peak at 1459cm^{-1} with that of Ag mode at 1467cm^{-1} of the same data. Fig.6.2.2a. and b. shows two Lorentzian fits to the Raman data of C_{60} film irradiated by 110 MeV Ni at a fluence of $7x10^{11}$ ions/cm^2 and 189 MeV Ag at a fluence of $1.7x10^{12}$ ions/cm^2. It is observed that polymerization initially increases upto a critical value and then starts decreasing. At high destruction polymerization was not observed. Both these are consistent with the understanding that damage and polymerization of C_{60} become competitive and damage overcomes the polymerization at higher fluences, as shown in Fig.6.2.1c. for 50MeV Si irradiation as a function of fluence.

Table 6.2.1a. shows the electronic and nuclear stopping powers used in the present work. These values were calculated using the code TRIM 95 [30]. It is seen that the energy deposited in the material due to electronic loss is about three orders of magnitude higher to that of the nuclear loss. The table also shows the percentage of destruction and polymerization of the film on irradiation.

6.2.3. Photoluminescence study:

The PL signal in C_{60} on irradiation showed oxygen related PL at 2.1eV (~590nm) as discussed by Ryskin et al. [31].Therefore it was necessary to characterize the film for oxygen determination. The oxygen content in the film was determined by Rutherford back scattering(RBS). The oxygen content in the pristine films was found to be 0.0134 per cent.

The energy gap between the highest occupied molecular orbital (HOMO) and the lowest occupied molecular orbital (LUMO) in C_{60} lies at about 1.9eV [32]. It has been observed by Reber et al. [33], that solid C_{60} exhibits a very weak luminescence at room temperature. This weak luminescence of C_{60} at room temperature has been explained as a result of the forbidden HOMO - LUMO transition and the very efficient intersystem crossing to the excited triplet state of C_{60} [34]. The luminescence is therefore observed below the forbidden HOMO - LUMO gap at 1.7eV [35]. Matus et al. [36] has also explained this in terms of self-trapped exciton model to explain the shift from 1.9eV to 1.7eV.

The PL measurements in the present work shows the characteristic C_{60} peak at 1.7eV (~730nm) [37] in unirradiated samples. However a PL at 2.1eV (~590nm) was observed for irradiated samples and the ratio of the PL peak at 1.7eV with the luminescence at 2.1eV was found to decrease with fluence. Table 6.2.3b. (i) and (ii) shows the PL intensity ratios for different fluences with an unirradiated for 50 MeV and 110 MeV Ni ion. To confirm our result that the PL at 2.1eV is due to formation of oxide in the film, we have performed PL measurement for unirradiated and irradiated films in air and vacuum (10^{-3} mbar). It is known that physisorbed oxygen which gets absorbed to C_{60} film with weak bonding energies (due to weak interaction) with orders of magnitude smaller than the energies of chemical bonds can be easily removed in vacuum. No oxygen related PL was observed for unirradiated films. However, the 2.1eV PL starts appearing in the irradiated samples in increasing intensity with dose. This suggests that irradiation damage of C_{60} increases the reactivity of the irradiated films with the molecular oxygen in air forming fullerene oxide with oxygen atoms attached to the fullerene cage and the same is not removed in vacuum. The increase in oxygen content with fluence has also been reported earlier for proton irradiation [19] where the closed non-reactive structure of C_{60} molecules can be changed into reactive structures on irradiation, with dangling bond orbitals forming fullerene oxides. Fig.6.2.3a. shows such PL spectra of unirradiated C_{60} film in air and in vacuum and PL of irradiated film with 50 MeV Si at a dose of 1.8×10^{12} ions/cm^2. The possibility requires further investigations if the samples, when removed from the

beam chamber after irradiation may have products which are susceptible to reaction with oxygen on exposure to atmosphere and cause oxidized products due to photoreaction [38].

6.3. Characterization of irradiated fullerene employing other techniques:

To obtain more information on the effect of high energetic heavy ion irradiation on C_{60}, we have also undertaken other techniques to study the induced modifications on its surface morphology, crystal structure and its chemical modifications. For the purpose we have undertaken the study on irradiated C_{60} thin films of thickness ~500nm with 180 MeV Ag ions at various doses ranging from 1×10^{10} to 5×10^{12} ions/cm^2.

6.3.1. X-ray Diffraction (XRD).

X-ray diffraction of C_{60} powder (Fig. 6.3.1a), pellet (Fig.6.3.1b) and unirradiated thin film of C_{60} (Fig. 6.3.1c) gave the peak characteristics of f. c. c lattice. The peak positions were obtained at $2\theta = 10.8^0$, 17.9^0, 20.8^0 corresponding to the planes of (111), (220), and (311) respectively. The peak characteristics (i.e. 2θ position) obtained were essentially the same as obtained by Zhong-Min Ren et al [18]. The lattice parameter as calculated from the peak positions was found to be 14. 10Å.

On irradiation it is observed that there is a decrease in the integrated peak intensities with fluence, specially from 5×10^{11} ions/cm^2. The broadening of the peaks indicates damage or fragmentation of C_{60} molecules [19], and arises due to form factor changes and subsequent reduced volume of the remaining ordered or organized material. The existence of all the peaks, though significantly reduced in intensity even at the highest fluence of 5×10^{12} ions/cm^2, suggests that there still remains undamaged C_{60} molecules exhibiting the crystalline structure.

6.3.2. Atomic Force Microscopy (AFM).

The surface morphology of C_{60} thin films was investigated using atomic force microscopy (AFM) to study the modified morphology on irradiation. Fig 6.3.2. (a), (b), (c) and (d) shows AFM pictures of pristine and irradiated C_{60} films over an area of ($1\mu \times 1\mu$).

AFM surface image shows that on an average, the size decreases upon irradiation. This may be due to grain boundary deterioration. It is observed that roughness decreases upon irradiation down to 5×10^{11} ions/cm^2 and then increases at 5×10^{12} ions/cm^2. This may be due to possible sputtering of light carbon by heavy Ag ions. AFM shows the film to be granular with layered structure with steps clearly seen. The average grain size is of about 340nm with a few extended growth of larger grains of about 400nm and almost similar for

smaller grains in the pristine film. But the grain shape are not well defined after irradiation. Corners of grains were seen to have smoothen out resulting in ellipsoidal or near square or circular shapes. This supports the view of grain boundary erosion. The surface roughening at the highest dose can be explained by formation of compact material in the radiation damaged surface layer. In some pictures of irradiated films one can see certain conical hillocks on a smooth layered structure background. Table 6.3.2a. gives the values of the changes in the grain size and roughness on irradiation for different areas.

6.3.3. Fourier Transformed Infra-red (FTIR) Spectroscopy.

From group theory calculations C_{60} is expected to have only four IR active vibrational modes (of species T_{1u}). Calculations have shown that it is expected to occur at about 1600 ± 200, 1300 ± 200, 630 ± 100, and 500 ± 50 cm_{-1} [39-42], the spread indicating variation from author to author in the calculated line positions.

We have observed the IR modes at 1426,1179, 573 and 528cm^{-1}. FTIR spectra (Fig. 6.3.3a), shows the four strong infrared peaks which corresponds to the four bands expected for C_{60} in the solid state [43-45]. Musket et al. [19], have calculated the four IR frequencies for isolated frequencies at 1429,1183, 576 and 526cm^{-1}. With respect to their results we assign the 1426 and 573cm^{-1} as attributed to combination of Hexagon and Pentagon stretching in opposite

directions respectively and 1179 and 528cm^{-1} due to "boat torsion angles". The other peaks present in the spectra may be due to presence of some $C0_2$, CO or due to mutual interaction of C_{60} molecules in the coating [1]. It is observed that IR bands at 1426 and 1179cm^{-1} decreases in intensity with fluence without significant changes in the peak position and widths, suggesting fragmentation/destruction of significant amount of C_{60} molecules in the film.

O'Brien et al. [46] has shown that photofragmentation of C_{60} leads to formation of even numbered clusters (C_{58}, C_{56}.....C_{82}). This suggests that the removal of carbon atoms from C_{60} through collision would result in formation of smaller caged clusters. Thus if on irradiation collision were the dominant effect on C_{60} then peak shifts due to inter-molecular distances and different vibrational frequencies would have been observed in FTIR and XRD. Since peak shifts were not significant except in the intensities, we conclude that the effect of energy loss due to collision is minimum.

References:

1. W. Kratschmer, L. D. Lamb, K. Fostiropoulos, and D. R. Huffman, Nature (London) 347 (1990) 354.
2. A. F. Hobard, M. J. Rosseinsky, R. C. Haddon, D. W. Murphy, S. H. Glarum, T. T. M. Palstra, A. P. Ramirez and A. R. Kortan, Nature (London) 350 (1991) 660.
3. M. Flemming, A. P. Ramitrez, M. J. Rosseinky, D. W. Murphy, R. C. Haddon, S. M. Zahurak, and A.V. Makhija, Nature (London) 352 (1991) 787.
4. H. W. Kroto, Science 242 (1988) 1139.
5. R. L. Whetter et al. The MRS Late News Session - Buckyball: New Materials Made from carbon soot. Videotape (Materials Research Society, Pittsburg, 1990).
6. H. W. Kroto, J. R. heath, S. C. O'Brien, R. F. Curl and R. E. Smalley, Nature (London) 318 (1985) 162.
7. R. F. Curl and R. E. Smalley, Science, 242 (1988) 242.
8. E. Brendsdal, J. Brunvoll, B. N. Cyvin, and S. J. Cyvin, in " Quasicrystals, network and Molecules of Fivefold Symmetry." VCH Verlags-Ges, New York Weinheim 1990, Ed. J. Hargittai, p 277.
9. L. Palmetshofer, J. Kastner, Nucl. Instr. and Meth. B96 (1995) 343.
10. F. Negri, G. Orlandi, and F. Zerbetto, " Quantum- chemical investigation of Frank-Condon, and John - Teller activity in the electronic spectra of buckminsterfullerene ". Chem. Phys. Lett. 144 (1998) 31.
11. T. Picher, M. Matus, J. Kurti and H. Kuzmany, Phy. Rev. B45 (1992) 13841.

12. S. Hobday, R. Smith, U. Gibson and A. Ritchter, Rad. Eff. and Defects in Solids 142 (1997) 301.

13. P. Zhou, A. M. Rao, K. Wang, J. D. Robertson, C. Eloi, M. S. Meier, S. L. Ren, X. X. Bi and P. C. Eklund Appl. Phys. Lett. 60 (1992) 2871.

14. B. Bhusan, B. K. Gupta, G. W. Van Cleef, C. Capp and J. V. Coe, Appl. Phys. Lett. 62 (1993) 3253.

15. P. D. Horak and U. J. Gibson, Appl. Phys. Lett. 65 (1995) 968.

16. E. B. Maiken and P. Taborek, J. Appl. Phys. 78 (1995) 541.

17. J. Kastner, H. Kuzmany, L.Palmetshofer, P. Bauer, and G. Stingeder, Nucl. Instr.and Meth.B80/81 (1993) 1456.

18. Zhong-Min Ren, Xin-Long Xu, Yuan-Chang Du, Zhi-Feng Ying, Xia-Xing X-iong and Fu-Ming, Nucl. Instr. Meth. B100 (1995)55.

19. R. G. Musket, R. A. Hawley-Fedder and W. L. Bell, Rad. Effects and Defects in Solids, 118(1991) 225.

20. A. Dunlop and D. lesueur, Rad. Effects and Defects in Solids 126 (1993)123

21. R. M. Papelo, A.Hallen, J. Eriksson, G. Brinkmalm, P. Demirev, P. Hakansson and B. U. R. Sundqvist, Nucl. Instr. and Meth. B 91 (1994) 124.

22. Ch. Dufour, E. Paumier and M. Toulemonde, Nucl. Instr and Meth. B122 (1997) 445.

23. D. Fink, R. Kleet, P. Szimkoviak, J. Kastner,L. Palmetshofer, L. T. Chadderton, L. Wang and H. Kuxmany, Nucl. Instr. and Meth. B 108 (1996) 114.

24. A. Itoh, H. Tsuchida, K. Miyabe, M. Imai and B. Imanishi, Nucl. Instr.and Meth. B129 (1997) 363.

25. T. Mori, and Y. Namba, Vac Sci Tech, A1 (1983) 23.

26. P. C. Ecklund, A. M. Rao, Y. Wang, P. Zoom and G. R. Ochoa, Fullerene and Photonics, Vol. 2 (1994).

27. R. A. Assink, J. E. Schirber, D. A. Loy, B. Morosin and G. A. Carlson, in "Novel forms of Carbon", edited by C.L. Renschler, J.J. Pouch and D.M. Cox, MRS symposia proc. No.270 (Materials Research Society, Pittsburgh 255. 1992).

28. A. M. Rao, P. Zhou, K. Wang, G.T. Hager, J. M. Holden, Y. Wang, W. T Lee, X. X. Bi, P. C. Eklund, D. S. Cornett, M. A. Duncan and I. J. Amster, Science, 259 (1993) 955.

29. K. Venkstesan and V. Ramamurthy, Photochemistry in Organized and Constrained Media,133, (1991).

30. J. F, Ziegler, J. P. Biersack. and V. Littmark, The stopping and Rangeof Ions in Solids, Pergaman Press New York,1985.

31. M. E. Ryskyn, V. I. Chernysh. S. A. Dorbin, T. Y. Kureneva and B. R. Shub, Optics and spectroscopy 78, (1995) 205.

32. S. H. Yang, C. L. Pttiette, J. Conceicao, O. Cheshnovsky, and R. E. Smalley, Chem. Phys. Lett. 139 (1987) 233.

33. C. Reber, L. Yee, J. Mckierman, J. I. Zink, R. S. Williams, W. M. Tong, D. A. A. Ohilberg, R.L. Whetton, and F. Diederich, J. Phys. Chem. 95 (1991) 2127.

34. A. Ankreoni, M. Bondani, and G. Consolati, Phy. Rev. Lett. 72 (1994) 844.

35. K. Pichler, S. Graham, O. M. Gelsen, R. H. Friend, W. J. Romanow, J. P. Mccauley, Jr., N. Coustel, J. E. Fischer, and A. B. Smith III, J. Phys. Condens. Matter 3 (1991) 9259.

36. M. Matus, H. Kuzmany, and E. Sohmen, Phys. Rev. Lett. 68 (1992) 2822.

37. C. Reber, L. Yee, J. Mckiernan, J. I. Zink, R.S. Williams, W. M. Tong, D. A. A. Ohlberg, R. L. Whetten, and F. Diederich, J. Phys. Chem. 95 (1991) 2127.

38. Menon, M. and Subbaswamy, K. R., Chem. Phys. Lett. 125 (1986) 459.

39. D. E. Weeks and W. G. Harter, J. Chem. Phys. 90 (1989)4744.

40. R.E. Stanton and M. D. Newton, J. Phys. Chem. 92(1988) 2141.

41. S.J. Cyvin, E. Brendsdal, B. N. Cyvin and J. Brunvoli, Chem. Phys. Letters 143 (1988) 377.

42. Z. C. Wu, D. A. Jelski and T. F. George, Chem. Phys. Letters 137 (1987) 291.

43. W. Kratschmer, K. Fostiropoulos and D. R. Huffman, Chem. Phys. Lett. 170 (1990) 167.

44. R. E. Hauffer, J. Conceicao, L. P. F. Chibante, Y. Chai, N. E. Byrane, S. Flanagan, M. M. Haley, S. C. O'Brein, C. Pan, Z. Xiao, W.E. Bilips, M. A. Ciufolini, R. H. Hauge, J. E. Margrave, L. J. Wilson, R. F. Curl, and R. E. Smalley, J. Phys. Chem 94 (1990) 8634.

45. H. Ajie, M. M. Alvarez, S. J. Anz, R. D. Beck, F. Diederich, K. Fostiropoulos, D. R. Huffman, W. Kratschmer, Y. Rubin, K. E. Schriver, D. Sensharma, and R. L. Whetten, J. Phys. Chem, 94, (1990) 8630.

46. S. C. O'Brien, J. R. Heath, R. L. Curl and R. E. Smalley, J. Chem. Phys. 88, (1998) 220.

Table. 6.1a.

I_h Point group Symmetry Table.

I_h	E	$12C_5$	$12C_5^2$	20_3	15_2	i	$12S_{10}$	$12S_{10}^3$	20_6	15 σ		
A_g	1	1	1	1	1	1	1	1	1	1		$x^2+y^2+z^2$
T_{1g}	3	1/2(1+√5)	1/2(1+√5)	0	-1	3	1/2(1+√5)	1/2(1+√5)	0	-1	Rx,Ry,Rz	
T_{2g}	3	1/2(1+√5)	1/2(1+√5)	0	-1	3	1/2(1+√5)	1/2(1+√5)	0	-1		
G_g	4	-1	-1	1	0	4	-1	-1	1	0		
H_g	5	0	0	-1	1	5	0	0	-1	1		$(2z^2-x^2-y^2)$, x^2-y^2, xy,yz,zx
A_u	1	1	1	1	1	-1	-1	-1	-1	-1		
T_{1u}	3	1/2(1+√5)	1/2(1+√5)	0	-1	-3	1/2(1+√5)	1/2(1+√5)	0	1	x,y,z	
T_{2u}	3	1/2(1+√5)	1/2(1+√5)	0	-1	-3	1/2(1+√5)	1/2(1+√5)	0	1		
G_u	4	-1	-1	1	0	-4	1	1	-1	0		
H_u	5	0	0	-1	1	-5	0	0	1	-1		
χ_i—	180	0	0	0	0	0	0	0	0	4		

Table. 6.1b. Contribution to character per unshifted atom.

Proper operation		Improper operation	
R	χ_R	R	χ_R
C_n^K	$1+2\cos 2\pi k/n$	S_n^k	$-1+2\cos 2\pi k/n$
$E = C_1^k$	3	$\sigma = S_1^1$	1
C_2^1	-1	$1 = S_2^1$	-3
C_3^1, C_3^2	0	S_3^1, S_3^5	-2
C_4^1, C_4^2	1	S_4^1, S_4^5	-1
C_6^1, C_6^2	2	S_6^1, S_6^5	0

(Table reffered from : Theory of IR and Raman vibrational spectra. Wilson,Decus and Cross)

Table 6.2.1a

C_{60} destruction and polymerization on irradiation with heavy ions at different energies and fluences. Absorbed energy densities $D_{elect,\ nucl} = (S_{elect,\ nulc} \times$ fluence)

Ion	Energy (MeV)	Fluence (ions/cm^2	Se [eV/Å]	Sn [eV/Å]	Delect [eV/Å^3]	Dnucl [eV/Å^3]	I_{1467} Dest	I_{1459} Polymer
^{107}Ag	189	1.42×10^{11}	1145	2.57	1.62×10^{-2}	3.6×10^{-5}	.92± 0.09	0.013±0.001
		2.8×10^{11}			3.2×10^{-2}	7.1×10^{-5}	.70± 0.07	0.052±0.005
		5.6×10^{11}			6.4×10^{-2}	1.4×10^{-4}	.40± 0.04	0.060±0.006
		1.7×10^{12}			1.9×10^{-1}	4.3×10^{-4}	.01 ± 0.01	0.105±0.01
^{58}Ni	110	9×10^{10}	687	.93	6.1×10^{-3}	8.3×10^{-6}	1±0.98	.0263±0.002
		1.8×10^{11}			1.2×10^{-2}	1.6×10^{-5}	.85±0.08	.082±0.008
		4.5×10^{11}			3.09×10^{-2}	4.1×10^{-5}	.45±0.04	.42±0.04
		7×10^{11}			4.8×10^{-2}	6.5×10^{-5}	.32±0.03	.42 ±0.04
^{28}Si	50	2.1×10^{11}	279	.26	5.8×10^{-3}	5.4×10^{-6}	.70±0.08	.19±0.01
		5.5×10^{11}			1.5×10^{-2}	1.4×10^{-5}	. 4±0.04	.6±0.02
		1×10^{12}			2.7×10^{-2}	2.6×10^{-5}	.215±0.02	.5±0.05
		1.8×10^{12}			5.02×10^{-2}	4.6×10^{-5}	.0461±0.004	.09±0.009

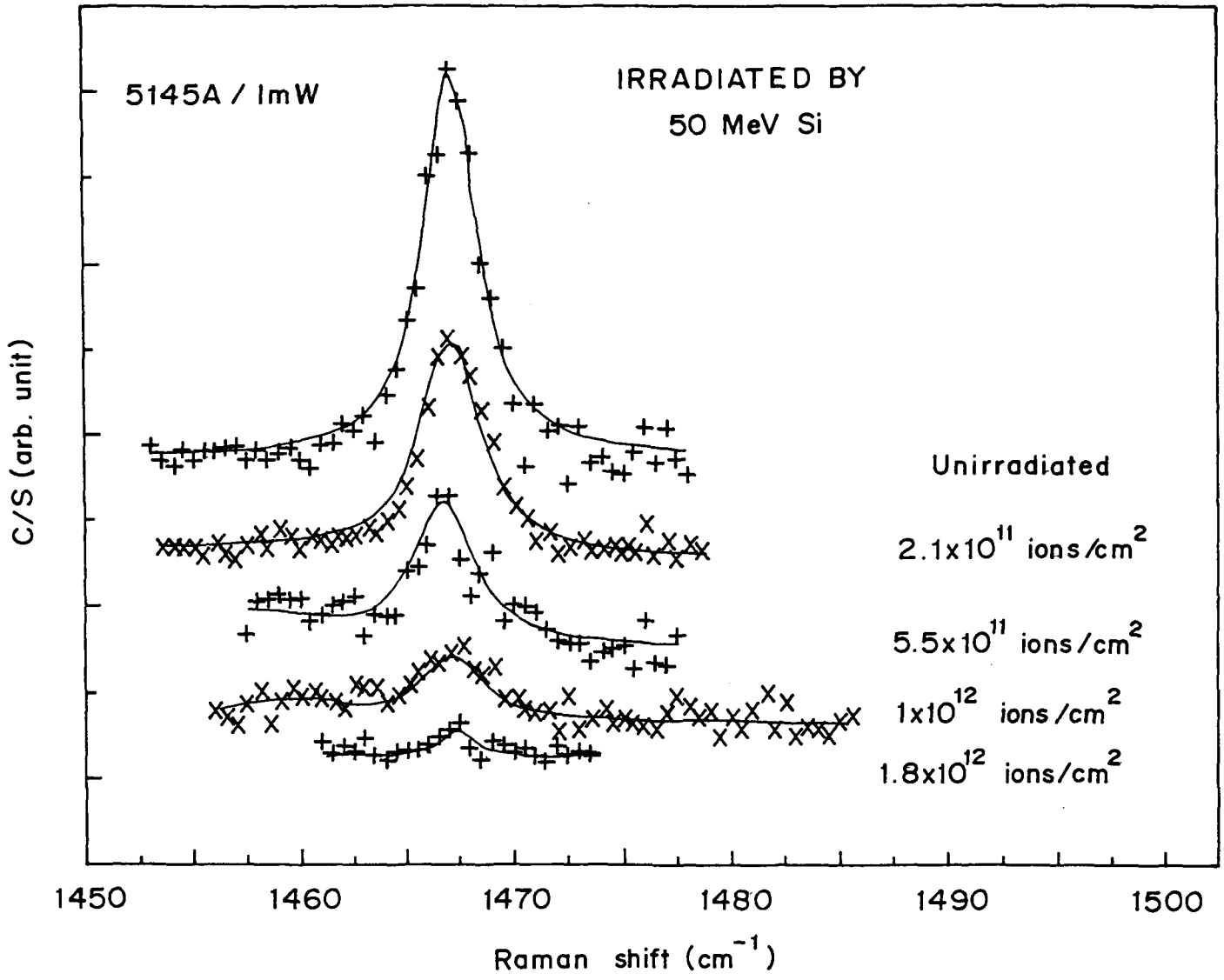

Fig. 6.2.1a Intensity decrease of the Ag mode 1467 cm^{-1} with fluence

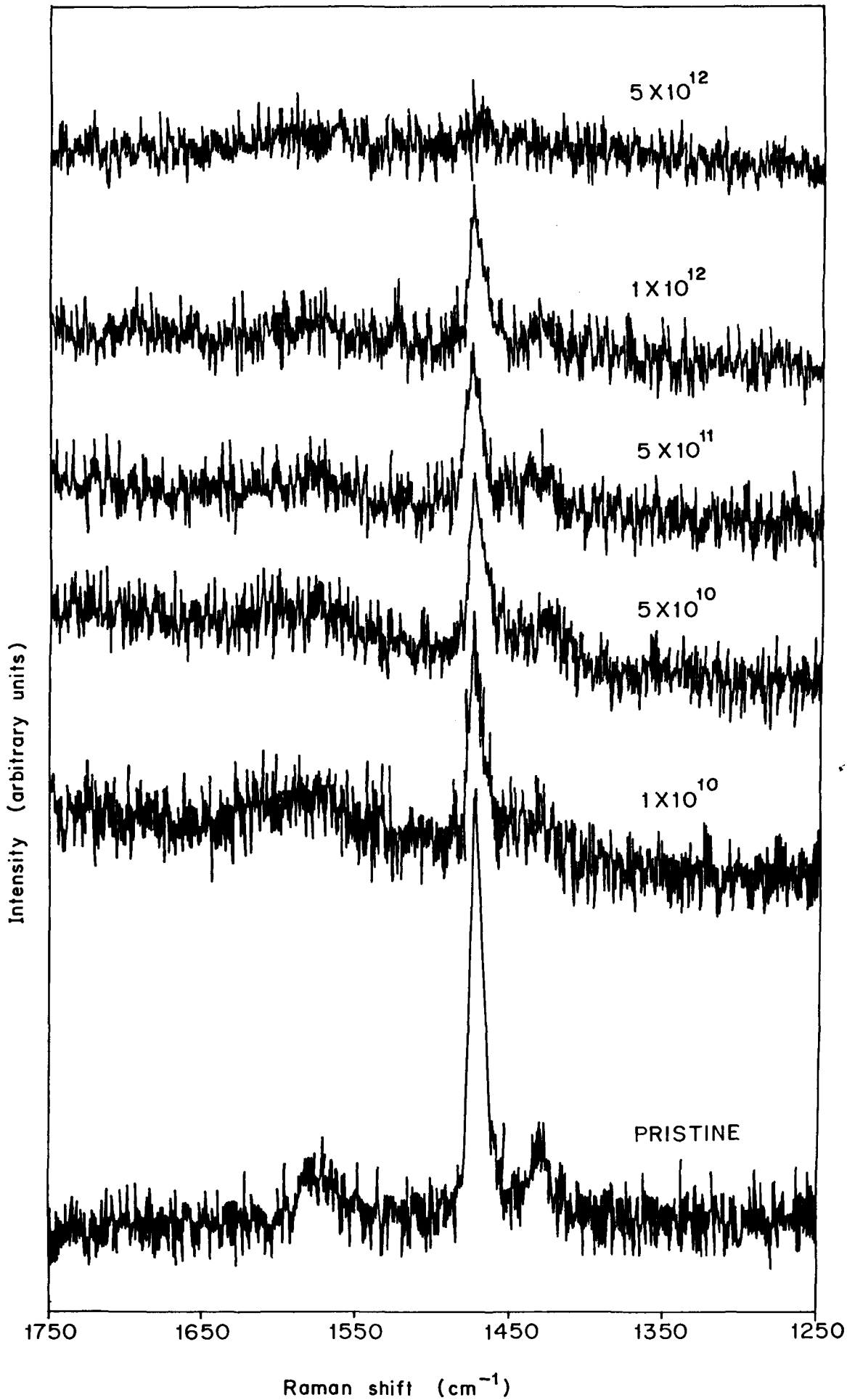

Fig. 6.2.1b Raman spectra from pristine and irradiated C_{60} targets by 180 MeV Ag ions

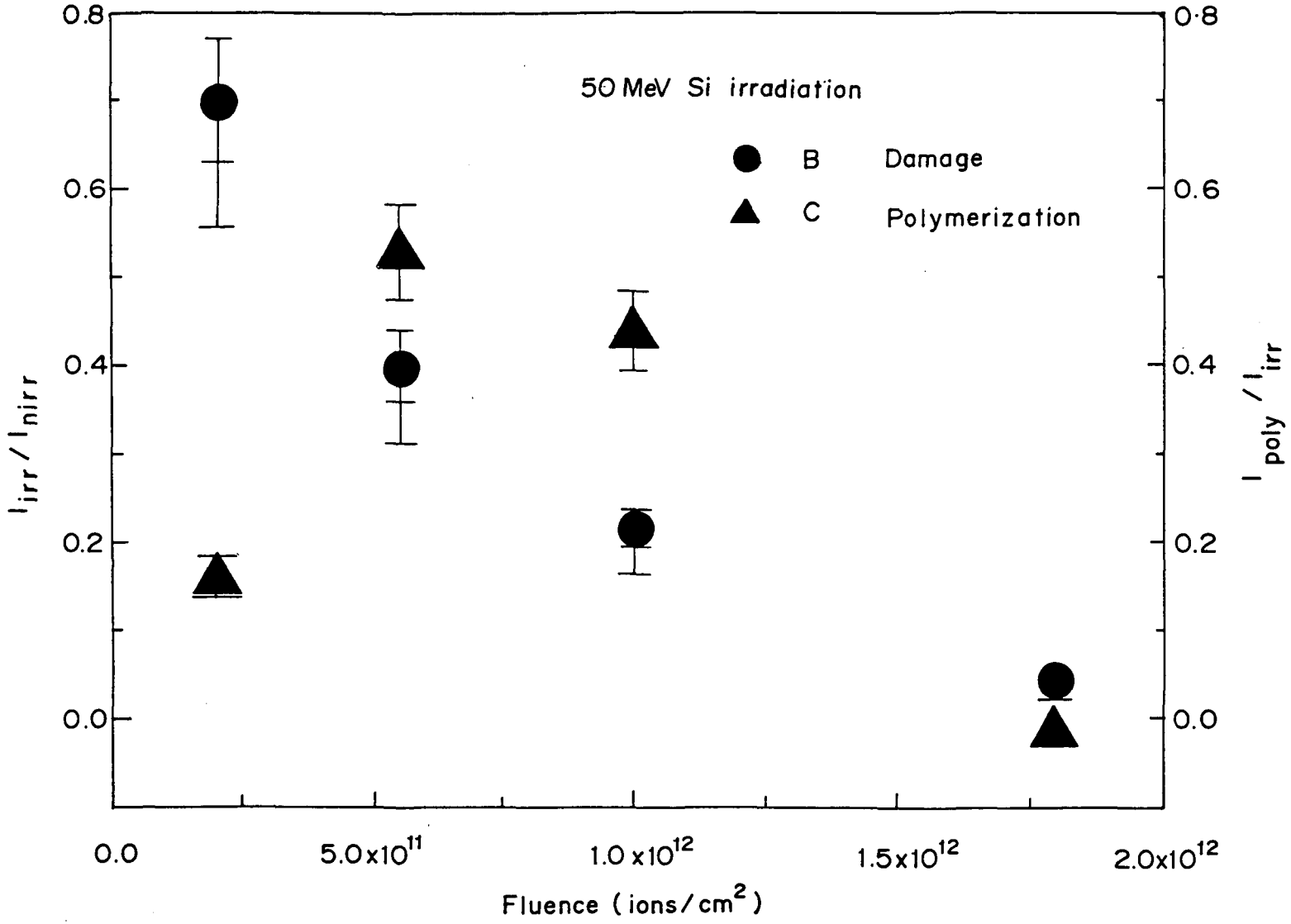

Fig. 6.2.1c Plot showing percentage of destruction and polymerization of C_{60} irradiated with 50 MeV Si ion

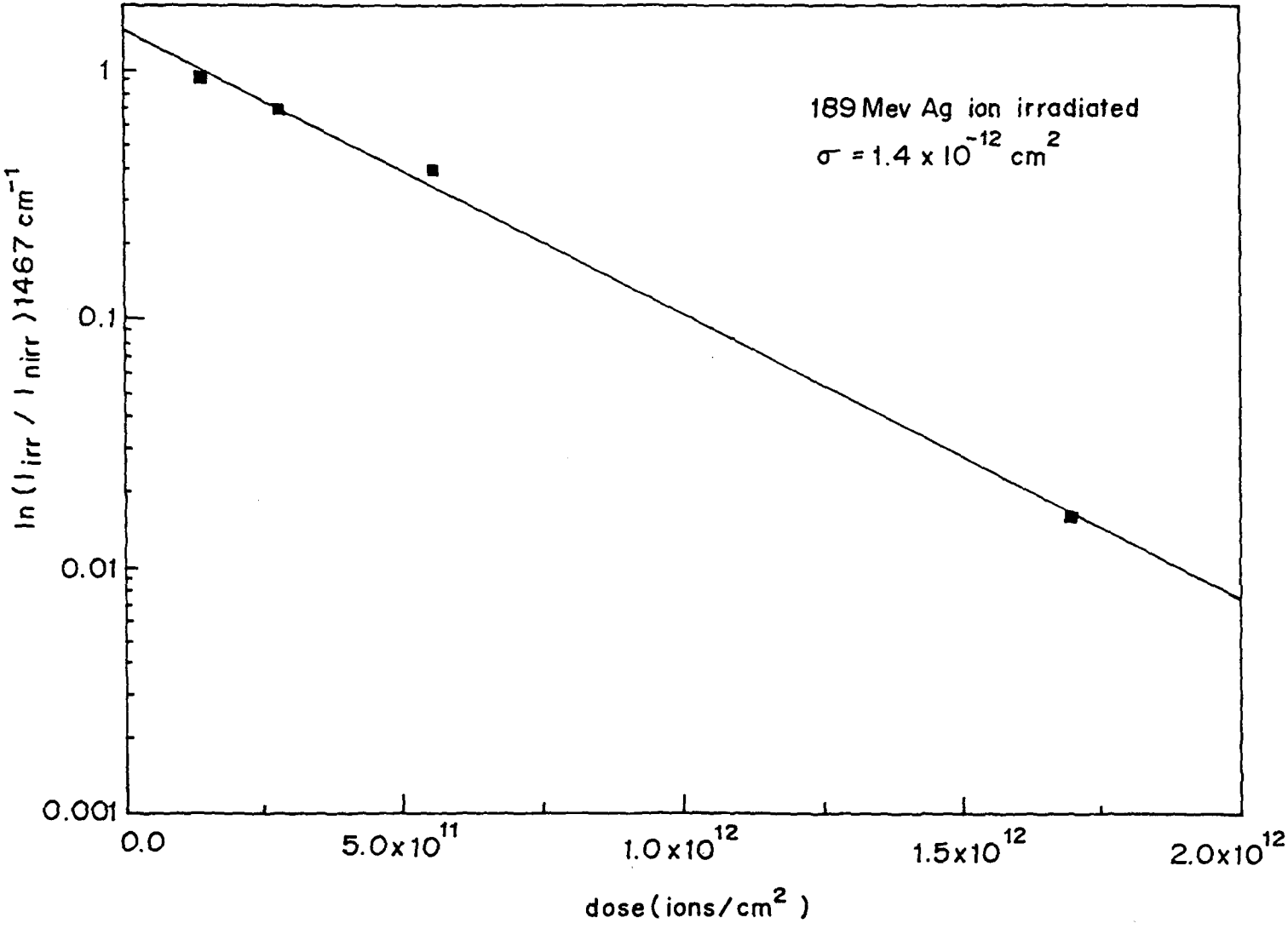

Fig. 6.2.1d Plote showing damage of C_{60} against fluence for 189 MeV Ag in

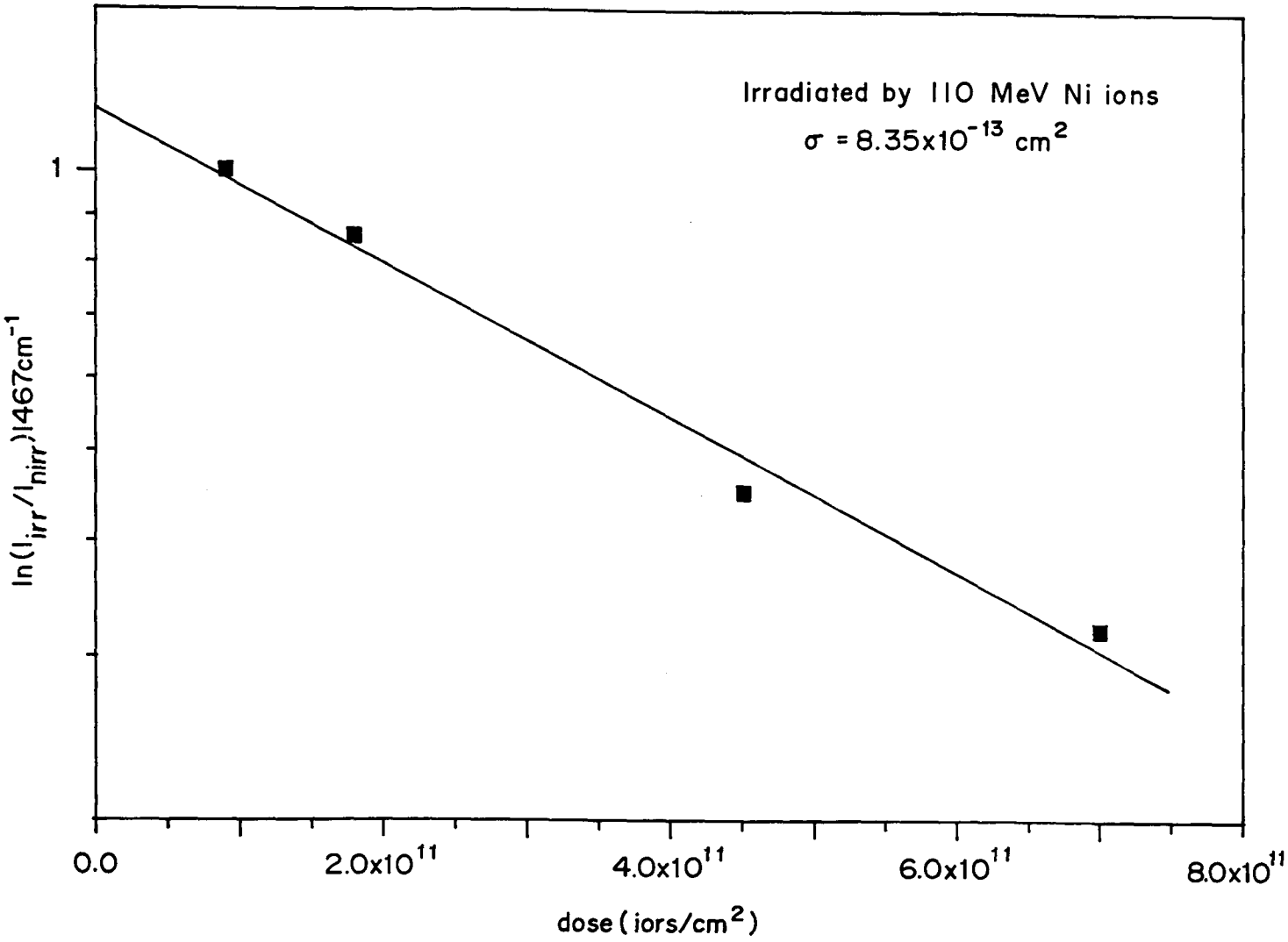

Fig. 6. 2.1e Plot showing damage of C_{60} against fluence for 110 MeV Ni ions

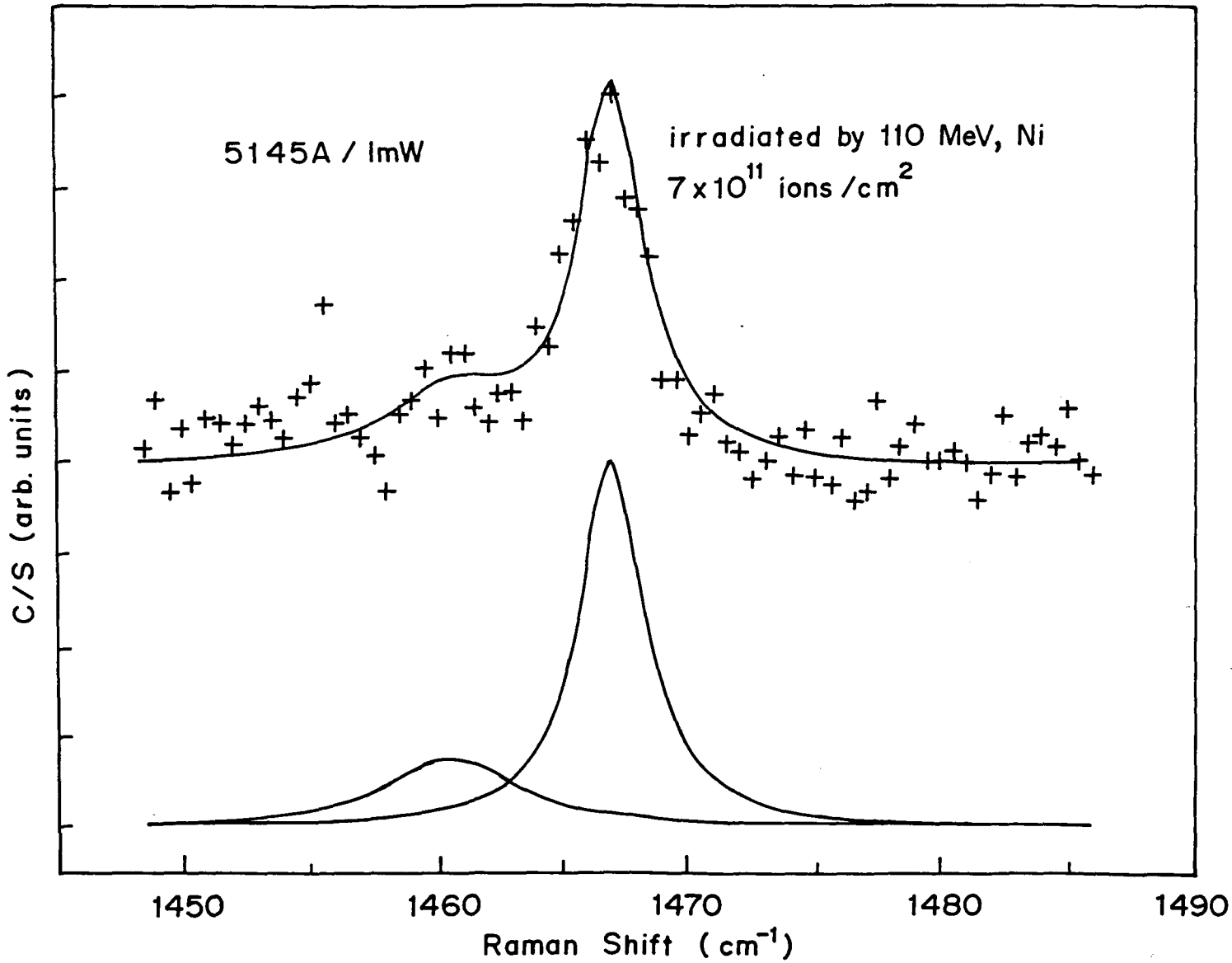

Fig. 6.2.2a Two lorentzion fit to 1459 cm^{-1} and 1467 cm^{-1}

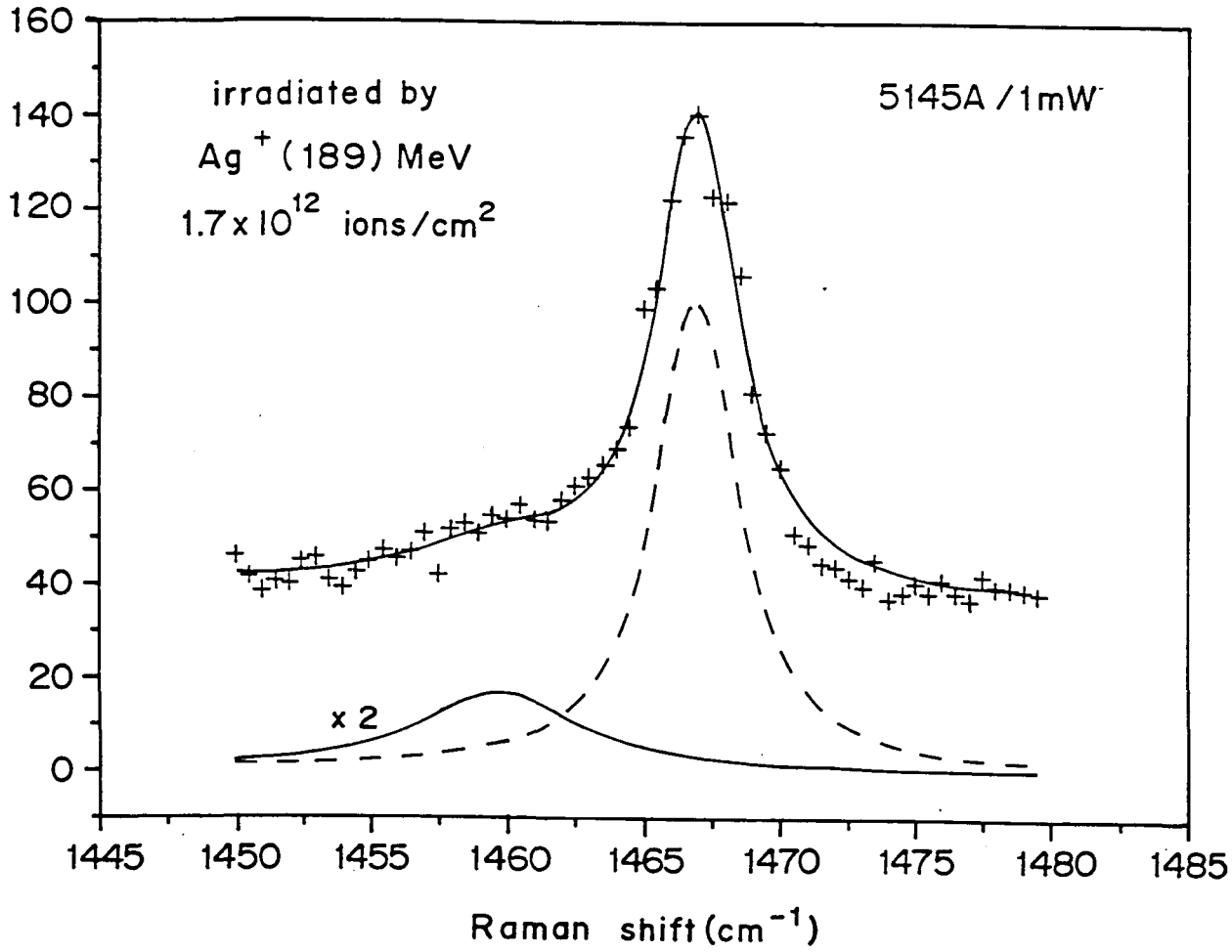

Fig. 6.2.2b Two lorentzian fit to 1459 cm^{-1} and 1467 cm^{-1}

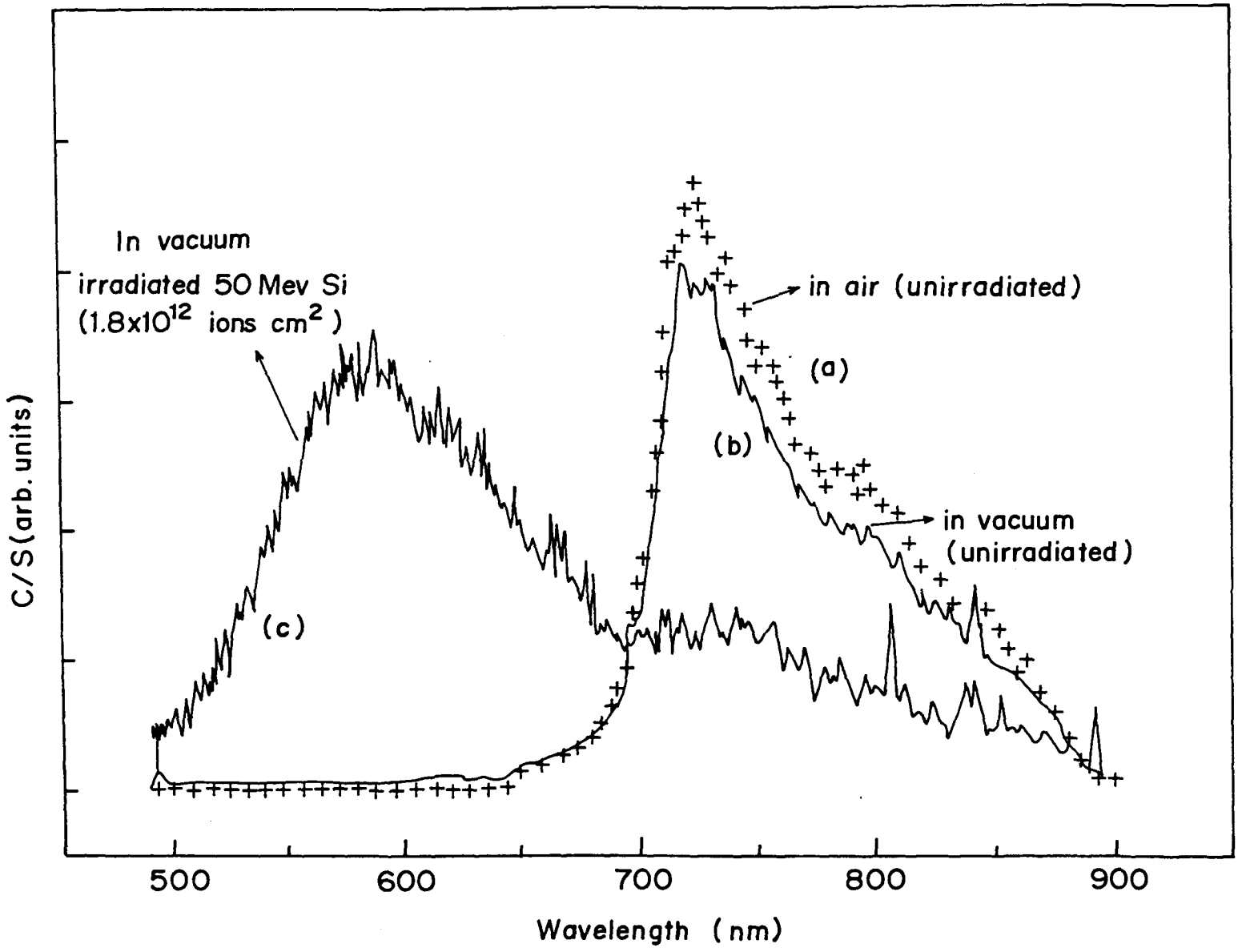

Fig. 6.2.3a PL spectra of pristine film in air, vacuum, and irradiated film with 50 MeV Si ion

Table 6.2.3b

(i). Table showing the ratios of the PL intensities at 1.7eV to 2.1eV of irradiated C_{60} films by 50 MeV Si ions.

Ion	Energy	Fluence (ions/cm^2)	S_e [eV/Å]	S_n [eV/Å]	PL 1.7eV/2.1eV
^{28}Si	50 MeV	$2.1x10^{11}$	279	.26	2.4 ± 0.24
		$5.5x10^{12}$			1.8 ± 0.18
		$1x10^{12}$			.357± 0.03
		$1.8x10^{12}$			.334±0.03

(ii). Table showing the ratios of the PL intensities at 1.7eV to 2.1eV of irradiated C_{60} films by 110 MeV Ni ions.

Ion	Energy	Fluence (ions/cm^2)	S_e [eV/Å]	S_n [eV/Å]	PL 1.7eV/2.1eV
^{58}Ni	110 MeV	$9x10^{10}$	687	.93	only 1.7eV peak
		$1.8x10^{11}$			only1.7eV peak
		$4.5x10^{11}$			4±.4
		$7x10^{11}$			0.833±0.08

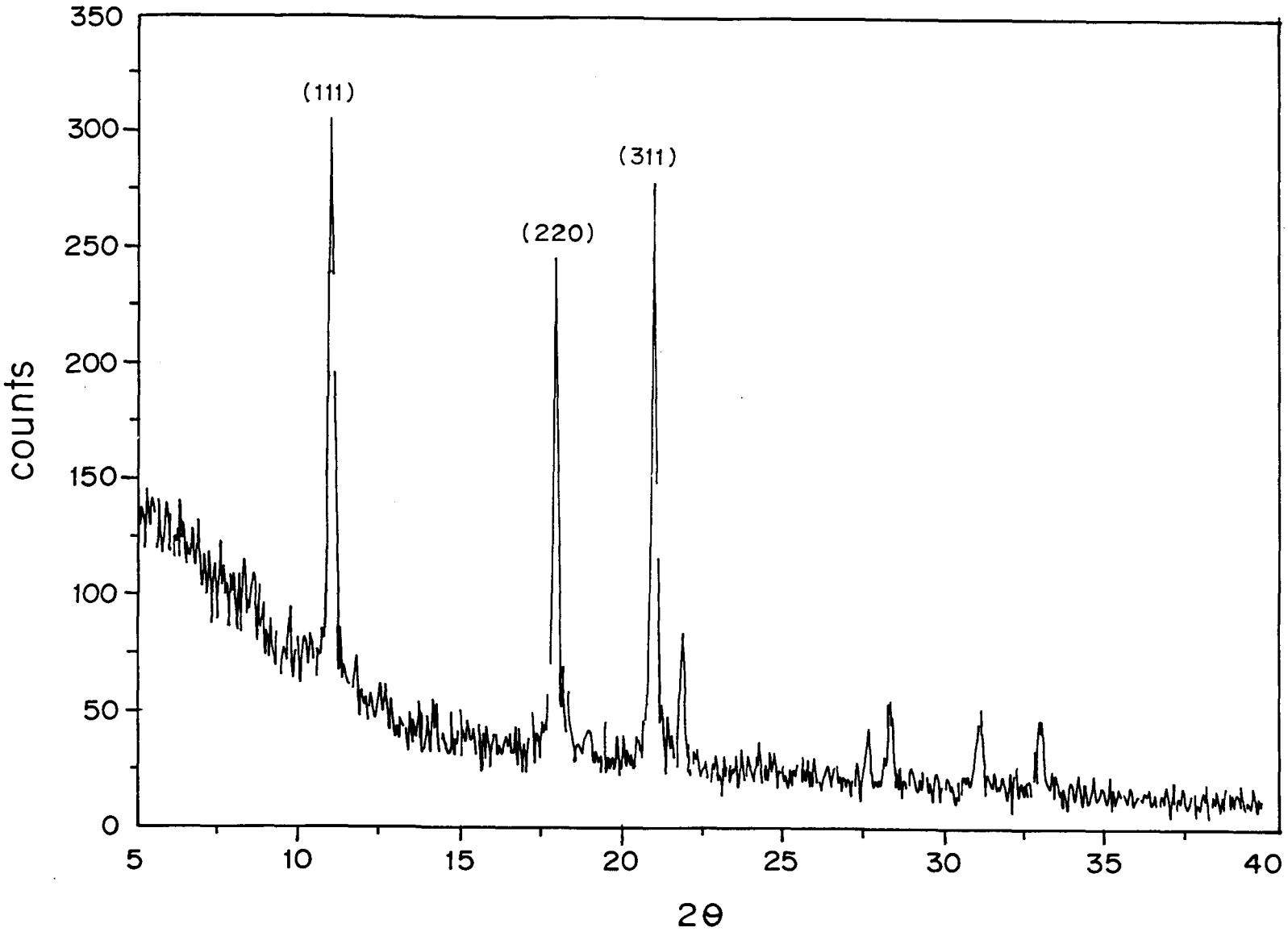

Fig. 6.3.1a X-ray diffraction pattern of C_{60} powder

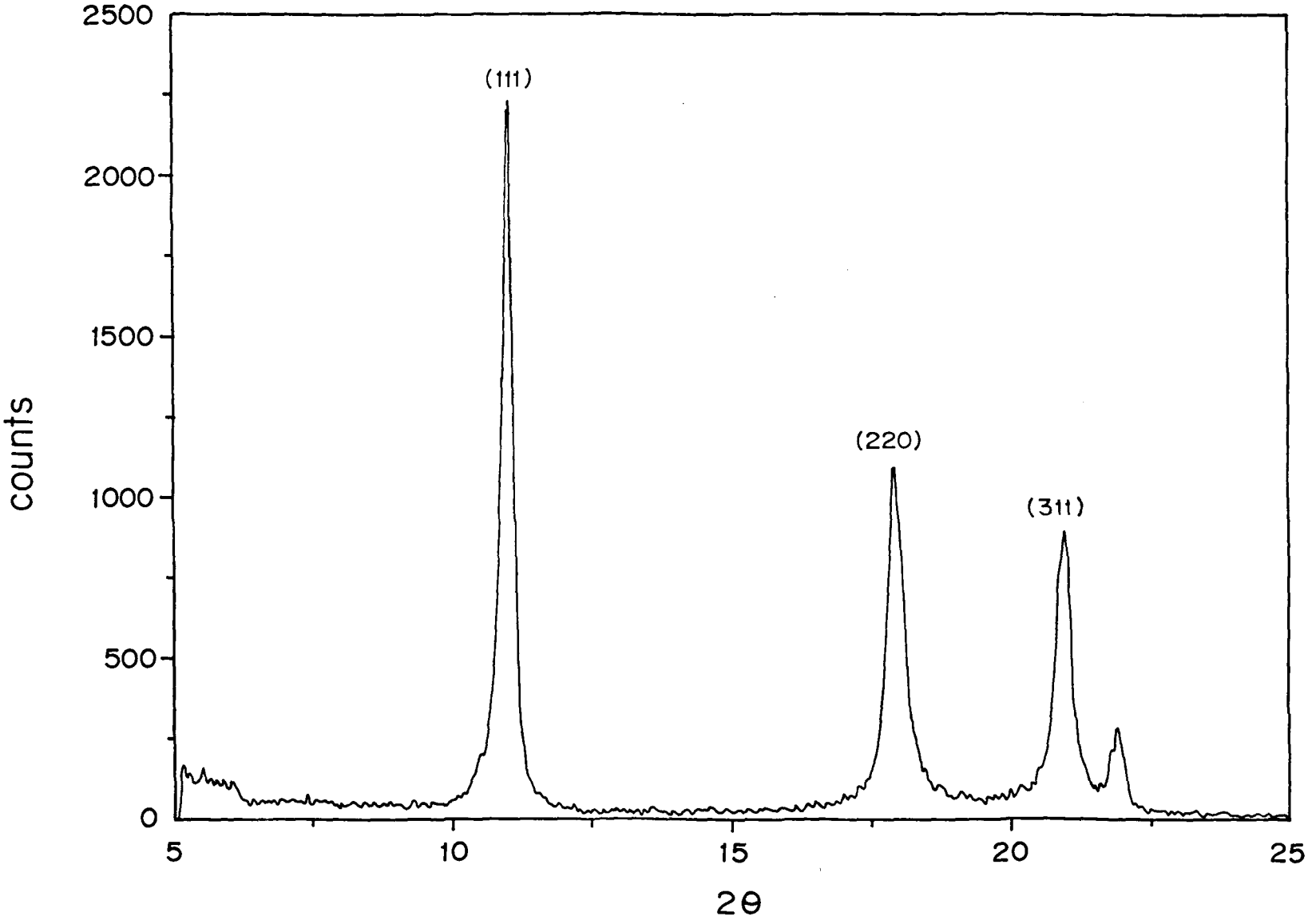

Fig. 6.3.1b. X-ray diffraction pattern of C_{60} pellet

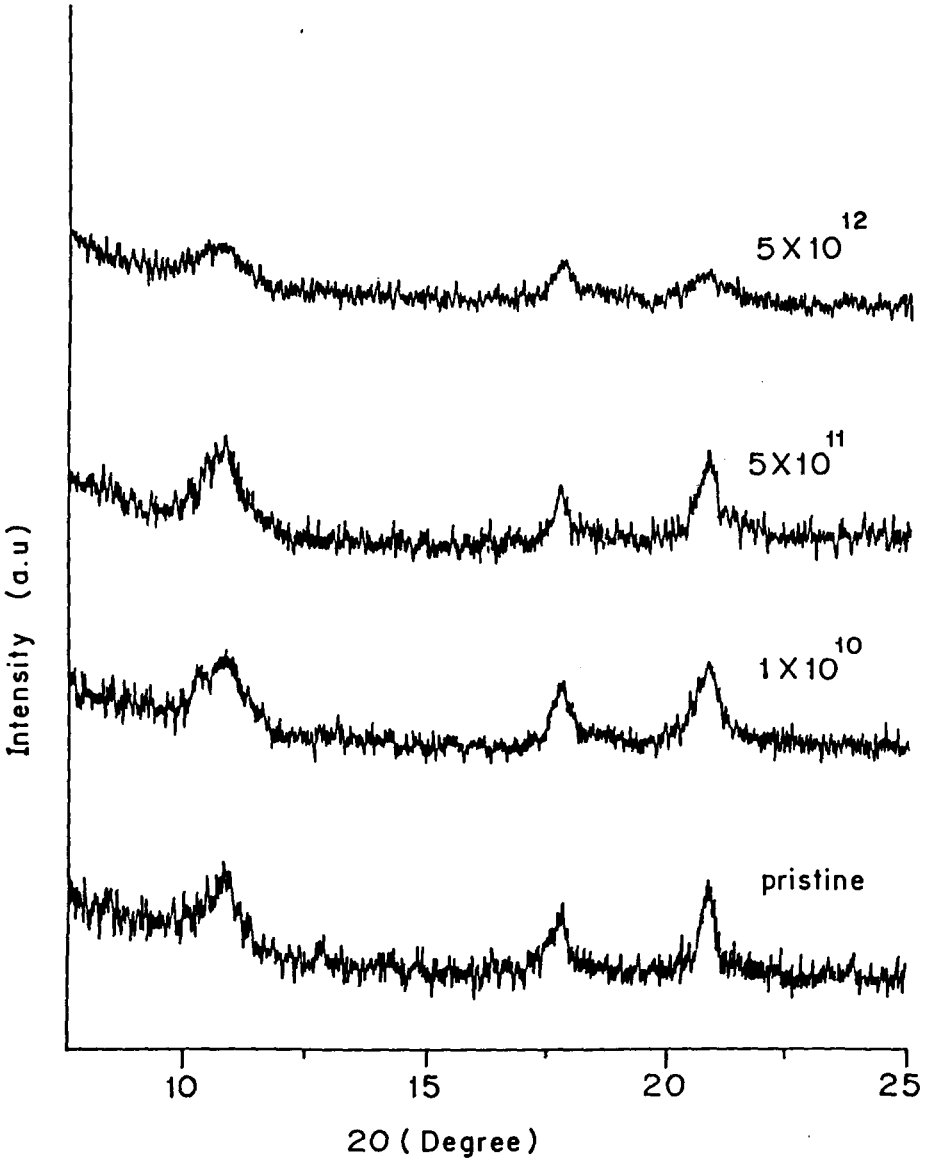

Fig. 6.3.1c XRD Spectra of unirradiated and irradiated thin films of C_{60} with 180 MeV Ag ions

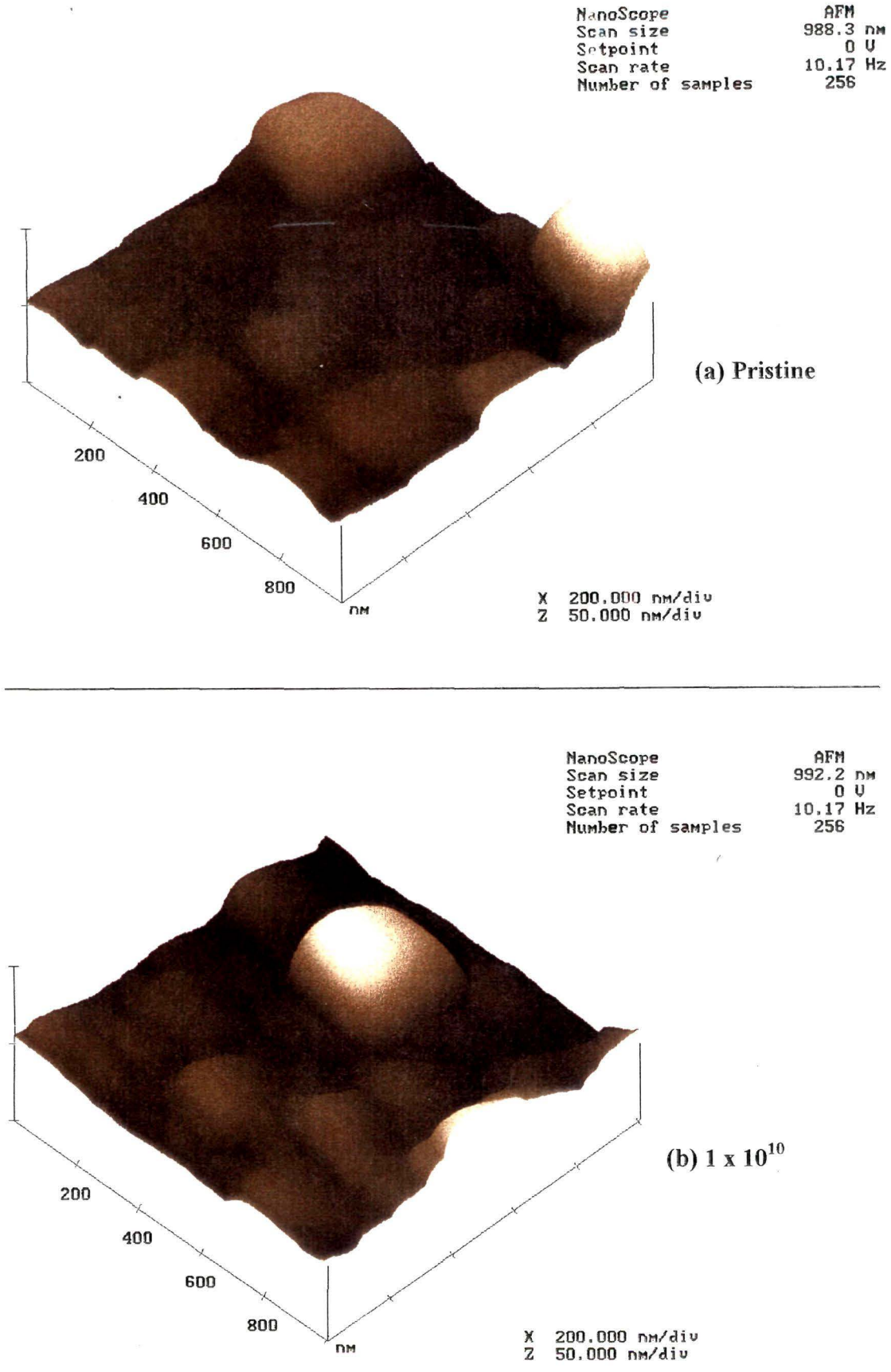

Fig. 6.3.2. AFM images of C_{60} films (a) pristine and (b), (c), (d) irradiated with 180 MeV Ag ions in cm^{-2}

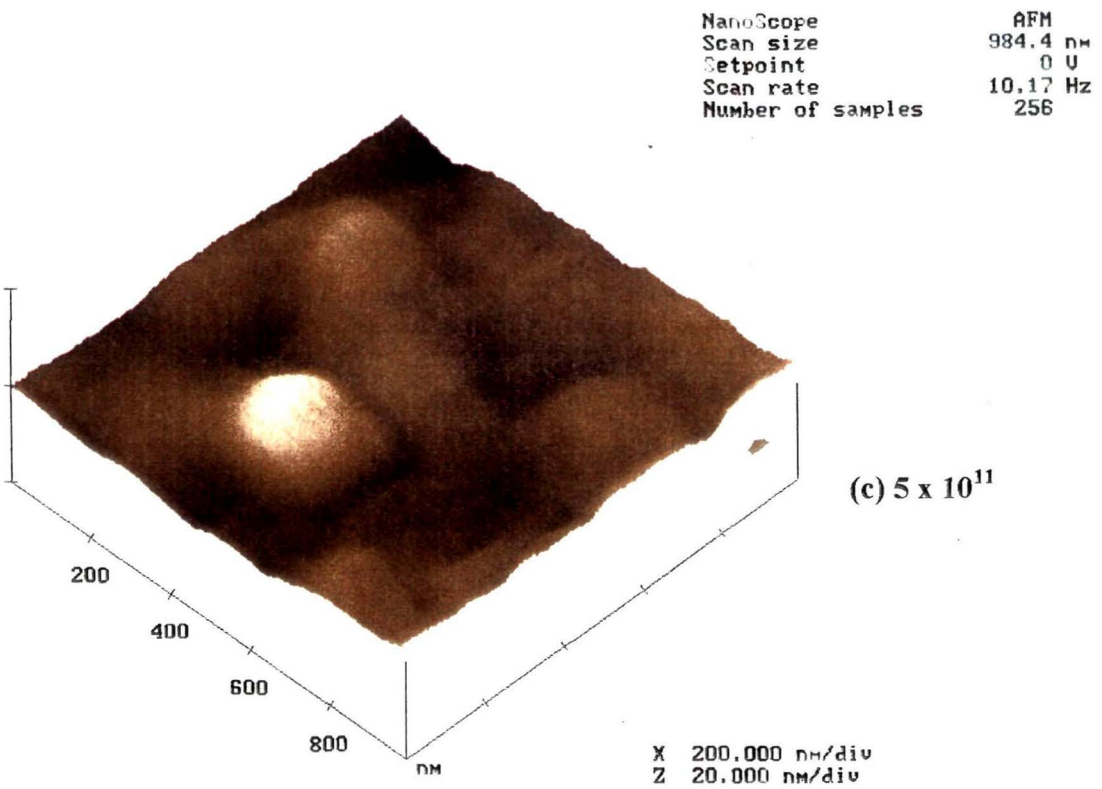

(c) 5 x 10^{11}

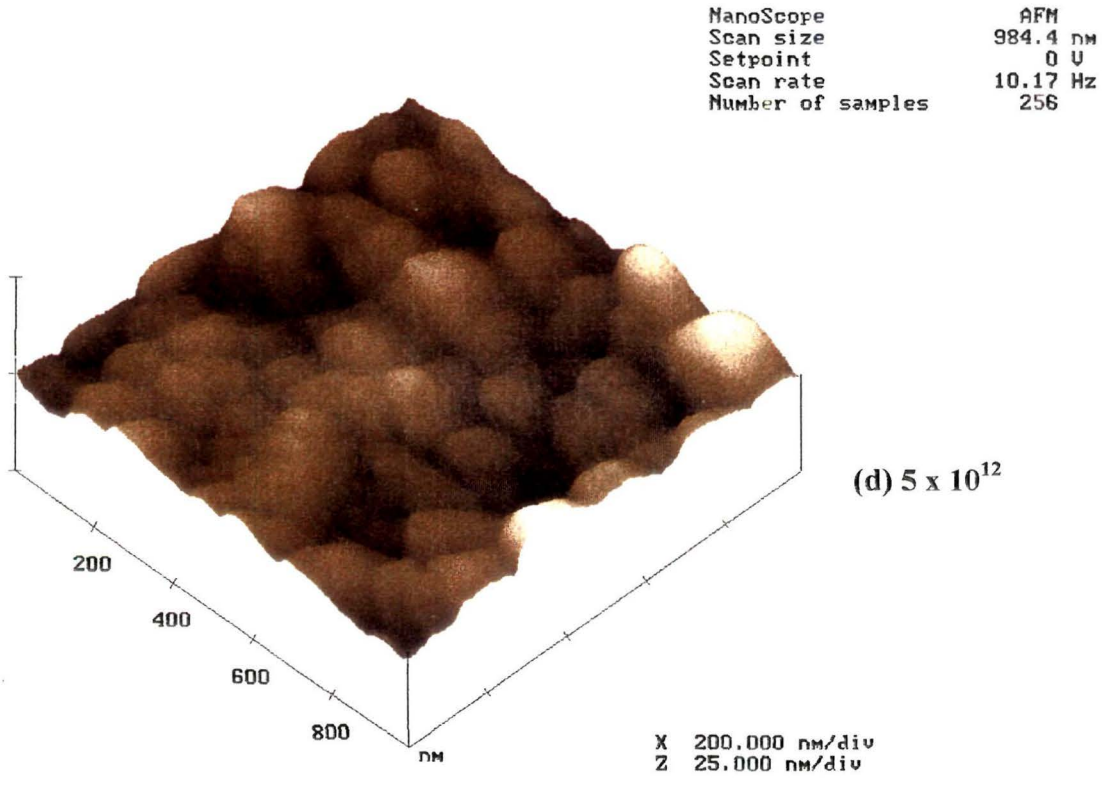

(d) 5 x 10^{12}

Table. 6.3.2a

AFM measurements of C_{60} thin films irradiated with 180 MeV Ag^+ ions.

$5\mu \times 5\mu$ (Area)	pristine	1×10^{10} (ions/cm^2)	5×10^{11} (ions/cm^2)	5×10^{12} (ions/cm^2)
Grain size(big) (nm)	423	359	292	644
Grain size(small) (nm)	267	260	255	193
Roughness (nm)	14.08	8.47	3.58	7.35
$2\mu \times 2\mu$ (Area)				
Grain size(big) (nm)	358	332	285	311
Grain size(small) (nm)	234	230	259	193
Roughness (nm)	12.41	10.48	3.18	6.63
$1\mu \times 1\mu$ (Area)				
Grain size(big) (nm)	373	316	161	260
Grain size(small) (nm)	206	-	-	-
Roughness (nm)	8.135	8.93	1.66	2.29

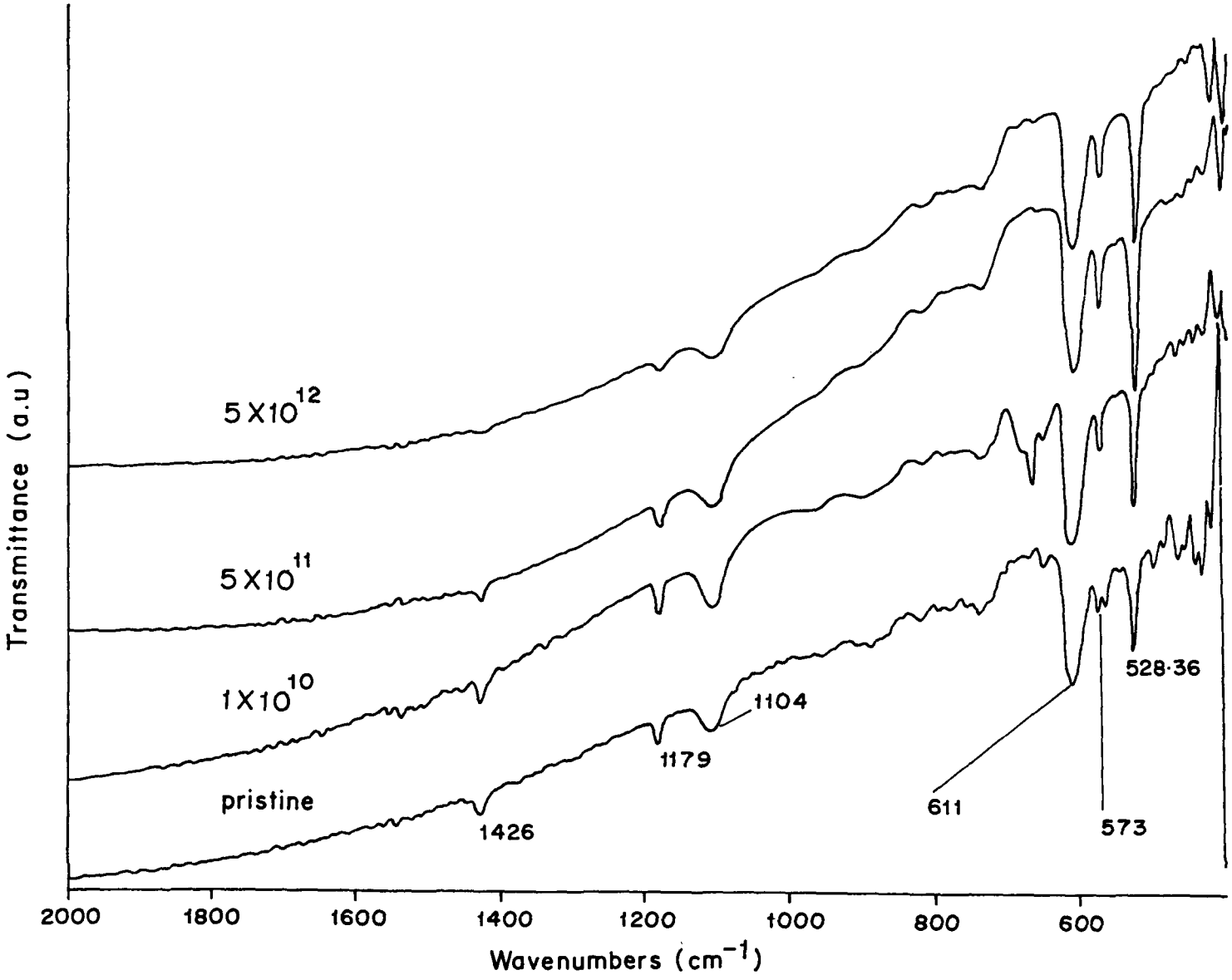

Fig. 6.3.3a FTIR Spectra of pristine and irradiated C_{60} films with 180 MeV Ag ions

CHAPTER - VII

7.0 CONCLUSION AND FUTURE SCOPE

High energy heavy ions passing inside a material lose their energy mainly through inelastic scattering, producing trail of excited/ionized atoms. The energy deposited produces a high energy density chemistry giving final products which are different from those generated by low energetic ions.

Along the ion trajectory a continuous trail of damage called latent tracks are formed, provided the electronic energy loss exceeds a certain threshold value depending on the material. These tracks consists of atomic displacements, broken molecular chains and free radicals. The formation of these tracks is largely is responsible for the material modification.

The energy deposited by swift heavy ions in materials can be varied by choosing the appropriate ion and their energies. This provides a possibility to create interesting modification in all types of materials. Thus the field of swift heavy ions in materials engineering and characterization offers much possibilities of applications.

In the present work we have therefore tried to characterize and analyze the effect of high energetic heavy ions at high electronic excitation of (2 keV/nm ~ 11 keV/nm) on polymers and fullerene (C_{60}) using different ions and varying doses.

7.1 Polymers:

The present investigation on polymers was undertaken to study :

(1) The loss of hydrogen on irradiation with different ions and energies and using the the technique of elastic recoil detection analysis (ERDA) for its determination.

(2) The effect of swift heavy ion irradiation on the radiochemistry and the melting characteristics of PET at high electronic energy transfer (~10 keV/nm) and using the techniques of Fourier transform infrared spectroscopy (FTIR) and Differential scanning calorimetry (DSC).

(3) The nature of chemical changes in PVDF by the irradiation of 180 MeV Ag and 95 MeV Ni ions was also studied employing the technique of FTIR.

From the study of hydrogen loss on irradiation by swift heavy ions we come to the conclusion that:

(a) The rate of hydrogen loss from irradiated polymers is proportional to the electronic energy loss.

(b) The loss of hydrogen is dependent on the type of C - H bonds in the polymers. For example PMMA and PP where there are CH_3 type bonds, the rate of hydrogen loss is higher than in other polymers.

(c) All hydrogen loss curves can be fitted by two exponential terms. The track radii estimated from the hydrogen release cross section to be 2 - 6 nm.

(d) As the ions pass through an insulating medium like a polymer, hydrogen gets partially released within the volume of the track. At the ion fluence when the track diameters start overlapping, it is observed that the rate of loss of hydrogen loss curve tends to flatten. This fluence also reveals the track radius.

The differential calorimetric(DSC) measurements of swift heavy ion irradiated PET shows significant changes in their melting property. Preliminary studies indicate that the melting temperature of irradiated PET increases with ion fluence and then decreases again. It appears that, whereas the pristine material

requires both the energy to induce oriented chain mobility at $T_{premelt}$ and the energy to enable orientation free chain mobility at T_{melt}, the ion irradiation suppresses oriented chain mobility, so that only the melting peak at T_{melt} remains. When ion track overlapping sets in, amorphization overtakes, leading to a reduction in the melting point. FTIR signals indicate a different trend of amorphization from earlier observations, which might support speculation of a transient recrystallization upon swift heavy ion impact. The XRD results show the appearance of a new peak at $2\theta = 37.33^{\circ}$ on irradiation, probably stemming from the reaction products, alongwith the decrease in the main peak at $2\theta = 25.62^{\circ}$.

Studies on the nature of chemical changes in PVDF by the irradiation of energetic ions of 180 MeV Ag ions indicated the formation of $=C=CF_2$ at low fluence which was found to decrease again at higher fluence. The C - H stretching modes sustained their identity even at a fluence of 5×10^{11} ions/cm^2. However the 95 MeV Ni ions irradiation at a fluence of 5×10^{13} ions/cm^2 suggested substantial modification of the polymer leading to simpler structural units.

7.2 Fullerene (C_{60}):

(1) Thin films of C_{60} were subjected to swift heavy ion irradiation of 189 MeV Ag, 110 MeV Ni and 50 MeV Si ions, spanning the region from 2 to 11keV/nm of electronic excitation at doses ranging from 1×10^{10} to 1.8×10^{12}

ions/cm^2. The irradiated thin films were studied using Raman and Photoluminescence spectroscopy.

(2) To obtain more information on the effect of high energetic heavy ions on C_{60}, characterization on the irradiated films of fullerene by 180 MeV Ag at doses ranging from $1x10^{10}$ to $5x10^{12}$ ions/cm^2 were also performed using the techniques of Atomic force microscopy (AFM), X-ray diffraction (XRD) and Fourier transform infra-red spectroscopy (FTIR).

The Raman scattering and Photoluminescence observations indicated structural transformations of C_{60}. Raman spectra indicated polymerization and damage of the film with ion fluence arising from high electronic loss deposition. The track radii as calculated from the damage cross section are found to be, T_r = 6 nm, T_r = 5 nm and T_r = 4 nm for Ag, Ni and Si whose electronic stopping power (S_e), corresponds to 11 keV nm^{-1}, 6 keV nm^{-1} and 2 keV nm^{-1} respectively. Photoluminescence spectroscopy of the irradiated film indicated a decrease in C_{60} phase with dose and increase in the intensity at the 590nm wavelength, which is attributed to increase in oxygen content.

X-ray diffraction studies of C_{60} powder, pellet and film gave the characteristic peaks of f. c. c. crystal. On irradiation it was observed that the peak intensities decreased and broadened indicating destruction of C_{60}

molecules. The film exhibited the crystalline structure even in the highest fluence of 5×10^{12} ions/cm^2, though the intensities were much reduced.

AFM pictures showed on the average there was a decrease in the grain size on irradiation, suggesting possible sputtering of carbon atoms from the film. The film showed surface roughening at the highest fluence. This is explained as the formation of compact material in the damaged surface layer.

Fourier transform infra-red spectroscopy (FTIR) spectra showed the strong four infrared peaks at 1426, 1179, 573 and 528cm^{-1} expected for C_{60} in the solid state. The 1426 and 1179cm^{-1} bands were found to decrease in intensity with fluence without changes in the peak position and widths, suggesting fragmentation/destruction of C_{60} molecules. It also suggests that the contribution of energy loss due to collision to the destruction of C_{60} molecules in the present case is minimum.

7.3 Future Scope:

From the results of the present work it is realized that this area offers a wide scope for further studies. For swift heavy ions the flexibility of varying the electronic energy transfer to the material by choosing appropriate ion and their energies itself offers unlimited area of interesting material modification. A few areas are suggested below in order to gain a deeper understanding on the mechanism of material modification by ion irradiation.

Polymers:

(a) The molecular emission quantification on irradiation at different energies and fluence may throw new insight on the chemical modification of the material.

(b) Electrical conductivity measurement of irradiated polymers in relation to the hydrogen loss may be useful information on hydrogen dependent conductivity.

(c) The concept of MeV heavy ion induced constructive phase transition in polymers is a field of interest, particularly in the light of interesting results obtained in this work at energy transfer ~10 keV/nm. It would be worthwhile to study the radiochemistry and melting behavior of a polymer in the energy transfer region above ~10keV/nm.

(d) High resolution electron microscopy would be very useful for visualizing the tracks generated by the energetic ions, whereby the track areas can be obtained.

(e) For changes in the physical properties like elasticity or chain flexibility of irradiated polymers the use of pulsed T_2 NMR would be very valuable.

(f) Hardness measurement for different doses on the irradiated polymers would also be a very important study area.

Fullerene (C_{60}):

(a) The study of destruction of C_{60} by comparing fullerene destruction by different projectiles with varying electronic but constant nuclear energy transfer, would be very informative. It would also clearly be useful to make a number of depth profile measurement of fullerene destruction.

(b) High resolution electron microscopy would be very useful to observe the possible track formation in C_{60} generated by the energetic ions.

LIST OF RESEARCH PAPERS

1. Effect of 80 MeV Si ion irradiation on C_{60} film.
   S. Lotha, D. K. Avasthi, Alka Ingale, K. C. Rustagi, Pratima Dhuri and Ajay Gupta 'Solid State Symposium' Mumbai Dec. 20 - 22 (1996).

2. Effect of Heavy ion irradiation in Polymers and C_{60}.
   S. Lotha, D. T. Khathing, V. K. Mittal, Alka Ingale, K. C. Rustagi, Ajay Gupta and D. K. Avasthi. Workshop 'SHIMS' IISc. Banglore March 10 - 11 (1997).

3. Ion Track radius estimation by on-line hydrogen release measurement.
   V. K. Mittal, **S. Lotha** and D. K. Avasthi
   'Swift Heavy ion in Polymers and Insulating Materials' Workshop
   GNDU, Amristar 23rd. Feb.(1998).

4. Electronic Excitation induced Transformation of C_{60}.
   S. Lotha, D. T. Khathing, A. Ingale, D. K. Avasthi, V. K. Mittal, S. Mishra, R. C. Rustagi, A. Gupta and V. N. Kulkarni.
   'SHIMEC' International Conference, NSC New Delhi.
   Oct 19 - 22(1998).

5. The Effects of Swift Heavy ion irradiation on the melting characteristics and crystallinity of PET

   and S. K. Bose.'SHIMEC' International Conference, NSC New Delhi.
   Oct 19 - 22(1998). Accepted for publication in Nucl. Instr. and Meth.B.
   May-27-1999.

6. Hydrogen loss under Heavy ion irradiation in Polymers.
   V. K. Mittal, **S. Lotha** and D. K. Avasthi
   Rad. Eff. and Def. in Solids 147(1999)199.

7. Effect of Heavy ion irradiation Effects on C_{60}
   S. Lotha, A. Ingale, D. K. Avasthi, V. K. Mittal, S. Mishra, R. C. Rustagi, A. Gupta V. N. Kulkarni and D. T. Khathing.
   Solid State Communication 111/1 (1999) 55

8. Resonant electronic Tunneling in single quantum well heterostructure junction of electrodeposited metal semiconductors using nuclear track filters.
   A. Biswas, D. K Avasthi, B. K. Singh, **S. Lotha,** J. P. Singh, D. Fink, B. K. Yadav and S. K. Bose, presented in the 3rd. International conference on ionizing radiation and Polymers (IRAP'98) held at Dresden, Germany Sep.19 - 24(1998). Nucl. Instr. and Meth B (in press) April (1999).

9. Swift Heavy ion induced radiolysis of Polymer (PET)
   A. Biswas, J. P. Singh, D. K. Avasthi, B. K. Yadav, V. J. Menon, **S. Lotha** and S. K. Bose, Communicated to Nucl. Instr. and Meth. B